Regulation of somatic stem cell precursor fates and proliferation during *Drosophila melanogaster* pupal ovary development resembles the signaling framework for adult stem cell behavior

Short title: Signals regulating Drosophila ovarian FSC development

Rachel Misner, Amy Reilein, Helen V. Kogan and Daniel Kalderon*

Department of Biological Sciences, Columbia University, 1212 Amsterdam Avenue, New York, NY10027 USA

* corresponding author: ddk1@columbia.edu

Abstract

Follicle Stem Cells (FSCs) in the Drosophila melanogaster ovary are maintained through independent regulation of division and differentiation to become proliferative Follicle Cells (FCs) to their posterior or quiescent Escort Cells (ECs) to their anterior. These behaviors are guided by graded extracellular Hedgehog (Hh) and Wnt signals emanating from cells anterior to FSCs and an inverse gradient of JAK-STAT pathway activity. Here, we used lineage analyses to investigate the development of ECs, FSCs and FCs from a common set of precursors during pupation. Previous studies found that the most anterior precursors divide slowest, with quiescence spreading from the anterior over time to include all ECs, that FSCs are specified simply by their location at eclosion, and that the first FCs derive from cells that accumulate posterior to the developing germline over the first 48h of pupation. We now provide evidence that those accumulating cells derive from migration out of the developing germarium. We found that Wnt pathway activity favored conversion of precursors to more anterior adult derivatives (ECs rather than FCs), while JAK-STAT pathway activity favored posterior outcomes. Posterior bias and faster division, explored by altering Cyclin E activity, both favored a precursor becoming an FSC. Both JAK-STAT and Hh signaling could increase precursor division rate. All of these characteristics resemble regulation of adult FSC behavior. We suggest that similar signaling networks and division rate dependence during maintenance and development may be general features for stem cells that are specified in parallel with tissue development and that exhibit division-independent differentiation.

Article Summary

Drosophila ovarian Follicle Stem Cell (FSC) behavior and regulation by graded Hedgehog (Hh), Wnt and JAK-STAT signals is well understood, motivating us to study mechanisms guiding development of FSCs and the neighboring cell types they maintain. The marked progeny of single cells labeled at pupariation were compared in adults for lineages with genetic alterations affecting signal transduction. Wnt and JAK-STAT had strong opposing influences on the anterior-posterior location, and hence identity of derivatives, while JAK-STAT and Hh (via Yorkie) stimulated cell division. Conversion of precursors to FSCs was favored by higher division rates.

Introduction

Many adult tissues are maintained by adult stem cells (Clevers and Watt 2018; Post and Clevers 2019; Kalderon 2022; Gao *et al.* 2023; Beumer and Clevers 2024). The two universal stem cell behaviors of cell division and initiating differentiation at appropriate, balanced frequencies are inevitably regulated by their physical and signaling environment, often known as the stem cell niche (Voog and Jones 2010; Biteau *et al.* 2011; Losick *et al.* 2011). Moreover, the further differentiation of immediate stem cell derivatives is often guided by additional cues from the mature adult tissue. Thus, stem cell function depends on the nature and spatial organization of the stem cells themselves, neighboring niche cells and more distant cells guiding full differentiation. The behavior and regulation of different types of adult stem cell is being studied productively for several paradigms. By contrast, the developmental mechanisms that place an appropriate number of stem cells in a suitable niche and larger tissue context are largely unknown. Understanding that process would have the potential

benefit of facilitating the creation of self-sustaining organoids and exploring developmental abnormalities leading to impaired adult stem cell function or cancer susceptibility.

The Drosophila ovary is an excellent paradigm for studying the development of adult germline and somatic stem cells (Giedt and Tootle 2023; St Johnston 2023). Each adult ovary consists of 15-20 ovarioles, with an anterior germarium and a series of developing egg chambers of increasing maturity, with each ovariole producing a mature egg as often as every 12h (Fig. 1A) (Spradling *et al.* 1997; Duhart *et al.* 2017; Giedt and Tootle 2023). This formidable cell production is fueled by 2-3 Germline Stem Cells (GSCs) (Eliazer and Buszczak 2011) and about sixteen somatic Follicle Stem Cells (FSCs) (Reilein *et al.* 2017; Hayashi *et al.* 2020; Kalderon *et al.* 2021; Kalderon 2022). The known biology of these two types of stem cell includes numerous interesting contrasts. GSCs generally remain in place at the anterior of the germarium, are individually long-lived, maintained by single-cell asymmetry and depend on anti-differentiation signals from immediately adjacent niche cells (Cap cells) (Kahney *et al.* 2019; Zhang and Cai 2020; St Johnston 2023). The differentiation of the immediate "cystoblast" derivative of a GSC depends on interactions with non-dividing somatic Escort Cells (ECs) (Kirilly *et al.* 2011) during posterior migration and is manifest as a set of four synchronized divisions with incomplete cytokinesis through region 1 to form a sixteen-cell region 2 cyst.

FSC cell bodies reside principally in two adjacent rings along the anterior-posterior (A/P) axis, surrounding a central germline stage 2b cyst and bounded on the other side by the basement membrane lining the germarium (Fig. 1A) (Reilein *et al.* 2017; Kalderon 2022). FSCs can exchange A/P locations and move circumferentially. They are maintained by population asymmetry with independent cell division and differentiation, characterized by frequent and variable, apparently stochastic, loss and expansion of individual cell lineages (Reilein *et al.* 2017; Reilein *et al.* 2018; Kalderon 2022). This picture of FSC organization and behavior differs markedly from an earlier model as a result of more thorough investigation and discarding earlier expectations of single-cell asymmetry, which led to highlighting only a minority of all FSC lineages (Margolis and Spradling 1995; Kalderon 2022). FSCs are responsible for producing about six founder Follicle Cells (FCs) for each future egg chamber. A few of these FCs arrest division soon afterwards and form specialized polar cells at the anterior and posterior termini of each egg chamber, as well as adjacent stalk cells, which connect adjacent egg chambers and allow budding of an egg chamber from the germarium (Fig. 1A) (Grammont and Irvine 2001; Assa-Kunik *et al.* 2007; Dai *et al.* 2017). Other FCs continue division in growing egg chambers to form an expanding single-layer epithelium of about 650 cells by mid-oogenesis (stage 6). These FCs acquire different identities according to their location, guided by JAK-STAT signals produced in polar cells and EGFR-stimulating signals from the oocyte, initially at the posterior of the germline cyst, and then from the oocyte nucleus after migration to an anterior cortical location that defines the future dorsal aspect of a developing embryo (McGregor *et al.* 2002; Xi *et al.* 2003; Merkle *et al.* 2020; St Johnston 2023). FSCs also produce new ECs in adults, albeit at a much lower rate than FCs (Reilein *et al.* 2017; Melamed and Kalderon 2020). The A/P location and differentiation of FSCs are guided principally by long-range signals, emanating from the anterior (multiple Wnt ligands from Cap cells and ECs) and posterior (JAK-STAT ligand Unpaired from newly-differentiating polar cells) to produce inverse gradients of those pathway activities across the stem cell domain, effectively defining the A/P extent of the FSC domain (Reilein *et al.* 2017; Melamed and Kalderon 2020). JAK-STAT pathway activity also stimulates FSC division in a graded fashion (Melamed and Kalderon 2020; Melamed *et al.* 2023). Hedgehog pathway activity also stimulates FSC division but may not contribute to the spatial pattern of FSC division (Vied and Kalderon 2009; Huang and Kalderon 2014). Other factors supporting the much faster division of posterior FSCs remain to be identified. The division rate of posterior FSCs approximately matches the rate of their conversion to FCs, so the

exchange of FSCs between anterior and posterior layers is roughly at equilibrium (MELAMED *et al.* 2023).

During development, germline and somatic gonadal cells are specified separately in the embryo and coalesce after germ cell migration to form an embryonic gonad (BOYLE AND DINARDO 1995; MURRAY *et al.* 2010; JEMC 2011). During larval stages, the ovary develops from anterior to posterior (initially termed apical to basal), starting with the specification of somatic Terminal Filament (TF) cells, which resolve into separate intercalated stacks that seed each individual ovariole (GODT AND LASKI 1995; GILBOA 2015). A Notch signal from TF cells recruits adjacent cells from a pool of somatic cells (Intermingled Cells: ICs) intermingled with germ cells, to become quiescent Cap cells (WARD *et al.* 2006; SONG *et al.* 2007; PANCHAL *et al.* 2017; ZAMFIRESCU *et al.* 2022). Germ cells that contact Cap Cells become the future GSCs, with other germ cells, in more posterior locations, initiating differentiation soon afterwards (ZHU AND XIE 2003; ASAOKA AND LIN 2004; GANCZ *et al.* 2011; GANCZ AND GILBOA 2013). As Cap cells and GSCs form in third instar larvae, somatic Swarm Cells migrate basally (towards the future posterior) around the TF cells to separate sets of developing ICs and germ cells into individual units (BANISCH *et al.* 2021). Then, during pupation, germ cells sequentially mature (towards the posterior) into sixteen-cell cysts, while somatic ICs amplify. These IC precursors eventually become ECs, FSCs and FCs, such that the newly-eclosed adult has a mature germarium structure, followed by four egg chambers of increasing size, allowing egg-laying to commence within about a day (REILEIN *et al.* 2021).

The specification of different ovarian somatic cell types during pupation has been studied by lineage analyses and direct morphological observation, including live imaging, yielding three major conclusions. First, FSCs are not specified at a particular time during development; instead, single-cell lineages generally include ECs and FCs together with FSCs, with the latter defined simply by occupying the appropriate A/P locations at eclosion (REILEIN *et al.* 2021). Thus, in this paradigm, the stem cells are not set aside early in development but derive from the same process that forms the whole adult tissue. Another study had suggested separate precursors for ECs and FSCs at the start of pupation, based on lineage analysis initiated by two GAL4 drivers (*Con-GAL4* and *bond-GAL4*) together with temperature sensitive GAL80 (SLAIDINA *et al.* 2020). That suggestion was, however, based on assuming that the additional presence of marked ECs in most adult ovarioles with marked FSCs was due to the presence of two or more lineages. Sparse induction of cell lineages showed this explanation to be incorrect; FSC-containing single-cell lineages almost always included ECs, revealing a common origin (REILEIN *et al.* 2021). Moreover, using the same reagents, it was apparent that neither the frequency, nor the time of lineage initiation could be controlled satisfactorily using the temperature-sensitive GAL80 technique, contrasting with lineage initiation using a heat-shock to activate recombinase encoded by a *hs-flp* transgene (REILEIN *et al.* 2021). Second, anterior somatic cell precursors divide more slowly than posterior precursors and terminate division during pupation. This feature appears to limit the number of the most anterior derivatives, Escort Cells (REILEIN *et al.* 2021). Third, the formation of the first FCs and the first egg chamber is morphologically very different from the process in adults, where newly-formed FCs are adjacent to a germline cyst and that germline cyst is subsequently surrounded by a monolayer of FCs before budding from the posterior of the germarium. Instead, many somatic cells accumulate posterior to the germarium (harboring all germ cells) during the first half of pupation and are then invaded by a germline cyst released from the germarium and migrating a considerable distance towards the posterior (REILEIN *et al.* 2021).

We would like to understand what orchestrates the movements and proliferation of somatic cells during pupation required to adopt appropriate adult identities and assemble a morphologically normal adult ovariole. As a first step, we have investigated cell-autonomous responses of somatic

precursors to genetic alterations by using lineage analyses during pupation to measure final outcomes as ECs, FSCs and FCs. We began by investigating signals and cellular properties known to influence the behavior of adult FSCs. This includes examining signals instrumental to FSC maintenance and differentiation (Wnt and JAK-STAT), signals and effectors important for FSC division (JAK-STAT, Hedgehog (Hh) and Yorkie (Yki)), and the effect of cell division rate on cell fate (ZHANG AND KALDERON 2001; SONG AND XIE 2003; VIED AND KALDERON 2009; WANG AND KALDERON 2009; VIED *et al.* 2012; WANG *et al.* 2012; HUANG AND KALDERON 2014; WANG AND PAGE-MCCAW 2014; REILEIN *et al.* 2017; HAYASHI *et al.* 2020; MELAMED AND KALDERON 2020; MELAMED *et al.* 2023). Among adult FSCs, there is competition for residence in the FSC domain, with conversion of FSCs to FCs or ECs balanced by FSC amplification through cell division. Hence, maintenance and amplification of an individual FSC lineage is cell-autonomously favored by genetic alterations that either increase the division rate or reduce the frequency of differentiation (REILEIN *et al.* 2017; REILEIN *et al.* 2018). We found that this principle and the roles of Wnt and JAK-STAT signaling apply also to the pupal development of FSCs, while responses to Hh and Yki are at least partly shared for stem cell development and adult maintenance. A key source of anterior signals (Wnt, Hh) is present at the start of pupal development. The original source of the ligand activating the JAK-STAT pathway, which guides FC formation from the start of pupation, is not defined but likely has a posterior bias; the major source, which instructs a robust gradient of pathway activity, emerges after the first egg chamber forms midway through pupation. These experimental findings and their rationalization suggest principles that may be shared generally among adult stem cells with division-independent differentiation that is guided by location: early establishment of niche signaling centers, continuous competition between division and differentiation for an individual cell to become or remain a stem cell, and regulation of division and cell location by the same signaling networks during adult stem cell development and maintenance.

Materials and Methods

Clone induction via MARCM

GFP-marked MARCM clones (LEE AND LUO 2001) were induced on different chromosome arms (2L, 2R, and 3R) using flies of the genotypes listed below ("X" and "Y" identities are listed subsequently; "*>*" indicates an FRT element, "*tub*" refers to the *αtub84B* promoter (LEE AND LUO 2001) and "*act*" to the *act5C* promoter (PIGNONI AND ZIPURSKY 1997)). In all cases, recombination is initiated at *FRT* sites by heat-shock induction of FLP recombinase, leading to marked clones lacking a *Gal80* transgene and expressing *UAS-GFP* from *tub-GAL4* and *act>GAL4* drivers. Simultaneously, a recessive allele ("X") becomes homozygous or a transgene ("*UAS-(Y)*") initiates expression, or both, or neither (controls).

(2L) *hs-FLP UAS-nGFP tub-Gal4*; *(X) FRT40A/tub-Gal80 FRT 40A*; *UAS-(Y)/act > CD2 > GAL4*
(2R) *hs-FLP UAS-nGFP tub-Gal4*; *FRT42D (X) / FRT 42D tub-Gal80*; *UAS-(Y)/act > CD2 > GAL4*
(3R) *hs-FLP UAS-nGFP tub-Gal4*; *+ / act > CD2 > GAL4, UAS-GFP*; *FRT 82B (X) / FRT 82B tub-Gal80*.

Studies conducted at 29C utilized flies of the genotype below (where an additional *act-GAL80* element on 2R is necessary to silence GAL4):

200 (2R) *hs-FLP UAS-nGFP tub-Gal4*; *FRT42D (X) / FRT 42D act-Gal80 tub-Gal80*; *UAS-(Y)/act > CD2 > GAL4*.
201
202 For 2L chromosome studies, (X) included *NM* (control), $cycE^{wx}$, smo^{2}, $pka\text{-}C1^{H2}$, smo^{2} $pka\text{-}C1^{H2}$,
203 $cutlet^{4.5.43}$, and (Y) included *DIAP1*, *CycE*, Yki^{S168A}; also, a $Su(fu)^{LP}$/ $Su(fu)^{LP}$ background was used for
204 *smo pka* clones.
205 For 2R chromosome studies, (X) included *sha* (control), ptc^{S2}, arr^{2}, yki^{B5}, ptc^{S2} yki^{B5}, $hpo^{42\text{-}47}$ and (Y)
206 included *Hop* together with *UAS-Dap*, as well as a *tub-yki* transgene that does not include the *UAS*
207 promoter.
208 For 3R chromosome studies, (X) includes *NM* (control), $apc1^{1}$ $apc2^{2}$, axn^{E77}, $kibra^{del}$, wts^{x1}, and
209 $stat^{85C9}$.
210
211 **Lineage analysis by MARCM in newly-eclosed flies**
212
213 From the time that pre-mated adults were put into a fresh vial (for 24h or less) to eclosion of the first
214 several adult progeny, sufficient for analysis, was most commonly 11 days (Reilein *et al.* 2021). Timing
215 of heat shocks to initiate lineages was determined with this 11-day course in mind. The larval-to-
216 pupal transition, where third-instar larvae are crawling up the sides of the vial and beginning
217 puparium formation, was generally 5 days before eclosion. Hence, adults collected 5d after heat-
218 shock were considered to have lineages initiated at pupariation ("0h APF"). At the time of heat-shock
219 (generally 6d after parents were first added to the vial), some animals were at pupariation; others
220 were slightly more advanced or delayed. Vials were cleared of any eclosed adults the evening before
221 collecting newly-eclosed adults over a period of no more than 6h centered on 120h after heat-shock.
222 Similar procedures were used for collection of adults with lineages designated as initiated 2 days
223 prior to pupariation ("-2d APF": heat-shock 4d after introducing parents; collect adult progeny over
224 6h, centered on 168h after heat-shock) and 36h after pupariation ("36h APF": heat-shock 7.5d after
225 introducing parents; collect adult progeny over 6h, centered on 84h after heat-shock). Vials were
226 heat shocked at 33C for 12 min (0h APF, 36h APF) or 20 min (-48h APF). These conditions were
227 chosen as the mildest conditions consistently inducing a similar yield of marked lineages at 0h APF, so
228 that many ovarioles would harbor a single marked lineage. To achieve a similar result, a longer period
229 of heat-shock was used at -48h APF because fewer precursors are present. Afterwards, vials were
230 incubated at 25C or 29C. Higher temperature increases GAL4 activity and was used for expression
231 of *UAS-Hop* and controls for that test (analogous tests in adult ovaries showed that 29C is necessary
232 to achieve strong activation of the JAK-STAT pathway (Melamed and Kalderon 2020)); all other flies
233 were incubated at 25C or room temperature (23C-25C). Flies were dissected on the day of eclosion
234 (0d).
235
236 **Adult ovary fixation and staining**
237
238 Adults were dissected in PBS using forceps by separating the entire posterior region of the abdomen,
239 revealing the ovaries within. Non-ovary material, such as fat bodies and other organs, was gently
240 shaken or teased out with forceps, and the ovaries (still attached to the cuticle) were transferred
241 using forceps to tubes containing 400 µl fixative. Ovaries were fixed in 4% paraformaldehyde in PBS
242 for 10 min at room temperature, rinsed 3x in PBS with 0.1% Triton and 0.05% Tween-20 (PBST), and
243 blocked in 10% normal goat serum (Jackson ImmunoResearch Laboratories) in PBST. Ovarioles were
244 incubated in primary antibody for 1 hr. Ovarioles were rinsed in PBST 3x and incubated for 1 hr in
245 secondary antibodies diluted 1:1000. Ovaries were rinsed 2x in PBST and 1x in PBS for 5 min each.
246 Ovaries were transferred using a p1000 with the narrow portion of the tip cut off to a well containing

PBS. The cuticle was then separated from the ovaries, which were transferred using forceps to a slide containing a drop of PBS. Each slide accommodates two drops, and each drop contained the ovaries from one individual animal. Ovaries were gently teased apart with extra sharp forceps, separating into clusters of 1-4 ovarioles, taking care to ensure that entire ovarioles remained intact and did not separate, as tracing the clones throughout the entire ovariole is crucial. After separation was complete, 25 µl of Flouromount-DAPI was applied to a coverslip and carefully placed over the portion of the slide with each sample.

Immunohistochemistry

Monoclonal antibodies against Fasciclin III (Fas3) and Vasa were obtained from the Developmental Studies Hybridoma Bank, created by the NICHD of the NIH and maintained at The University of Iowa, Department of Biology, Iowa City, Iowa 52242. 7G10 anti-Fasciclin III was deposited to the DSHB by C. Goodman, and was used at 1:250. Anti-Vasa (used at 1:10) was deposited by A. C. Spradling/D. Williams and used for staining adult ovaries. For pupal ovaries, the monoclonal rat anti-Vasa was not effective and instead rabbit anti-Vasa (gift from R. Lehmann, MIT) was used. Other primary antibodies used were anti-GFP (A6455, Molecular Probes) at 1:1,000; and goat FITC-anti-GFP (Abcam ab6662) at 1:400. Secondary antibodies were Alexa-488, Alexa-546, Alexa-594 or Alexa-647 from Molecular Probes. DAPI-Fluoromount-G (Southern Biotech) was used as mounting medium for all experiments. Images were collected with a Zeiss LSM700 or LSM800 laser scanning confocal microscope (Zeiss) using a 63x 1.4 N.A. lens.

Scoring and Analysis of marked lineages in adult ovaries

Ovaries were stained using antibodies to Vasa, Fas3 and GFP. Vasa staining assists in classifying cysts of regions 1 (fewer than 16 cells) versus regions 2a and 2b (16-cell cysts). The anterior border of strong Fas3 expression corresponds to the border between FSCs and FCs, with cells immediately adjacent and anterior to this boundary, together with their immediate anterior neighbors (three rings of cells anterior to the boundary of strong Fas3 staining), classified as FSCs. Escort cells were scored as r1 or r2a based on measurements that were performed with wild-type ovaries to determine the lengths of these regions. We previously examined EdU incorporation in ovaries of newly -eclosed flies and measured the distance from cap cells to the end of region 1 as determined by the presence of cysts that incorporated EdU. Region 1 cysts are going through mitosis and Region 2a cysts have the complete complement of 16 germ cells. The length ratio of regions 1:2a is about 3:1 in newly-eclosed adults. To measure the percentage of each terminal egg chamber covered by marked FCs, the ratio of GFP-marked cells to unmarked cells (stained with DAPI) was estimated throughout all z-sections. The total number of ovarioles containing any GFP-positive cells (“clones” or “lineages”) was recorded, along with the total number of ovarioles, for each coverslip, which has a pair of ovaries from one animal. Each ovariole was scored for GFP-positive cells by counting the number of r1 ECs, r2a ECs, and FSCs. FCs were scored for presence (yes or no) in the following regions: “Immediate Daughter” (region 2b), “Germarium” (region 3), “1”, “2”, “3”, or “4” (corresponding to the four egg chambers typically present in ovaries of newly-eclosed flies; sometimes “5” also), and “BS” (Basal Stalk; a cluster of about 10 cells around the polar cells at the posterior of the terminal, most mature, egg chamber). Notes were also added if labeled cells of a specific genotype were present at unusual frequencies in certain locations, including polar cells and stalk cells. Each scored ovariole was then labeled with its broad clone type (EC, EC/FSC, EC/FSC/FC, EC/FC, FSC, FSC/FC, or FC). This classification, together with the exact number of GFP-labeled r1 and r2a ECs, FSCs, and the presence or absence of FCs in the

regions listed above, was recorded in each row of a spreadsheet for a given genotype in an experiment. For each genotype in an experiment, we aimed to score at least 50 marked ovarioles across at least three coverslips. The data from each such spreadsheet were aggregated in order to measure several parameters, as described in the next section.

Estimating single-cell lineage outcomes underlying raw observations

Although we used a mild and brief heat-shock in order to induce only low activity of a *hs-flp* transgene, it is inevitable that some adult ovarioles will include lineages from more than one marked precursor. Previously, two methods were considered for estimating single-cell lineage outcomes from raw observations (Reilein *et al.* 2021). One assumed that every marking event is independent (zero-clone frequency method, below). Another used information about the frequency of ovarioles with marked ECs and FCs (but no marked FSCs) as a likely indicator of the presence of more than one lineage. For wild-type lineages, the latter method (of the two) indicated a higher frequency of ovarioles with more than one lineage for a given sample, and was the preferred method (because we believed it to be more accurate). Here, that method cannot be used because different genotypes may greatly alter EC and FC frequencies, as well as producing single lineages with only marked ECs and FCs (from selective loss of prospective FSCs). Past experience suggested that the "zero-clone" frequency method used here will underestimate the number of ovarioles with more than one lineage. An indicator of that potential error is the proportion of deduced single-cell lineages with only EC and FCs; the average frequency of that lineage category was 5% for controls. However, during the course of the studies reported here we learned that lineages with just ECs and FCs can arise from loss of FSCs from a single EC/FSC/FC lineage rather than representing simultaneous EC-only and FC-only lineages. Thus, the error in estimating single-cell lineage frequency and composition by the method described below is less than initially anticipated and overestimated by the EC/FC frequency.

Zero-clone frequency method

We assume all marking events are independent and use binomial calculations to derive the expected frequency of ovarioles with 1 and 2 lineages by deriving the probability of a recombination event in each precursor cell.
Although we need to use an estimate of the total number of cells present at the time of recombination, the numerical outcomes are not very sensitive to this exact number.
From prior published work (Reilein *et al.* 2021), lineage data estimated 24 or 17 precursor cells at pupariation (different experiments and labeling techniques). The number of precursor cells directly observed was 38 at 12h APF and 51 at 24h APF. This leads to an estimated number at 0h APF (assuming similar expansion from 0-12h and 12-24h APF) of 38 x 38/51= 28 cells
Since MARCM (the same technique used here) was used to deduce 24 precursors, we use that number.

If the frequency of ovarioles with no marked cells = f and p is the probability of recombination in a single cell,
$f = (1-p)^{24}$
The proportion of ovarioles with a single clone will be $24p(1-p)^{23} = f(24p)/(1-p)$.
Hence, the frequency of single-cell clones among labeled ovarioles = $f(24p)/((1-p)(1-f))$.
The frequency of ovarioles with 3 or more clones (estimated by this method) will likely be <20% of remaining ovarioles. Hence, we approximate, for simplicity, that all of the remaining ovarioles (non-

zero and non-single cell clones) contain two clones. We also round up to a whole number for the estimated percentages of ovarioles with zero, 1 or 2 lineages (adding to 100).

For lineages induced 48h before pupariation, we previously estimated there might be 10 precursor cells.
So, $f = (1-p)^{10}$
and the frequency of single-cell clones among labeled ovarioles = $f(10p)/((1-p)(1-f))$.

Estimating single-cell lineage type frequencies

After establishing the estimated number of ovarioles with one and two lineages for a given experimental sample, we deduce the total number of single-cell lineages present and then estimate the fraction of those of specific types. The major types are outlined first and then sub-divisions are brought in.

We start with raw data of major phenotypes: EC, EC/FSC, FSC, FC, EC+FC
Single-cell clone frequencies are named: EC(q), EC/FSC (r), FSC(s), FC (t), EC+FC(m)
Single lineage frequency = p1, two-lineage frequency = p2

Observed EC only = $q.p1 + q^2.p2 = q^2.p2 + q.p1$
Hence, we can calculate q directly

Observed FC only = $t.p1 + t^2.p2 = t^2.p2 + t.p1$
Hence, we can calculate t directly

Observed FSC only = $s.p1 + s^2.p2 + 2s.t.p2 = s^2.p2 + s(p1+2.t.p2)$

Observed EC+FC = $m.p1 + m^2.p2 + 2.p2.m(q+t) + 2.p2.q.t$
$= m^2.p2 + m\ (p1+2.p2.\ (q+t)) + 2.p2.q.t$

Observed EC/FSC = $1- (q+s+t+m)$

Then, for r1 (a) and terminal FCs (z)
Observed r1 only = $a.p1 + a^2.p2 = a^2.p2 + a.p1$

Observed “Terminal FC only” = $z.p1 + z^2.p2 = z^2.p2 + z.p1$
Note- here, “Terminal FC only” means there are marked cells in the terminal egg chamber and there are no marked cells other than FCs.

r1 ECs + FC (b) and EC + terminal FC only (y) can also be inferred.

Observed r1+FC = $b.p1 + b^2.p2 + 2.p2.b(q+t) + 2.p2.a.t$
$= b^2.p2 + b\ (p1 + 2.p2\ (q+t)) + 2.p2.a.t$

Observed EC + terminal FC only = $y.p1 + y^2.p2 + 2.p2.y(q+t) + 2.p2.q.z$
$= y^2.p2 + y\ (p1 + 2.p2\ (q+t)) + 2.p2.q.z$

The above two equations exclude EC + FC with no r1 only or terminal FCs but that is a very small error.

For "only Term FC", x, meaning no marked cells (even FCs) anterior to the penultimate egg chamber, and a similar category of EC + only Terminal FC, w, there are analogous equations.

Observed "only Terminal FC" = $x.p1 + x^2.p2 = x^2.p2 + x.p1$

Observed EC+ only Terminal FC = $w.p1 + w^2.p2 + 2.p2.w(q+x) + 2.p2.q.x$
$= w^2.p2 + w\ (p1 + 2.p2\ (q+x)) + 2.p2.q.x$

Added categories

(a) "Normalized" numbers to acknowledge that EC+FC category sometimes includes an EC-only and an FC-only lineage.

We acknowledge that the zero-clone frequency method might underestimate multiple clone frequency. Hence, the EC+FC category may include some EC-only and FC-only clones.
However, it is (i) reasonable that some prospective FSCs might be lost for WT from EC/FSC/FC lineages to give EC+FC lineages, (ii) genotypes with reduced division rate may cause selective loss of FSCs (this work), converting prospective EC/FSC/FC to EC+FC lineages. This may also occur to a degree for all genotypes. So, taking EC+FC as possibly composite (2 lineages) should be avoided if there is a division defect and is likely an overestimate of composite clones in all cases.

Method: assume all EC+FC (fraction m) are really single EC and single FC clones. Hence, m is added to EC-only & FC-only proportions (same for EC+FC specifically with term FCs or r1 ECs) and the total clone number is multiplied by (1+m) to give "normalized" EC and FC values.
These values appear in supplementary spreadsheets but are not discussed in the text.

(b) Clones with any terminal FC or r1 EC representation.

This is useful for considering cell allocation to the most extreme A/P locations (independent of other issues).
After deriving single-cell lineage frequencies,
Observed raw # of ovarioles with marked terminal FCs = "ObsTerm"
Raw ovarioles with clones = x
Deduced fraction of ovarioles with two lineages = f
Fraction of single-cell lineages with marked terminal FCs = T

$ObsTerm = x(1-f)T + xf(T^2+2T(1-T))$
$= xT-xfT+xfT^2+2xfT-2xfT^2$
$= T(x+xf)-T^2xf$

$(xf)T^2 – x(1+f)T + ObsTerm = 0$

Quadratic solution = $((x(1+f)-SQRT[(x+xf)^2-4xf.ObsTerm]))/(2xf)$

Same for r1, using Obsr1 to calculate R

Criticisms/shortcomings

If clone frequency varies more from fly to fly than ovariole to ovariole (within the same fly), then these corrections ought theoretically to be applied to each fly/coverslip. However, this is impractical (the methods cannot work well when n is low). To minimize this deficiency, it is best if all scored coverslips have roughly similar clone frequencies. We therefore instituted the criterion that coverslips (containing ovaries from a single fly) scored for clone phenotypes should have ovarioles with labeled cells at a frequency of 75% or lower (there were one or two experiments where we included coverslips with higher frequencies because there was no choice). We also instituted a minimum clone frequency of 15%. This was for two reasons. First, so that all clone frequencies were in a narrower range, so that errors due to single-cell lineage estimations would not vary widely among samples. Second, we had observed previously that there is occasional cell marking in the absence of deliberate heat-shock. Such lineages arise at unknown times (if originating from recombination; most appear to be single EC marks of unknown origin). Such background is less than 5% and has minimal impact if deliberately-induced lineages are prevalent. For controls, the average frequency of marked ovarioles scored was 42% at pupariation and 63% 48h before pupariation.
Because any error in single-cell lineage estimations likely depends on clone frequency, we experimented with splitting each control sample into two of similar number, with the lowest lineage frequency flies segregated from the highest lineage frequency flies. We processed the data separately and then aggregated. The final outcomes were almost identical, so we treated all fly ovaries from one experiment as a single batch for single-cell lineage estimations.

Terminal FC labeling with or without other FCs

"Only terminal FC" means labeled cells in the basal stalk and/or terminal egg chamber (which may extend to the penultimate egg chamber) but nowhere else in the ovariole.
"FC-only with terminal FCs" includes the category above, but also includes lineages with terminal FCs and additional FCs anterior to the penultimate egg chamber, but no ECs or FSCs.
Subtracting the category above from "FC-only" gives the FC-only lineages that do not include any labeled terminal FCs.
Thus, within the FC-only category, frequencies can be derived for only Terminal FCs, no terminal FCs, and a mix of terminal and non-terminal FCs.
These calculations were performed only for control lineages in order to determine if there were common precursors of FCs of terminal and non-terminal egg chambers.

Cells per clone: EC-only lineages

We considered only EC-only, and not EC+FC, raw data because some of the latter may derive from EC/FSC/FC clones that have lost FSCs.
We calculated raw ECs per EC-only clone (and used the same principle for r1 ECs only) and multiplied by the ratio of raw EC-only clone frequency to calculate single-clone EC-only frequency. Because this is a derived number, we use raw observations of EC number in EC-only clones to estimate standard deviation (and then, standard error).

Cells per clone: EC/FSC/(FC) lineages

Single-cell EC/FSC clones will all be within this raw data category. This is an inclusive category- most clones have FCs but those without FCs are also included. However, (a) such clones in raw data will sometimes also include an EC-only or an FSC-only clone and (b) the correct number of EC/FSC clones deduced by single-cell lineage estimations should be used.

Single-clone EC/FSC frequency = r

Observed EC/FSC = $r.p1 + r^2.p2 + 2.p2.r.(q+m) + 2.p2.r.s + 2.p2.(q+m).s$

(a) Subtractions from total counted cells

Additional ECs come from EC only clones at (average cells per EC-only clone)(total number of single clones= actual clone number plus deduced number of double-clones)(2p2.(q+m).r)

Additional ECs come from EC only clones at (average cells per EC-only clone)(total number of single clones= actual clone number plus deduced number of double-clones)(2p2.s.r)

(b) Total number of single-cell EC/FSC clones in observed EC/FSC samples

= r. total number of single-cell clones in sample

= r. total clones in sample (1+p2)

Because the final estimates are derived numbers, we use raw observations of EC and FSC number in EC/FSC clones to estimate standard deviation (and then, standard error)

All of the above calculations are in the supplementary spreadsheet that includes all samples for lineages induced at different times: “Single-cell 0hAPF calculations” and “Single-cell -2dAPF calculations”.

Evaluation of Controls

Expected variability

If we assume that we are examining single-cell clones and that the chance of hitting each type (location) of cell in a given developing ovariole is independent (and given by the average frequency of that clone type (p) in a sample with n single clones), we expect to see a binomial distribution of the frequency of outcome p.

We therefore calculated the “expected” SEM for this process for each average frequency of lineage category over all 12 controls for lineages induced at pupariation. For binomial distributions the expected standard deviation= SQRT[np(1-p)]

We also calculated the observed SEM among the 12 individual values for each category.

The ratio of the two values (observed/expected) was mostly in the range of 1-2, consistent with the random sampling (by recombination events) of the starting A/P location of precursors being a major contributor to variation.

These data are presented in the supplementary spreadsheet “0h APF Controls Variation”.

Significant Differences

The significance of differences for the frequency of a specific type of lineage for an experimental sample versus controls was estimated using Fisher’s exact two-tailed test. The data on the spreadsheets described above was copied (as values) on to separate spreadsheets to add some extra summary categories. Calculated p values (from an online calculator) were then added when these

were either very low or of importance to acknowledge as not being low (i.e., values above 0.05 were generally not entered). Altogether, we tested the following types of condition as both reduced or increased by genetic manipulation- cell division rate, Wnt signaling, JAK-STAT signaling, Yki activity, and Hedgehog signaling, translating to 10 broad conditions. It may therefore be of special interest to know when p values are below 0.05 and below 0.005, so we designated those values by "*" and "**" in graphs. Supplementary spreadsheets with these p values are named "0h APF Significance Fisher" and "-2d APF Significance Fisher".

Inferring clone types, FSC and EC numbers in newly-eclosed adults from scoring 2d-old adults

In order to make quantitative conclusions about the developmental process up to eclosion from scoring clonal outcomes in 2d-old adults we made the following assumptions and adjustments. We assumed that EC numbers and locations did not change during this 2d interval because ECs generally appear to be quite long-lived. ECs are, however, produced from FSCs during adulthood, so it is likely that a small number of marked ECs scored at +2d were produced from FSCs after eclosion. The proportion of marked ECs arising from FSCs is very likely small based on known rates of FSC conversion to ECs and the observed high frequency of FSC clones with no ECs (44%) from control -2d samples. Individual marked FSCs can be lost, mainly by becoming FCs, or amplified at high rates during adulthood. If one or more marked FSCs were present at 0d but became FCs by +2d those marked FCs would reside around the two germarial cysts or in the two youngest egg chambers because egg chambers bud roughly every 12h, allowing four cycles of FC recruitment over 2d. We therefore scored an ovariole as containing an FSC clone (FSC-only or FSC/EC, according to EC content) if there were any marked FCs up to and including the second egg chamber, even if there were no marked FSCs at +2d. In those cases, we scored the number of marked FSCs as zero. On average, the number of marked FSCs should remain constant from 0d to +2d, so we should obtain a very good estimation of FSC numbers at 0d by scoring the numbers of marked FSCs at +2d, provided we include all examples where marked FSCs were lost altogether as containing zero FSCs. By using these guidelines, we could surmise the exact number of different types of lineage at 0d and the exact number of constituent ECs and FSCs from data collected by scoring clones in 2d-old adults.

Dissection and staining of pupal ovaries

Pupae were removed from the vial wall by adding a drop of water and transferred with forceps into a well of a Corning PYREX glass spot plate (Corning, cat. no. 7220–85) containing either PBS or 4% paraformaldehyde solution with care taken not to damage or pierce the posterior end of the pupa. If the dissection was done in fixative solution, it could take no longer than 10 min (ovaries were rocked in clean fixative for a minimum of 15 min, but for no longer than 30 min). Ovaries from 72h APF and older had fewer tears in them when dissected directly into fixative. Using a dissecting microscope, pupae were held against the bottom of the well using forceps and the posterior tip was cut off using Vannas Spring Scissors (2.5mm straight edge, Fine Science Tools, Foster City, CA, item number 15000-08) about a third of the way in from the posterior end. The anterior part of the pupa was removed to a discard well. The posterior end was searched for ovaries (clear, spherical, striated structures) by gently dislodging fat tissue surrounding the ovaries so as not to cloud the well with debris. This was done by gently tearing apart the contents of the pupal case or swirling them in the well using two pairs of forceps. As soon as they were spotted, ovaries were transferred to a new well of fixative by the following process. A 20µl pipette tip with a pipettor set to 20µl was coated in 10% Normal Goat Serum (NGS) by pipetting up and down several times. The pipettor was set to 5µl to

573 pipette up the ovary from the dissection well to transfer into the fixative well. Ovaries were fixed by
574 rocking in the well for 15 min at room temperature. Fixative (and all liquid in subsequent steps) was
575 removed in either of two ways: with a 1000µl pipette set to 270µl to slowly and carefully pipette up
576 the liquid; or, using the same method to transfer ovaries above, with a 20µl pipette tip with a
577 pipettor set to 20µl, which was coated in 10% Normal Goat Serum (NGS) by pipetting up and down
578 several times. The pipettor was set to 5µl to pipette up the ovary from the fixative well to transfer
579 into a fresh well with PBST. Ovaries were rinsed 3x in 2% PBST 0.5% Tween solution for 5, 10, and 45
580 min at 4C by rocking very slowly in a horizontal plane. The glass dissection dish was covered with a
581 large pipette tip box. Ovaries were rinsed for 30-60 min in 10% NGS solution at 4C, and then rocked
582 gently in primary antibody overnight. Ovaries were rinsed 3x with 0.5% PBST and then incubated for
583 1 hour (covered, cold room, rocker set on 2) in secondary antibody diluted 1:1000 with 0.5% Triton.
584 Ovaries were rinsed 2x with 0.5% PBST and 1x with PBS. To mount ovaries, a 20µl pipette tip coated
585 in 10% NGS solution, as described above, was set to 5µl and used to capture the ovary and transfer to
586 a glass slide. 20-25µl of DAPI Fluoromount was added to a coverslip, and then placed on top of the
587 slide with the ovaries. Care was taken to avoid pressing the coverslip and potentially disfiguring the
588 mounted ovaries. In some studies of older pupal ovaries, specifically 72h APF and onwards, forceps
589 were used to gently tear apart the ovarioles to separate germaria for clearer imaging. A sharpie was
590 used to draw arrows to mark the location of the ovaries on the coverslip.
591
592 **Staging of pupae (Fz3-RFP experiments)**
593
594 Third-instar larvae were sorted to select females, transferred to a vial with food and checked every
595 hour to mark the time each individual developed into a puparium (white, but immobile, with small
596 anterior spiracles). This time is 0 hours APF (after puparium formation). We found that keeping
597 animals in the light at night and in the dark during the day on a 12h/12h cycle, allowed more of them
598 to pupate during the daytime. We used a programmable outlet timer (Nearpow) together with a
599 manual LED soft white nightlight (Energizer cat. 37099) installed in a dark incubator at 25C.
600
601 **Imaging and quantitation of Fz3-RFP profiles**
602
603 Fz3-RFP flies (made by Ramanuj DasGupta, Genome Institute of Singapore and a gift from Erika Bach,
604 NYU, USA) were dissected and stained for Fas3 and DAPI. Ovaries were imaged with a 63 × 1.4 N.A
605 lens on a Zeiss LSM 800 confocal microscope (Carl Zeiss). Zeiss Zen Blue was used to acquire
606 microscope images of 1024x1024 pixels at 16-bit depth with line averaging 2. Zeiss Zen was used to
607 measure the intensity of RFP in cells along an edge of a germarium in a line starting adjacent to Cap
608 cells and ending at the border of Fas3 expression. Measurements were taken in 5 µm distance
609 increments within a z-stack range that did not exceed 8 µm. If there was more than one cell within
610 the same 5 µm increment, both cells would be measured. If there was no suitable cell within the 8
611 µm z-stack range at a specific 5 µm increment, no measurement was collected. Fz3-RFP intensities
612 were measured by circling the nucleus of a cell in the DAPI channel using the spline contour tool and
613 obtaining the average intensity value in the 561nm channel for the enclosed area from the Z-stack
614 with the highest RFP intensity. The 561nm laser intensity was set at 1.1% for 21-36h APF germaria
615 and reduced to 0.3% beginning at 48h-APF through adult in order to keep RFP within the linear range.
616 Because overall RFP levels varied from germarium to germarium, individual RFP profiles were
617 constructed for each germarium; RFP intensities for each germarium were normalized to the
618 brightest cell on the edge of that gemarium. Normalized intensities were then averaged for each time
619 point. In order to reflect the relative RFP brightness from 27h to 36h-APF, the averaged, normalized

values were divided by the laser intensity at which they were taken. The averaged normalized values for every distance along the 27h-APF and 36-APF curves were divided by 1.1. The averaged normalized values for every distance along the 48h-APF, 60h-APF, and adult-stage curves were divided by 0.3. The 27h-APF, 36h-APF, 48h-APF, 60h-APF, and adult were then normalized to the highest value in all of the graphs to reflect relative intensities and display the gradient profiles. Because the 21h-36h germaria were necessarily acquired with a higher laser intensity, output levels in Photoshop were reduced from 255 to 100 to indicate the greatly reduced RFP intensity of those samples. The distances from Cap cells to the border of strong Fas3 expression on the edge of the germarium and to the posterior end of the germline in the center of the germarium were also measured for every germarium and averaged for each time-point.

Results

Cell lineage methods and analysis

The cell-autonomous effects of genetic alterations on cell fate can generally be studied by comparing outcomes for marked cells, with or without a genetic alteration, over the relevant developmental period. Here, we are interested in examining all somatic cells of an ovariole from pupariation (when mature third instar larvae cease movements) to adulthood. We therefore induced FRT-catalyzed recombination events to mark and modify any ovarian somatic cell at a chosen developmental stage by using a heat-shock inducible Flp recombinase transgene. Prior studies using this approach for wild-type cells suggested that the number and identity of adult somatic cells in a marked lineage depends principally on the A/P location of the marked precursor at pupariation (Reilein *et al.* 2021). Anterior precursors become ECs, posterior precursors become FCs, and precursors in intermediate locations produce mixed lineages that include ECs, FSCs and FCs (Fig. 1A). Moreover, posterior precursors divide faster and, unlike EC-only precursors, they do not cease division during pupation (Reilein *et al.* 2021). Here, we use equivalent lineage studies with specific genetic alterations to identify factors that guide patterned cell division, differentiation of FCs during pupation, and anterior-posterior (A/P) migration of somatic ovarian precursors, which dictates EC and FSC fates in the adult germarium. There are, however, some significant technical challenges and limitations.

First, the marked cells in a single adult ovariole ideally derive from a single precursor within a pool of about two dozen precursors at pupariation. We therefore used a very mild heat-shock protocol, carefully administered for uniformity, to induce mitotic recombination in a MARCM (Mosaic Analysis with a Repressible Marker) strategy (Lee and Luo 2001). In practice, this generally leads to about 30-50% of all ovarioles with at least one labeled cell (Fig. 1B). Some of these ovarioles will, however, include derivatives of two or more initially marked cells. We therefore estimated this fraction from the percentage of unlabeled ovarioles by assuming that all recombination events are independent, and we then inferred the frequency and composition of single-cell lineages (see Methods). An example of the results of this conversion of raw data to deduced single-cell lineage data is shown for a control sample (Fig. 1C). In all other presented data, only the deduced single-cell lineage data are shown (with sample numbers in figure legends referring to raw data; all raw data and conversion details are in supplementary data spreadsheets).

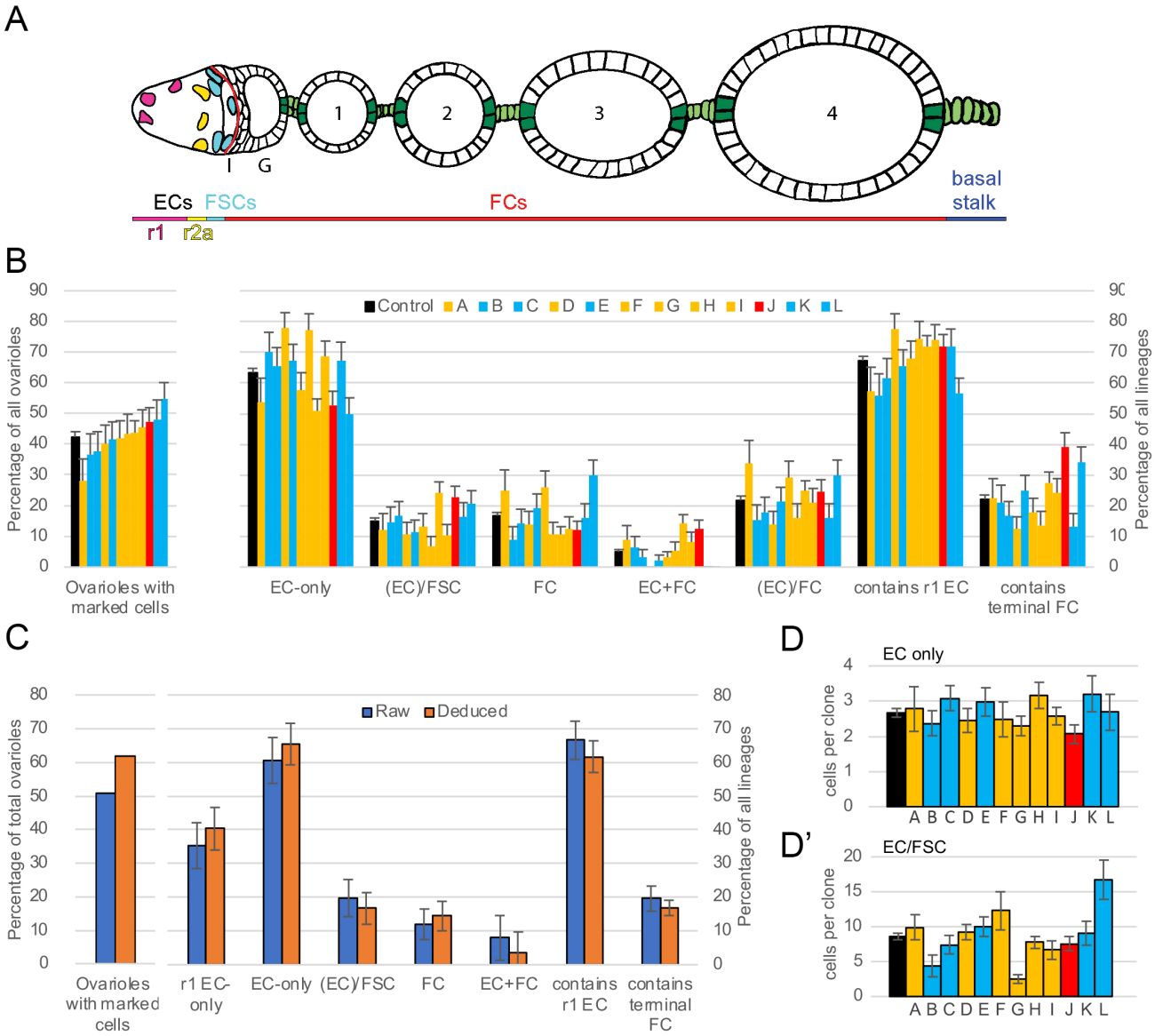

Figure 1: Estimation of single-cell lineage outcomes and cell numbers in control samples.
(A) Illustration of somatic cells of an ovariole in a newly-eclosed fly. The germarium (anterior, left) produces budded egg chambers (posterior, right), four of which (numbered 1-4) are typically present in each ovariole in a newly-eclosed fly. Escort Cells (ECs) are divided according to their location, as region 1 (r1: magenta) and region 2a (r2a: yellow). FSCs (cyan) reside principally in two A/P rings, just anterior to the anterior border of strong Fas3 cell surface expression ("Fas3 border": red line). FCs (mostly without a filled color), posterior to the Fas3 border, are classified by their location: Immediate (Region 2b, I), Germarium (Region 3, G), egg chamber 1, 2, 3, and 4. Specialized FC sub-types colored are polar cells (dark green), stalk cells (light green) and basal stalk cells (light green). **(B)** MARCM controls from 12 experiments, analyzed in newly-eclosed flies after 0h APF clone induction. Colors indicate the recombinant FRT site: 40A (yellow), 42D (blue), 82B (red). Black is the non-weighted average of all control values. The first cluster reports the percentage of all ovarioles with any marked cells. The number of marked ovarioles ranged from 36 to 121 (36, 41, 51, 54, 58, 56, 48, 121, 62, 98, 49, 65, respectively) and the total number of ovarioles from 102 to 277 (128, 112, 135, 135, 140, 134, 111, 277, 136, 207, 102, 119, respectively). Other clusters report the deduced frequency of the named lineage categories among marked lineages after estimating single-cell lineage frequencies (see methods). The number of FSC-containing lineages without ECs is generally very low and is therefore combined with lineages containing ECs and FSCs (written as (EC)/FSC); almost all of these lineages also contain marked FCs. Ovarioles with ECs and FCs but no FSCs are thought mostly to contain two lineages. The EC+FC category therefore gives an indication of the limitations of the method used to convert raw data to estimates of single-cell lineages. Here, the (EC+FC) and FC-only frequencies have also been added to give the

(EC)/FC category. The final two clusters show the percentage of all lineages that includes at least one marked r1 EC or terminal FC. **(C)** An individual control from (**B**) (control C, third control) to show raw values (blue) compared to deduced single-cell lineage values (orange). **(D, D')** Deduced average number of **(D)** cells per EC-only clone (total cell number: 54, 68, 103, 103, 116, 80, 85, 195, 110, 107, 106, 87, respectively) and **(D')** EC plus FSC cells in EC/FSC clones (total EC + FSC cell number: 40, 24, 79, 56, 71, 116, 12, 266, 58, 194, 85, 281, respectively; the number of EC/FSC lineages for samples B and G are notably low) for all MARCM controls analyzed in newly-eclosed flies after 0h APF clone induction. (**B-D**) SEMs shown. For raw data and calculations please see supplementary spreadsheets titled 0h APF Graphs Fig1,3; 0h APF Controls Variation; Compilation of Numbers Figure 1 Controls.

Second, although the chosen approach can simultaneously report on the behavior of all precursors in a variety of AP locations, it necessarily includes a sampling error. For example, if we are examining the fate of the roughly 20% of precursors that would normally become FCs, the sample of such cells will not always be exactly 20%. We have performed many sets of experiments, each including a control ("wild-type") genotype. Those multiple controls allow experimental evaluation of sampling variability. They also provide a cumulatively large control sample to produce reliable measures for each parameter deduced from lineage studies. For MARCM clones induced at pupariation, the standard deviation among controls for the frequency of a given lineage type (Fig. 1B) was generally similar to that expected for random sampling of individual cells from the estimated number of somatic precursors present at pupariation (see Methods and cited supplementary spreadsheet).

Third, clone sizes provide only limited insight into the spatial regulation of division rates. First, the deduced average number of marked ECs per EC-only clone was consistently between 2 and 3 for controls, consistent with limited division of the most anterior precursors and providing little opportunity to measure significant quantitative deficits (Fig. 1D). Second, almost all lineages with FSCs also include ECs and FCs. The number of ECs and FSCs in such lineages (average of about 8 for controls) (Fig. 1D') provides some indication of the amplification of a subset of the precursors, but this excludes the large and variable numbers of FCs generally present in such lineages. It is not possible to measure the number of marked FCs that first associate with a germline cyst (which would be the key number to measure divisions in and around the prospective FSC domain) because each such cell generally divides many further times as the egg chamber forms and grows. Thus, the sum of ECs and FSCs in an FSC-containing lineage only provides limited information about division rates in regions that give rise to ECs, FSCs and FCs. The fraction of cysts with marked FCs in FSC-containing lineages provides a second measure. The number of marked cells in the most posterior egg chamber can report on proliferation of the most posterior precursors. Additional information comes from measuring the frequency with which such lineages extend into the penultimate egg chamber.

Fourth, the MARCM method has the key virtue of clear positive marking, so that every lineage (even a single cell) and every marked cell within a lineage can be identified readily. A well-known disadvantage is, however, that GAL80 gene products must first be diluted and degraded before GAL4-driven *UAS-X* transgene products can accumulate. Strong accumulation of GFP from *UAS-GFP* in somatic ovarian cells takes at least 3d using our genetic reagents, and a similar delay is therefore expected before any *UAS*-driven transgene begins to exert maximal effect. Thus, both the onset and plateau of phenotypic responses to activation of a *UAS*-driven transgene in a MARCM clone can only be estimated and will generally be later than for the generation of a loss-of-function homozygous mutation. These and other relevant methodological considerations are discussed at greater length in the context of specific results obtained for variant genotypes.

732
733 **Terminal FC source is not distinct from other EC, FSC and FC precursors**
734
735 We are interested in understanding how somatic cells are instructed to occupy various
736 positions in the adult germarium to function subsequently as FSCs and ECs. We are also especially
737 interested in how the first FCs are specified during pupation. This is an intriguing question because FC
738 formation in adults relies on signals from previously produced FCs. We therefore first sought to clarify
739 the origins of the FCs on the first-formed egg chamber.
740 At the start of pupation, about 20-30 somatic cells are dispersed among germline cells to form
741 a primitive germarium (Fig. 2A). These intermingled cells (ICs) express the transcription factor, Traffic
742 Jam (TJ) (LI *et al.* 2003). Numerous additional TJ-negative somatic cells, referred to as basal cells
743 (Swarm cells after migration; not shown in Fig. 2A and not the same as basal stalk cells), are present
744 in a more posterior location, as a seemingly contiguous group, rather than associated with individual
745 developing ovarioles. Over the next 48h, TJ-positive somatic cells accumulate posterior to the
746 developing germarium (beyond the most posterior germline cyst) to form a structure termed the
747 Extra-Germarial Crown (EGC) (REILEIN *et al.* 2021). In the most posterior portion of the EGC, somatic
748 cells are intercalated to form a "basal stalk", which also includes some TJ-negative cells at the
749 posterior (KING *et al.* 1968; GODT AND LASKI 1995; VLACHOS *et al.* 2015; REILEIN *et al.* 2021). Thereafter (at
750 about 56h APF on average), the most posterior germline cyst moves away from the germarium, into
751 the EGC and basal stalk, as cells in that extra-germarial territory, including some originally TJ-negative
752 cells, move anteriorly along the cyst to form a monolayer epithelium, leaving a short residue of basal
753 stalk at the posterior end that persists until eclosion (REILEIN *et al.* 2021). Most of the mid-pupal
754 (around 48h APF) EGC and basal stalk cells become FCs (or adult basal stalk cells) on the first budded
755 (terminal) egg chamber but some contribute to the next (penultimate) egg chamber, alongside FCs
756 derived from IC precursors present within the germarium around 48h APF (Fig. 2A). These deductions
757 derive from fixed images at successive stages, live imaging cell tracing and lineage analyses initiated
758 by a heat-shock at 36h APF (REILEIN *et al.* 2021). Many such 36h APF lineages contained only marked
759 FCs or basal stalk cells on the terminal egg chamber (purple lineage in Fig. 2A), while other lineages
760 had marked FCs only in more anterior locations (cyan and yellow lineages in Fig. 2A). Each type of FC-
761 only lineage sometimes included marked FCs in the penultimate egg chamber. Thus, at 36-48h APF,
762 only precursors in the EGC or basal stalk contribute terminal FCs and only IC precursors yield FCs
763 anterior to the two terminal egg chambers.
764 The remaining question is whether the precursors of the first FCs (EGC and basal stalk cells)
765 emerge from germarial ICs over the first 48h of pupation. This hypothetical migration out of the
766 developing germarium has not been visualized directly. There is extensive division outside the
767 germarium, so there may be only a modest ongoing exodus from the germarium that escaped
768 detection during live imaging. An alternative possibility is that the EGC and basal stalk cells seen at
769 48h APF have a separate origin from IC cells, conceivably deriving from extra-germarial basal cells
770 present at pupariation (KING *et al.* 1968) and acquiring TJ expression over the following days. These
771 possibilities can be distinguished by lineage analysis. An FC-only lineage (induced prior to 36h APF)
772 that includes FCs in both the terminal egg chamber ("terminal FCs") and at least one location anterior
773 to the penultimate egg chamber ("non-terminal" FCs) would provide evidence of a common
774 precursor of ICs and EGC/basal stalk cells present before 36h APF.
775

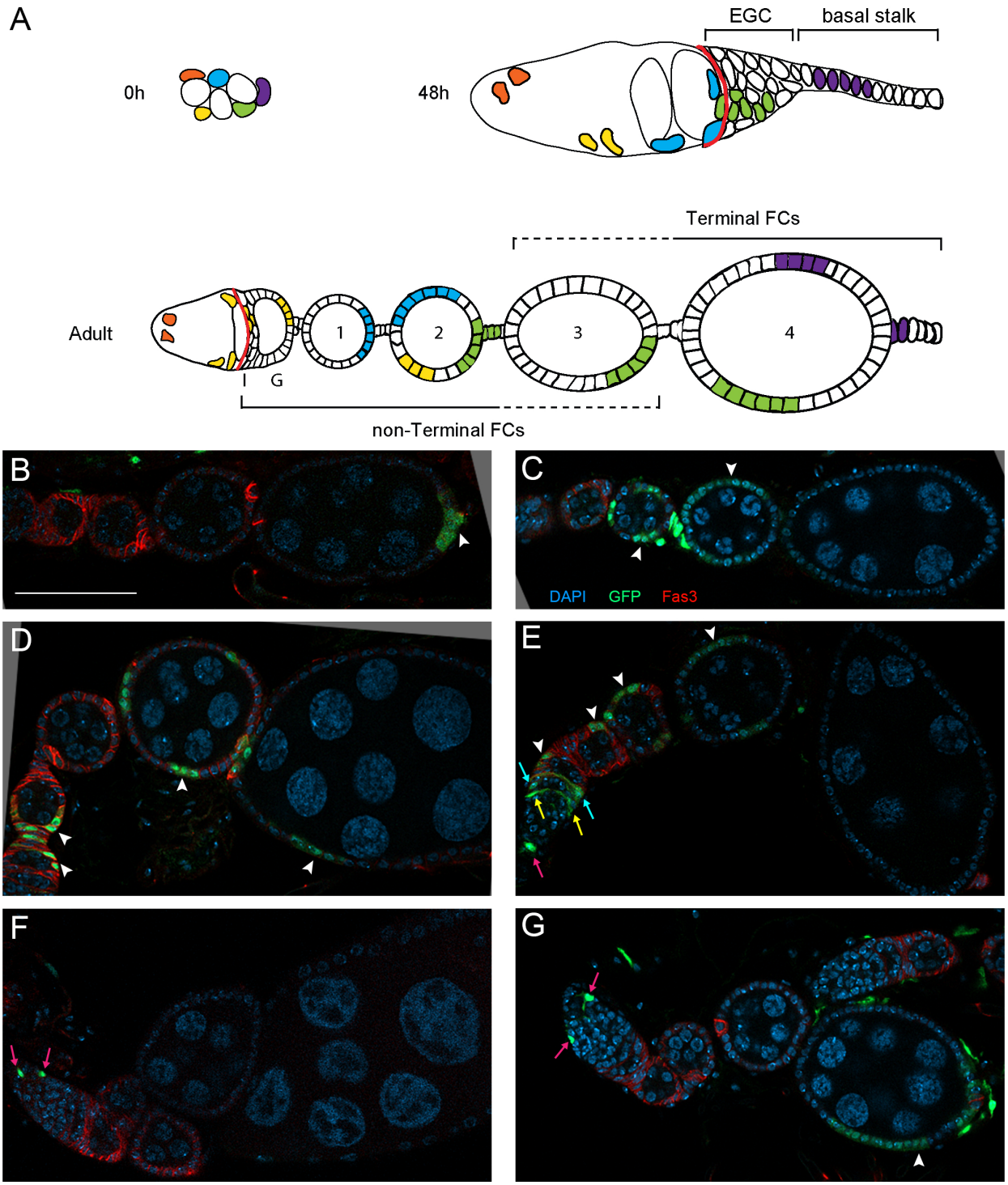

Figure 2: Terminal and non-terminal Follicle Cells derive from germarial ICs at pupariation.
(A) Illustration of selected individual precursors at pupariation (0h APF) and their progression over time. At 0h APF, the somatic cells are interspersed with single germline cells and 2-cell cysts. By 48h APF, the most mature germline cysts have 16 cells and a single such cyst occupies the most posterior position in the germarium. At this time, more posterior somatic cells express Fas3 (anterior border of expression indicated by the red line). The relationships between precursors at 48h APF and adult derivatives have previously been established. Specifically, precursors within the Extra-Germarial Crown (EGC) and Basal Stalk, which contain no germline cells and are therefore considered extra-germarial, give rise to FCs in the terminal egg chamber or adult basal stalk (with some derivatives extending into the penultimate egg chamber but no

further anterior). Precursors within the germarium at 48h APF give rise to adult ECs only (orange), ECs, FSCs and non-terminal FCs (yellow) or non-terminal FCs only (blue). It was not known whether cells in the EGC and basal stalk migrated out of the germarium between 0 and 48h APF (as indicated by the colors in the diagram) or if they derived from precursors in another location. The existence of precursors at pupariation producing adult FCs in terminal and non-terminal locations (as indicated for green cells) would support a germarial origin of terminal FCs. It would still be expected that some precursors at 0h APF would give rise only to terminal FCs (as shown for purple cells). The outcomes shown for green and purple cells were found, as illustrated in (b) and (D). **(B-G)** Representative images of lineages induced at 0h APF in ovarioles of newly-eclosed flies. **(B)** Terminal FC-only; **(C)** non-Terminal FCs only (egg chambers 2 and 3); **(D)** non-Terminal and Terminal FCs, showing that all FCs derive from germarial cells at pupariation; **(E)** EC/FSC/FC (designated as EC/FSC in graphs), **(F)** EC-only, **(G)** EC plus Terminal FC (presumed to be two lineages in the same ovariole because lineages derived from a single cell generally occupy largely contiguous territory). Scale Bar 50 µm for all images. White arrowheads indicate marked Follicle Cells; magenta arrows, r1 ECs; yellow arrows, r2a ECs; cyan arrows, FSCs. DAPI, blue; GFP, green; Fas3, red.

From 12 separate control experiments for lineages initiated at pupariation, the average fraction of FC-only lineages with terminal FCs (n=101) that also included marked FCs anterior to the penultimate egg chamber was (0.253/0.685) 0.37. This argues strongly for a single cell often acting as a precursor to both terminal and non-terminal FCs. Such precursors, like other non-terminal FC precursors, are therefore within or contiguous with the IC population, meaning that EGC and basal stalk cells derive from posterior migration of ICs out of a primitive germarium. Thus, it appears that some precursors in the germarium at pupariation produce only terminal FCs (Fig. 2B; purple cell in Fig. 2A), others produce only non-terminal FCs (Fig. 2C; blue cell in Fig. 2A), while several produce both terminal and non-terminal FCs (Fig. 2D; green cell in Fig. 2A). More anterior precursors produce EC/FSC/FC lineages (Fig. 2E; yellow cell in Fig. 2A) or only ECs (Fig. 2F; orange cell in Fig. 2A).

It is possible that our method for estimating single-cell lineage composition from raw observations underestimates the frequency of “double-clones” in a single ovariole (see Methods). To estimate the potential impact of an underestimation of this type we looked at the average frequency of lineages with terminal FCs that also include ECs (Fig. 2G). This incidence (0.039/(0.102 + 0.039)= 0.26) was previously considered mostly due to the presence of two lineages. To estimate the frequency of a second lineage including non-terminal FCs rather than ECs (which are much more frequently marked) due to “double-clones”, we multiply by the relative frequency of the latter two lineages ((0.154-0.064)/0.644) = 0.14). This gives an expected incidence of (0.26 x 0.14) = 0.036, which is far below the observed incidence of 0.37. In fact, further studies reported here suggest that some lineages containing only marked ECs and FCs are potential EC/FSC/FC lineages that have lost FSCs rather than indicating two superimposed lineages. Hence, the incidence of “double-clones” in our deduced single-cell lineages is likely even lower than estimated above. We can therefore be confident that ICs and extra-germarial somatic cells at 36-48h APF have a common origin at pupariation, with the terminal FC precursors migrating out of the nascent germarium. This means that we can use altered genotypes in lineage analyses to look for differences in the production of terminal FCs in order to identify factors that regulate posterior migration out of the developing germarium over the first 48h of pupation. The lineage studies provide evidence that the migration must occur prior to 48h APF but do not define when the migration occurs. There are some Traffic-Jam-positive cells posterior to all germ cells even by 12h APF (Reilein *et al.* 2021), so it is likely that some migration is early.

835 **Consequences of altered precursor division rate**
836
837 In an adult ovariole, the division rate of a marked FSC over a period of several days cannot
838 simply be assessed by counting the number of marked derivatives, principally because FC derivatives
839 are initially highly proliferative, so that the number of FCs directly produced from marked FSCs
840 cannot be counted. The analogous limitation applies to any pupal precursors that give rise to a
841 mixture of FCs and other cell types during pupation. The number of divisions for EC-only lineages can
842 be measured, but the average size of control EC-only clones is only 2.7 (Figs. 1D and 3I'), providing
843 only a small range for detecting reduced division rates. The most posterior somatic precursors at
844 pupariation contribute principally to FCs of the first-formed egg chamber (purple cell in Fig. 2A). The
845 division frequency of a posterior precursor can therefore theoretically be estimated as the proportion
846 of FCs in the terminal egg chamber that are marked (ignoring lineages that only mark polar cell and
847 stalk cells, which cease division soon after specification).
848 We wanted first to establish whether changes in division rate can be measured in pupal ovary
849 precursors in various locations and then to determine whether altering the rate of cell division has a
850 systematic effect on developmental outcomes. We have previously shown that a specific
851 hypomorphic *cycE* allele (*cycE*^{WX}) reduces the division rate of adult FSCs without affecting
852 differentiation significantly, and that this leads to loss of marked FSCs over time (WANG AND KALDERON
853 2009; REILEIN *et al.* 2018). The reduced competitiveness of slowly dividing FSCs is an important
854 characteristic that results from division and differentiation being independent processes for these
855 stem cells (as in some other population asymmetry paradigms) (VERMEULEN AND SNIPPERT 2014; REILEIN
856 *et al.* 2018). Essentially, this is because the marked *cycE* mutant stem cells drain from the stem cell
857 domain at the normal rate through differentiation but are replenished by division at a lower rate.
858 We found that the average number of marked ECs per EC-only clone for *cycE* induced at 0h
859 APF was 1.9, compared to 2.7 for controls (Fig. 3I'). This is consistent with reduced division of the
860 most anterior somatic ovarian precursors but likely does not report the magnitude of the effect well
861 because wild-type *cycE* products likely perdure for the short duration of pre-EC divisions. The most
862 posterior somatic precursors at pupariation contribute principally to FCs of the first-formed egg
863 chamber (purple cell in Fig. 2A). The division frequency of a posterior precursor can therefore
864 theoretically be estimated as the proportion of FCs in the terminal egg chamber that are marked. The
865 average fraction of marked FCs among terminal FCs with main-body FC labeling was 3.0% for *cycE*,
866 compared to nearly 50% for the direct control (Fig. 3A, B). This measure might be distorted if the
867 altered genotype affects the likelihood of precursors becoming stalk or polar cells, which proliferate
868 less than other FCs. However, marked stalk or polar cells were no more prevalent for *cycE* (2/14
869 samples) than for controls (5/10 samples). Thus, it appears that reduced CycE activity associated with
870 the *cycE*^{WX} allele greatly impaired cell division rates for posterior ovarian precursors.
871 Reduced precursor division frequency might be anticipated to have different consequences
872 on lineage outcomes depending on precursor location. First, we might hypothesize that slowly-
873 dividing *cycE* cells in regions giving rise to future FSCs will be outcompeted by normal precursors,
874 depleting marked FSCs, exactly as seen for adult-induced FSC lineages. The logic here is that since
875 there is a certain A/P domain where precursors reside to become FSCs, the survival of a lineage in this
876 domain requires cell division to balance posterior loss. When induced at pupariation and analyzed in
877 newly-eclosed adult ovaries, there was a large reduction in the frequency of *cycE* clones that included
878 one or more FSCs (2% vs 15% for controls; $p<0.005$) (Fig. 3I). Out of all marked ECs and FSCs, only 1%
879 of *cycE* cells were FSCs vs 23% of control cells, confirming the substantial deficiency in FSC
880 production. The frequency of ovarioles harboring marked cells of any type was not significantly

altered (47% *cycE*, 42% in the direct, side-by-side control), suggesting that the *cycE* mutation does not impact cell survival and is therefore unlikely to be depleting FSCs through selective cell death. The results therefore support the hypothesis that severely reduced cell division substantially reduces the probability of a cell emerging from pupal development as an FSC. Selective loss of FSCs from prospective EC/FSC/FC lineages would be expected to result in an unusually high frequency of lineages containing only marked ECs and FCs. This was observed for *cycE* lineages (Fig. 3G, I; $p<0.005$).

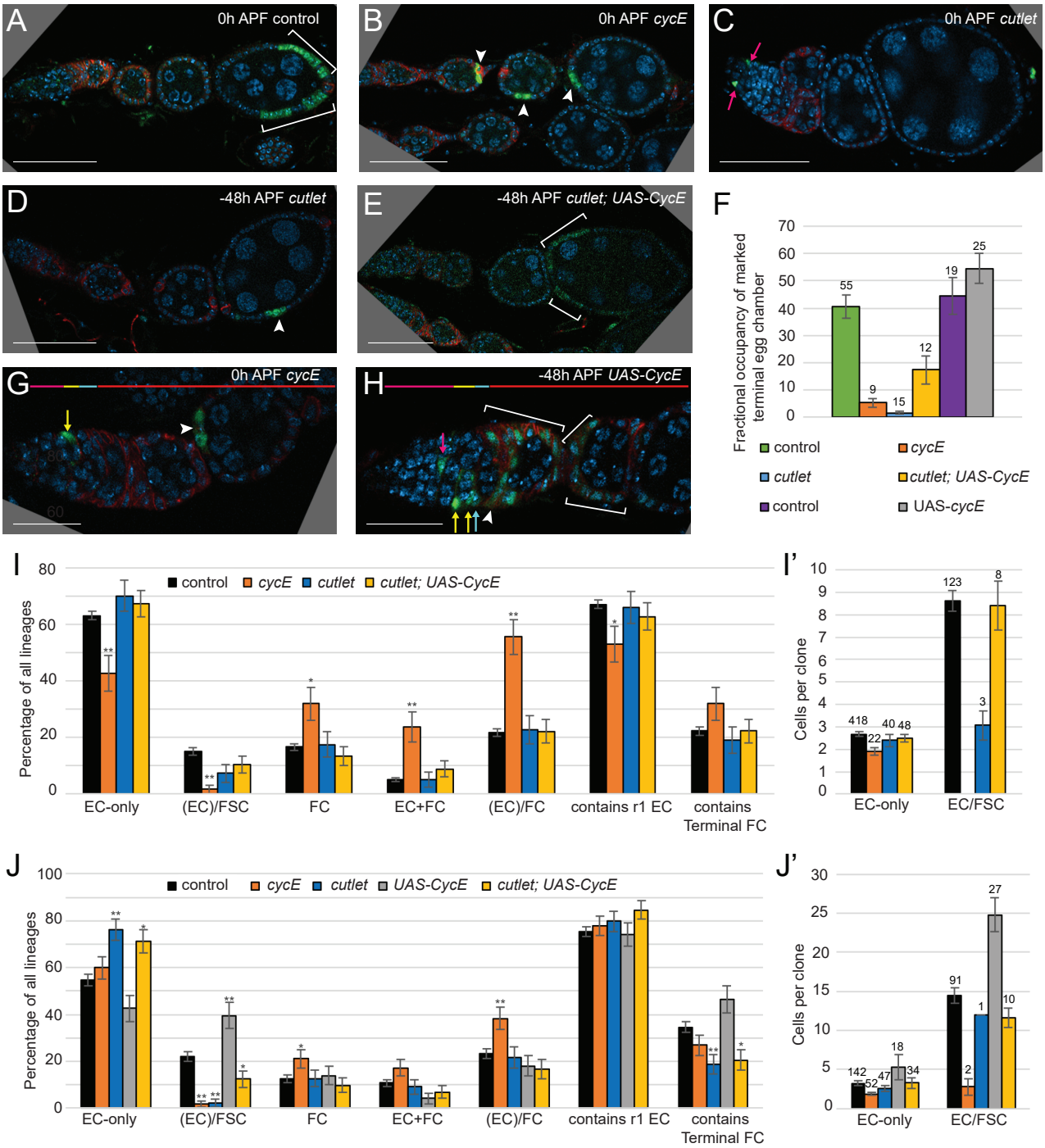

Figure 3: Effects of altered division frequency on lineage outcomes.
(A-F) Fractional occupancy of terminal egg chamber by marked FCs, when present, as an approximate measure of division frequency for posterior precursors. **(A-C)** show lineages induced at pupariation and **(D-F)** are lineages induced 48h prior to

pupariation for the indicated genotypes. **(F)** Percentage of marked cells out of total cells in terminal egg chamber for lineages of the indicated genotypes induced 48h before pupariation. Direct controls precede other genotypes for each experiment. **(G, H)** Ovarioles with **(G)** a *cycE* EC/FC lineage induced at 0h APF, illustrating the increased frequency of such lineages, potentially due to selective loss of FSCs from EC/FSC/FC lineages and **(H)** a *UAS-CycE* EC/FSC/FC lineage, present at elevated frequency, induced 48h before pupariation. White arrowheads indicate Follicle Cells; magenta arrows, r1 ECs; yellow arrows, r2a ECs; cyan arrows, FSCs. DAPI, blue; GFP, green; Fas3, red. Scale Bar **(A-E)** 50 µm and **(G-H)** 20 µm). **(I, J)** Deduced frequency of the indicated types of single-cell lineage as a percentage of all lineages and **(I', J')** average number of cells per EC-only or EC/FSC lineage (ECs and FSCs only) induced at **(I)** 0h APF and **(J)** -48h APF. Error bars show SEM. One asterisk (*) indicates p<0.05; two asterisks (**) indicates p<0.005 (Fisher's two-tailed exact test). **(I)** Number of marked ovarioles = 739 (control), 50 (*cycE*), 60 (*cutlet*), 78 (*cutlet; UAS-CycE*). **(J)** Number of marked ovarioles = 319 (control), 93 (*cycE*), 119 (*cutlet*), 85 (*UAS-CycE*), 75 (*cutlet; UAS-CycE*). **(I,' J')** Number of lineages indicated above bars. For raw data and calculations please see supplementary spreadsheets titled 0h APF Graphs Fig1,3; -2d APF Graphs; FC occupancy aggregate**;** Compilation of Numbers Figure 3 Division -5d; Compilation of Numbers Figure 3 Division -7d.

A second hypothesis is that reduced division rate may result in reduced posterior movement of precursors. The somatic cell population grows and expands posteriorly over the first 48h of pupation to occupy a wider A/P territory prior to the budding of the first egg chamber. While it is more likely that posterior expansion is fueled by pressure from growth and division of germline cysts and somatic cells that lie anterior, it is possible that the division of a cell has some cell-autonomous contribution to its posterior movement. If such an effect were significant, we might expect that *cycE* mutant cells would less frequently contribute to FCs of the terminal egg chamber and would more frequently become ECs, especially region 1 ECs. Contrary to that hypothesis, the fraction of lineages including terminal FCs was higher (32% vs 22%; p= 0.09) and the fraction with r1 ECs was lower (53% vs 67%; p<0.05) for *cycE* lineages compared to controls (Fig. 3I). The frequency of EC-only lineages was also reduced for *cycE* (43% vs 63%; p<0.005), while the frequency of FC-only lineages was increased (32% vs 17%; p<0.05) (Fig. 3I). These results therefore suggest an unexpected cell-autonomous posterior movement of *cycE* mutant cells relative to surrounding precursors over the whole A/P range.

To test whether the posterior movement of *cycE* mutant precursors was due to reduced division or another action of CycE we tested an allele of the replication factor gene *cutlet*, which reduced division rate in adult FSCs (WANG *et al.* 2012). The mean number of marked ECs per EC-only was 2.4 compared to 2.7 for controls (Fig. 3I'), while the average fraction of marked FCs among terminal FCs was 7.4%, compared to 24.3% for the direct control (Fig. 3C). These results are consistent with reduced cell division rates for *cutlet* mutant cells, albeit to a lesser degree than observed for the $cycE^{WX}$ allele. The fraction of lineages with marked FSCs was 7%, compared to 15% for controls (Fig. 3I). EC-only clone frequency increased slightly relative to controls (70% vs 63%) but the frequencies of FC-only lineages (17% vs 17%), labeling of r1 ECs (66% vs 67%) and of terminal FCs (19% vs 22%) were largely unchanged (Fig. 3I). Thus, there was selective loss of *cutlet* mutant FSCs without any significant A/P bias of precursor fates. Loss of FSCs for both *cycE* (15% to 2%) and *cutlet* (15% to 7%) is consistent with the conclusion that reduced cell division rates lower FSC production. By contrast, a large deficit of r1 EC-only lineages, an increase in FC-only lineages far exceeding that expected just from FSC loss, and an increase in terminal FCs were observed only for *cycE,* suggesting that these measures of net posterior movement of precursors do not result from a reduced division rate.

We then assessed the effects of overexpression of CycE, using *UAS-CycE* expression with *tub-GAL4* plus *act-GAL4* as drivers of expression (our standard MARCM condition) in marked lineages induced 48h before pupariation. The timing was chosen so that increased CycE levels might start to accrue roughly coincident with pupariation. In adult FSC lineage studies, *UAS-CycE* increased the

division rate of FSCs but not ECs, which are quiescent in adulthood (MELAMED AND KALDERON 2020; MELAMED *et al.* 2023). EC precursors are still dividing early in pupal development, so they might be stimulated to divide more frequently if excess CycE is provided at the start of pupation. Excess CycE would certainly be expected to increase the division rate of more posterior somatic cell precursors. Hence, by the converse of the logic explained earlier for reduced CycE, faster division might increase the representation of marked FSCs. The number of marked cells per EC-only clone was higher for *UAS-CycE* (5.3) than for controls (3.2) (Fig. 3J'). The average fraction of marked FCs among terminal FCs was also increased, from 45% to 55% (Fig. 3C). Among EC/FSC/FC lineages (where FC production cannot be counted, limiting the accuracy of estimating division rates), the average number of marked germarial cells (ECs and FSCs) rose from 14.5 (including 9.5 ECs) for controls to 24.8 (including 17.4 ECs) for *UAS-CycE* (Fig. 3J'). Thus, *UAS-CycE* increased the division rate of precursors in all locations. *UAS-CycE* produced a slightly higher clone rate (frequency of ovarioles with marked cells) than the side-by-side control (65% vs. 56%), demonstrating that excess CycE does not reduce cell survival. Importantly, *UAS-CycE* lineages contained FSCs (40%) more frequently than controls (23% for direct control; 22% for average controls; $p<0.005$) (Fig. 3H, J). These results support the hypothesis that increased division rate during pupal stages can increase FSC allocation, just as faster division increases FSC representation in adult FSC lineages.

The observed increased representation of EC/FSC/FC lineages is expected to be because potential FSCs are less frequently lost to yield lineages with just ECs and FCs. Indeed, the frequency of (EC+FC) lineages was lower for UAS-CycE (4% vs 11% controls for lineages induced 48h prior to pupariation) and higher for reduced *cycE* activity induced 48h prior to pupation (17% vs 11%) or at pupariation (24% vs 6%). These results suggest that a wild-type precursor in a location that can yield ECs, FSCs and FCs because of modest A/P spread during pupal development will occasionally contain only adult ECs and FCs because cells in prospective FSC locations were not replenished fast enough to counter continuous drain to more posterior FC locations. That, in turn, suggests that a significant fraction of (EC+FC) lineages result from single precursors, rather than the super-position of an EC-only and an FC-only lineage, as previously thought (REILEIN *et al.* 2021) and that our estimation of single-cell lineages numbers derived from raw data is better than we had believed on the basis of the deduced (EC+FC) lineage frequency.

The frequencies of both EC-only (43% vs 55%; $p=0.1$) and r1-only lineages (24% vs 43%; $p<0.005$) were decreased for *UAS-CycE*. This could simply be because the increased number of cells per lineage inevitably results in several clones crossing posterior boundaries, into r2a EC and FSC territory, respectively. The frequency of FC-only lineages was unaltered (14% vs 13%), suggesting there is no large systematic displacement of all marked cells towards the posterior. Rather, the principal response was that the representation of a central population, which become FSCs, was increased.

Since *UAS-CycE* was found to restore survival of adult FSC lineages with *cutlet* mutations (albeit assessed prior to more definitive measures of FSC competition introduced in 2017) (WANG *et al.* 2012), we tested whether excess CycE might ameliorate the key phenotypes of *cutlet* mutant lineages induced 48h prior to pupariation (deficiency of FSCs and indications of reduced division rate). *UAS-CycE* increased the average number of number of cells in EC-only lineages from 2.5 to the control value of 3.2 (Fig. 3J'). The average fraction of marked FCs among terminal FCs was greatly increased, from 2% to 17%, indicating substantial rescue of division rate towards control values (Fig. 3C). The frequency of lineages with FSCs was also partially restored (from 2% to 12%) towards the control value (22%) (Fig. 3D, E, J). In the EC/FSC lineages there were now similar numbers of ECs (8 vs 9.5) and FSCs (3.5 vs 5.0) to controls (Fig. 3J', sum shown). The FC productivity of FSC-containing lineages can

986 be roughly estimated by counting the proportion of egg chambers, region 2b and region 3a germline
987 cysts with associated marked FCs; this measure would be increased by recruitment of more future
988 FSCs or a higher division rate of those cells. The low proportion of cysts with marked FCs for *cutle*t
989 (1/11; 9%) was increased by *UAS-CycE* (33/54; 61%) towards the control value for this experiment
990 (128/156; 82%). These results are all consistent with substantial correlated restoration of cell division
991 rate and FSC production. A smaller restoration of FSC-containing lineages (from 7% to 10%) towards
992 control values (15%) was seen for the addition of *UAS-CycE* to *cutlet* loss of function in lineages
993 initiated at pupariation (Fig. 3I). The proportion of cysts with surrounding marked FCs in FSC-
994 containing lineages was also increased from 14% (3/21) for *cutlet* to 46% (25/54) by the addition of
995 *UAS-CycE*, towards the control value of 65% (26/40). The delayed expression of excess CycE in
996 lineages initiated at pupariation likely accounts for the lesser rescue.
997 Reduced CycE activity was also tested in lineages induced 2d prior to pupariation (Fig. 3J). The
998 major phenotype was a large loss of lineages with FSCs, similar to *cutlet*. There was also an increase
999 in FC-only and EC/FC lineages combined ("(EC)/FC") for *cycE* (38%) relative to *cutlet* (22%) and
1000 controls (23%), similar to results for lineages induced at pupariation. However, there was neither an
1001 increase for terminal FC representation (27% vs control 35%), nor a large reduction in r1 EC
1002 representation (80% vs 75%) seen for lineages initiated at pupariation. Thus, the strong phenotype of
1003 FSC loss was seen for both stages of lineage induction, while the unexpected posterior movement of
1004 precursors due to loss of *cycE* was prominent only for lineages induced at pupariation.
1005 This set of studies suggests that the primary consequence of cell-autonomously reducing the
1006 rate of precursor division within a competitive environment of normal cells during pupation is a large
1007 reduction in the frequency of lineages containing FSCs in newly-eclosed adults. This was observed for
1008 both loss of *cycE* and loss of *cutlet*, initiating lineages at pupariation and 2d earlier. The converse was
1009 seen in response to increasing the division rate. No other consequence was consistently seen for both
1010 *cycE* and *cutlet* loss of function mutations, while excess CycE also appeared only to affect FSC
1011 representation.
1012
1013 **Wnt signaling magnitude strongly influences precursor fates across the whole A/P domain**
1014
1015 We wished to investigate the roles of Wnt and JAK-STAT signaling on somatic ovarian
1016 precursor development because these are the two major pathways regulating adult FSC behavior
1017 (VIED *et al.* 2012; REILEIN *et al.* 2017; MELAMED AND KALDERON 2020). Canonical Wnt signaling is initiated
1018 by binding of ligand to Frizzled and LRP5/6 (Arrow in Drosophila) family co-receptors, leading to
1019 release of β-catenin from a destruction complex scaffolded by Axin (Axn) and its subsequent
1020 association with nuclear TCF/LEF (TCF in Drosophila) to convert TCF from a repressor to an activator
1021 of transcription (WIESE *et al.* 2018).
1022 We used the strong axn^{E77} allele (which truncates the protein after Q406 to eliminate DIX,
1023 GSK3, β-catenin and protein phosphatase 2A binding domains to behave like a null in several assays)
1024 to create marked homozygous *axn* mutant precursors at pupariation and measure the spectrum of
1025 lineages obtained consequent to increasing Wnt pathway activity cell autonomously during pupal
1026 development. Almost all lineages consisted of only marked ECs (91%, compared to 63% in controls)
1027 (Fig. 4A, D, F), with an elevated yield of lineages confined to r1 ECs (61% vs 49% control) and of
1028 lineages containing at least one marked r1 EC (81% vs 67% control). Only 2% of lineages contained
1029 marked FCs without FSCs (22% for controls) and only 6% contained any marked FSCs (15% for
1030 controls) (Fig. 4F). Thus, it appears that all marked precursors have preferentially moved anteriorly
1031 during pupal development in a cell-autonomous response to increased Wnt pathway activity, leading

1032 to a near-absence of marked posterior derivatives, FSCs and FCs. In adult FSCs, loss of *axn* leads to
1033 strong net anterior movement, producing a high frequency of marked ECs over time but it also
1034 severely reduces cell division (REILEIN *et al.* 2017; MELAMED AND KALDERON 2020). Based on *cycE* and
1035 *cutlet* mutant phenotypes over pupal development, reduced division would be expected to reduce
1036 the yield of FSCs but some of the "lost" FSCs would become FCs. The drastic loss of both FSCs and FCs
1037 for *axn* mutant precursors argues for a strongly altered behavior (anterior migration) other than
1038 reduced division. The average number of cells per EC clone was slightly lower for *axn* (2.5) than the
1039 control value (2.7). However, this is not a sensitive test and the *axn* mutant ECs, on average, also
1040 occupy a slightly more anterior set of EC positions than control derivatives, which may lead to earlier
1041 cessation of division. Since almost all *axn* precursors become ECs, there were too few FSC and FC *axn*
1042 derivatives to assess cell division rates of more posterior precursors. Thus, it is not clear whether
1043 increased Wnt signaling directly affects cell division during pupation but there is a strong phenotype
1044 of anterior bias for adult derivatives of precursors in all locations.
1045 To investigate the effects of loss of Wnt pathway activity we used a strong or null *arrow* allele
1046 (arr^2) that introduces a premature stop codon. We also added *UAS-DIAP1*, which was found in adult
1047 FSC derivatives to increase the yield of labeled *arr* mutant ECs (MELAMED AND KALDERON 2020). Other
1048 studies have found that adult ECs, especially those at the far anterior, are subject to apoptosis when
1049 Wnt pathway activity is severely reduced (WANG *et al.* 2015; WANG AND PAGE-MCCAW 2018). Relative to
1050 controls, *arr* mutant lineages induced at pupariation (with *UAS-DIAP1*) had a strong deficit of lineages
1051 with only r1 ECs (23% vs 49% control), only ECs (34% vs 63% control) or any r1 EC (36% vs 67%
1052 control) (Fig. 4B, C, F). By contrast, there was an increased fraction of lineages with marked FSCs (27%
1053 vs 15% control), only FCs (33% vs 17%) or containing terminal FCs (41% vs 22% control). The average
1054 number of marked germarial cells in each EC-only (2.1 vs 2.7) or EC/FSC/FC lineage (7.4 vs 8.6) was
1055 largely unchanged. Thus, as in adult FSC lineages, loss of Wnt pathway activity appears to have no
1056 major effect on the rate of cell division but causes a strong posterior shift in location, leading to a
1057 deficit of ECs and an excess of FCs. The increase in lineages with FSCs can be rationalized as due to a
1058 greater numerical shift of would-be ECs (which are the most numerous) to FSCs than of would-be
1059 FSCs to FCs. These conclusions explain the unexpected observation long ago that loss of *arr* increased
1060 FSC clonal yield if induced at larval stages and assayed 10 days later, despite reducing FSC longevity in
1061 adult FSC lineages because of a posterior shift increasing conversion of FSCs to FCs (VIED *et al.* 2012).
1062 In other words, the same primary consequence of preferential posterior movement due to
1063 autonomous loss of Wnt signaling reduces FSC yield in adults because marked FSCs cannot be
1064 replenished from marked ECs, but increases FSC yield during pupation because marked EC precursors
1065 can move into FSC locations; in both situations there is faster depletion of marked FSCs posteriorly to
1066 become FCs.
1067 The effects of altered Wnt pathway activity on the conversion of precursors to adult ECs and
1068 FSCs can also be evaluated by counting the total number of these derivatives over all examined
1069 lineages (FC numbers cannot be evaluated in this way). This analysis has the virtue that it does not
1070 rely on whether marked cells in an ovariole derive from one or more precursors. In line with the
1071 analysis of lineage types above, the proportion of derivatives that became FSCs (control 20%) was
1072 greatly reduced for *axn* clones (6%) and markedly increased for *arr* clones (35%), while the proportion
1073 that became r1 ECs (control 54%) was similar for *axn* clones (50%) and markedly decreased for *arr*
1074 clones (31%). The unchanged proportion of r1 ECs for *axn* is somewhat deceptive because FCs are not
1075 included in this analysis. Control samples include many FCs whereas *axn* lineages do not. Hence, r1 EC
1076 frequency as a proportion of all marked cells (including FCs) is actually lower for controls than for *axn*.

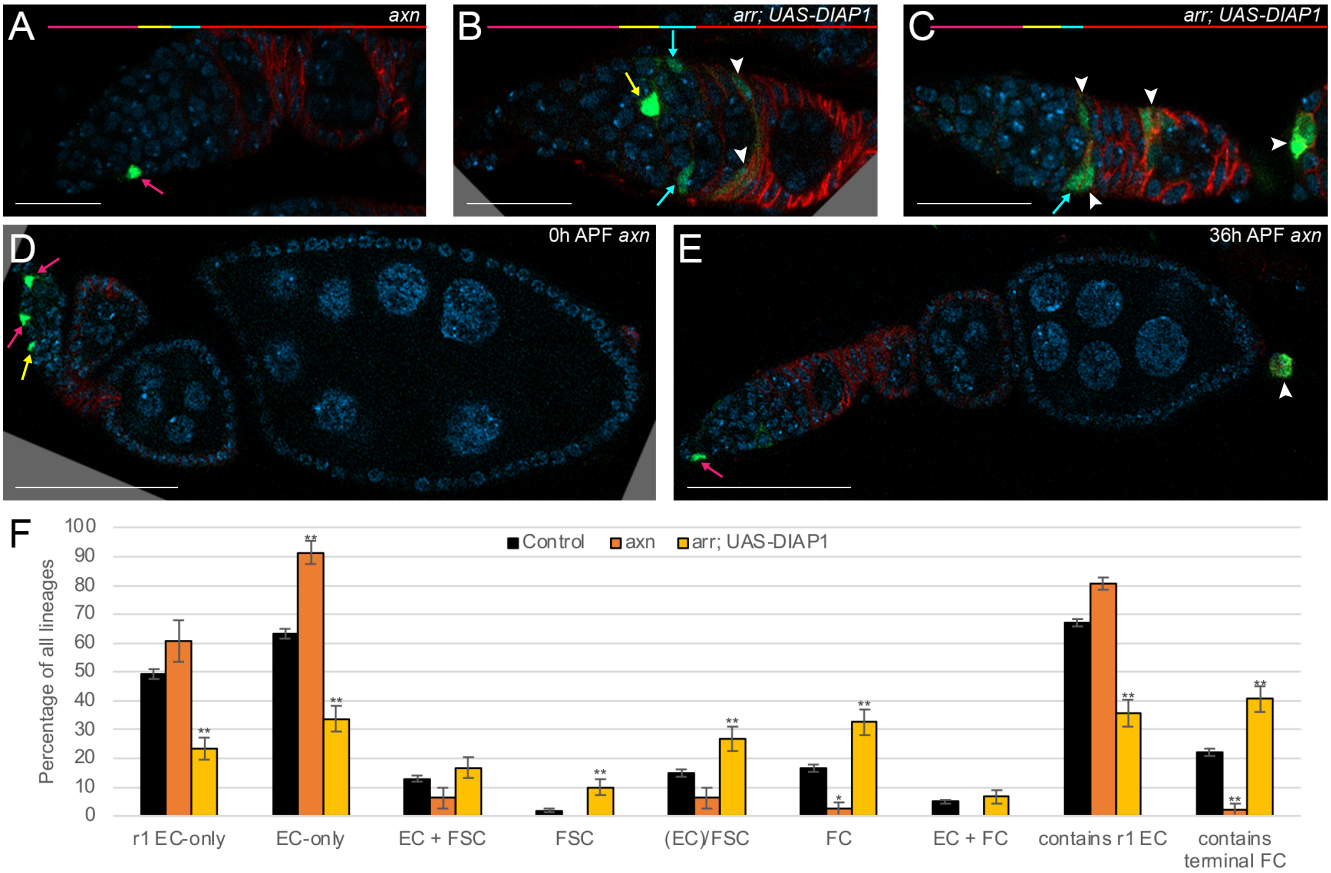

Figure 4: Higher Wnt pathway activity promotes anterior precursor movement during pupation.
(A-E) Representative lineages induced at (**A-D**) 0h APF or (**E**) 36h APF for the indicated genotypes. White arrowheads indicate Follicle Cells; magenta arrows, r1 ECs; yellow arrows, r2a ECs; cyan arrows, FSCs. DAPI, blue; GFP, green; Fas3, red. (**A-C**) The r1 EC, r2a EC**,** FSC and FC domains are shown in corresponding colors in the horizontal bars above. Characteristic phenotypes with elevated frequency included **(A)** an *axn* r1 EC-only lineage and **(B, C)** *arr; UAS-DIAP1* lineages containing FSCs and FCs, (**B**) with or (**C**) without ECs (the latter is rarely observed for control lineages). **(D, E)** Ovarioles with an *axn* lineage induced at **(D)** 0h APF, with only ECs, and at **(E)** 36h APF, with marked terminal FCs in the basal stalk (arrowhead). Scale Bar 20 µm for (**A-C**) and 50 µm for (**D, E**). **(F)** Deduced frequency of the indicated types of single-cell lineage as a percentage of all lineages induced at 0h APF. Error bars show SEM. One asterisk (*) indicates $p<0.05$; two asterisks (**) indicates $p<0.005$ (Fisher's two-tailed exact test). Number of marked ovarioles = 739 (control), 44 (*axn*), 95 (*arr; UAS-DIAP1*). For raw data and calculations please see supplementary spreadsheets titled 0h APF Graphs Fig4-10; Compilation of Numbers Figure 4 Wnt.

Wnt pathway activity limits cell migration out of the germarium during the first half of pupation

We have shown that EGC and basal stalk cells, the progenitors of terminal egg chamber FCs, derive from precursors that migrate posteriorly out of the germarium over the first 48h of pupation, and that increased Wnt signaling throughout pupation strongly reduces the acquisition of terminal FC identity cell-autonomously (Fig. 4F). To refine the key period of action, we induced control and *axn* lineages at 36h APF, estimating that genetically increased Wnt signaling would be delayed by a further few hours to coincide roughly with the completion of EGC/basal stalk formation and the migration of the most posterior germline cyst out of the germarium. At 36h APF there are many more somatic cell precursors per ovariole than at pupariation, so even the mildest heat-shock conditions produce MARCM clones in almost all ovarioles. Consequently, most ovarioles will contain more than one lineage and it is not possible to derive single-cell lineage frequencies accurately; raw

1103 observations are therefore presented for that time-point. The clone frequency for *axn* (97%) was
1104 higher than for the direct control (58%), so that multiple lineages per ovariole are likely more
1105 frequent. Nevertheless, there was clearly no deficit in the fraction of marked ovarioles with labeled
1106 terminal FCs (46% vs 31% control) (Fig. 4E; Supplementary spreadsheet "-3.5d axn August 2023
1107 Numbers"). This is markedly different to the result for lineages initiated at pupariation, indicating that
1108 the near absence of terminal FCs for those samples is caused by failure of precursors to migrate
1109 posteriorly out of the germarium over the first 48h of pupation, with no subsequent deficit in
1110 surviving as terminal FCs.
1111 The frequency of lineages that included terminal FCs was much higher for *arr* (41%) than for
1112 control lineages (22%) when induced at pupariation, indicating that Wnt signaling normally limits
1113 terminal FC formation (Fig. 4F). When lineages were induced 24h APF there was a similar clone
1114 frequency for control (84%) and *arr* plus *UAS-DIAP1* (73%) and a similar proportion of ovarioles that
1115 included marked terminal FCs (29% control vs 30%; Supplementary spreadsheet "-4d arr DIAP
1116 Numbers"). Thus, the increased representation of terminal FCs seen for lineages induced at
1117 pupariation is absent 24h later. We deduce that normal Wnt signaling restrains posterior movement
1118 of precursors out of the germarium at the start of pupation. These consequences of elevated and
1119 reduced Wnt signaling on generation of the first FCs parallel the effects seen in adults for conversion
1120 of FSCs to FCs, in which a precise level of Wnt signal is required for normal FSC production and
1121 optimal FSC maintenance, even though FC formation in adults and for the first egg chamber in pupae
1122 are morphologically very different.
1123
1124 **Wnt activity is influential throughout pupation**
1125
1126 The above results mostly showed a strong effect of Wnt signaling favoring more anterior
1127 precursor locations when changes in Wnt pathway activity were applied throughout pupal
1128 development. Additionally, strong effects on terminal FC formation were seen for genetic changes
1129 initiated at pupariation but not if initiated at 24h APF (*arr*) or 36h APF (*axn*), showing that Wnt
1130 signaling levels are critical very early in pupariation for migration of precursors out of the germarium
1131 to form the first FCs. In theory, further insight into critical times of action can be gained by initiating
1132 lineage tracing and a change in Wnt signaling at a full range of developmental times. However, a
1133 limitation of using MARCM clones is that a strong GFP signal only develops after 3d because of
1134 perdurance of GAL80 products. We therefore induced clones at 6d, 5d, 4d, 3d and 2d before eclosion
1135 and examined lineages in adults two days after eclosion. A drawback of this approach is that the first
1136 egg chambers produced during pupal development have matured into deposited eggs and are no
1137 longer present in 2d-old adults, so marked FCs cannot be scored comprehensively. Hence, our
1138 analysis focused only on ECs and FSCs. Also, FSCs present at eclosion are not scored directly but must
1139 be inferred (see Methods). The experiment was performed for *axn* and also for loss of a different β-
1140 catenin destruction complex member (using a double mutation, *apc1 apc2*) with similar results, for
1141 *arr*, and for three control genotypes. Results, expressed as the percentage of all marked ECs/FSCs
1142 (Supplementary Fig. 1), and were summed for all controls, two *arr* tests and the two genotypes (*axn*
1143 and *apc1 apc2*) producing excess Wnt pathway activity. A small deficit of FSCs was apparent for
1144 *axn*/*apc* in lineages initiated 2d before eclosion (48% vs 55% control) and a larger deficit was seen at
1145 5d and 6d prior to eclosion (14% vs 33% control in each case), suggesting that increased Wnt pathway
1146 activity provokes movement of precursors away from FSC-producing AP locations throughout pupal
1147 development (Supplementary Fig. 1). Loss of *arr* activity produced a strong r1 EC deficit (5% vs 16%
1148 control) and a substantial FSC surfeit (84% vs 55%) even from 2d prior to eclosion, showing that

1149 normal Wnt signaling influences A/P movement of precursors in the last two days of pupal
1150 development. The excess frequency of FSCs among ECs and FSCs for *arr* relative to controls averaged
1151 over -2d and -3d clone initiation times was 32%; it was 64% averaged over -6d and -5d initiation
1152 points. (Supplementary Fig. 1 and supporting information spreadsheet). These data suggest that loss
1153 of Wnt activity, and hence normal Wnt signaling, has an effect on cell location within EC/FSC
1154 precursor territory, as well as on terminal FC precursors, early in pupal development. The above
1155 deductions have the limitation that they are based on FSC or r1 EC representation among non-FC
1156 precursors rather than all precursors. Both *axn* and *arr* alter the proportion of precursors that
1157 become FCs and the magnitude of this effect may vary during pupation, contributing to changes in
1158 the measured representation of FSCs and r1 ECs over time.
1159
1160 **Pattern of Wnt pathway activity during pupal ovary development; an A/P gradient**
1161
1162 Wnt pathway activity in adult germaria, measured with a Fz3-RFP reporter that responds to
1163 genetic pathway manipulations in that tissue (WANG AND PAGE-MCCAW 2014; DAI *et al.* 2017; REILEIN *et*
1164 *al.* 2017), is uniformly high in ECs and declines over the FSC domain to zero in the earliest FCs (Fig.
1165 5L). The sources of Wnt in the adult germarium include high levels of Wg and Wnt6 production in Cap
1166 cells and lower levels of Wnt 2 and Wnt4 in ECs (SAHAI-HERNANDEZ AND NYSTUL 2013; WANG AND PAGE-
1167 MCCAW 2014; WANG AND PAGE-MCCAW 2018).
1168 In pupal germaria, Fz3-RFP was first detected 27h APF and showed a marked increase in
1169 intensity between 36h and 48h (Fig. 5A-G, J). At all stages, Fz3-RFP was higher in anterior than
1170 posterior regions, consistent with the possibility that Cap Cells, which are specified at the anterior of
1171 the germarium very close to the start of pupation, and even developing EC precursors, may be major
1172 sources of Wnt ligand, as in the adult. The delay in reaching high levels of pathway activity might be
1173 due to maturation of Cap Cell properties but is perhaps more likely due to functional differentiation
1174 of ECs from precursors, most of which cease division, starting from the anterior, by 48h of pupation
1175 (REILEIN *et al.* 2021). At 48h APF the spatial decline in Fz3-RFP was spread over the posterior two-
1176 thirds of the germarium (Fig. 5G, J). By 60h APF, the domain of consistently high Fz3-RFP expression
1177 occupied a larger anterior territory, extending roughly halfway to the region of strong Fas3
1178 expression, followed by a steeper decline to background levels (Fig. 5H, K). At all stages, the anterior
1179 border of strong Fas3 expression coincided with very low levels of Wnt pathway reporter activity. In
1180 adult germaria and in pupal ovarioles prior to release of the first germline cyst, cells at, and posterior
1181 to, the strong Fas3 border have committed to becoming FCs. The persistent coincidence of this Fas3
1182 border with a decline of Wnt pathway activity to near zero suggests that low Wnt signaling may be a
1183 pre-requisite for FC formation at all stages. This hypothesis is supported by the near-complete block
1184 of FC formation during pupal development in *axn* mutant precursors and the increased propensity of
1185 *arr* mutant precursors to form FCs throughout pupal development. These responses to altered
1186 signaling appear to be mediated by net A/P migration throughout the precursor domain. Thus, *arr*
1187 mutant cells are not depleted immediately anterior to potential FC-producing zones because there is
1188 also enhanced migration to those positions from the EC precursor domain; in fact, adult FSC
1189 production from *arr* precursor cells was increased overall. Conversely, *axn* mutant cells that do not
1190 become FCs do not accumulate extensively in the neighborhood of FSCs; there was, instead, a net
1191 loss of FSC fates in favor of EC production.
1192

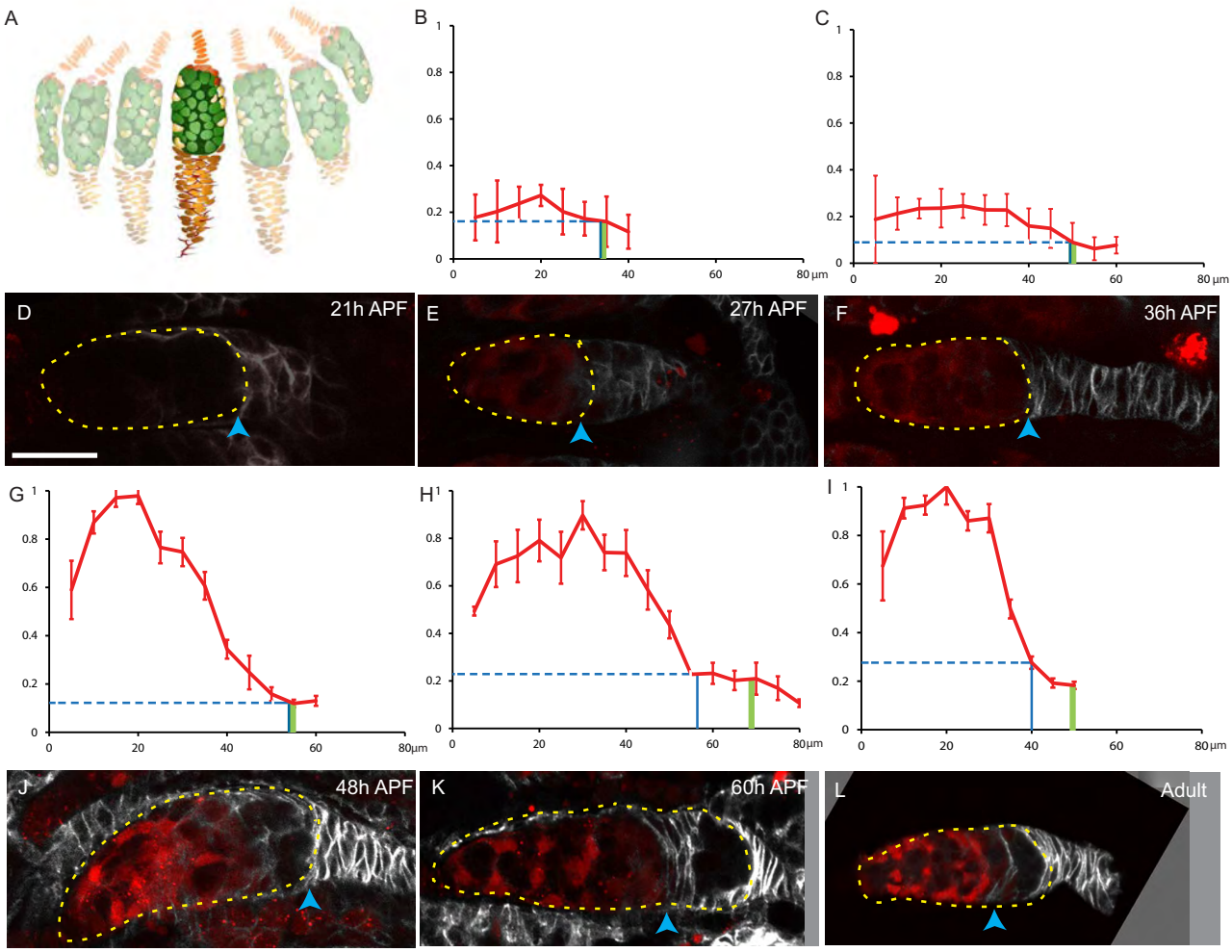

Figure 5: Development of a Wnt signaling gradient in pupal germaria.
(A-L) Results from pupae expressing Fz3-RFP as a reporter for Wnt pathway activity. **(A)** Diagram of a 30h APF ovary. An individual germarium is highlighted with anterior at the top. **(D-F, J-L)**. Individual germaria at the noted stages, oriented anterior to the left, with the germarial region (containing germline cells) outlined in yellow and the anterior border of strong Fas3 staining indicated by a blue arrowhead. Samples were stained for Fas3 (white) and pupal samples were imaged intact, without separating developing ovarioles. **(B, C, G-I)** RFP profiles were constructed by measuring RFP intensities (y-axes) at 5 µm intervals along the edge of the germarium where most somatic cell bodies are located, starting adjacent to Cap Cells (0 on x-axes) and moving posteriorly. Individual germaria varied in RFP brightness and therefore the profile for each germarium was normalized to the brightest cell in that germarium. Normalized curves were averaged and SEM calculated to show the average Fz3-RFP profiles derived from germaria at **(B)** 27h APF (n=50 cells in 7 germaria), **(C)** 36h APF (n=108 cells in 14 germaria), **(G)** 48h APF (n=138 cells in 15 germaria), **(H)** 60h APF (n=178 cells in 14 germaria) and **(I)** adults (n=178 cells in 14 germaria). The average location of the border of strong Fas3 expression (blue vertical line), Fz3-RFP levels at that location (horizontal dashed line) and the location of the average posterior end of the germline cells in the germarium (green vertical line; measured from the Cap Cells to the central point at the posterior of the germline) are indicated. **(D-F, J-L)** Multiple z-sections were combined in a maximum intensity projection to show Fz3-RFP in cells along the length of germaria. **(D)** Fz3-RFP was not detected at 21h APF, **(E)** was present at low levels with an anterior bias at 27h (4 µm-thick z projection) and **(F)** at 36h APF (5 µm-thick z projection) before **(J)** accumulating to high anterior levels with a steep decline ending close to the strong Fas3 border at 48h APF (4 µm-thick z projection) and **(K)** 60h-APF (5 µm-thick z projection), similar to **(L)** the profile in newly-eclosed adults (10 µm-thick z projection). Scale bar of 20 µm applies to all images. For raw data please see supplementary spreadsheet titled Fig5 Fz3RFP Graph.

1217 **JAK-STAT activity promotes FC formation and favors more posterior ovarian precursor fates**
1218
1219 In Drosophila, Unpaired ligands activate a receptor to promote cross-phosphorylation and
1220 activation of the receptor-associated Janus kinase (JAK), Hopscotch (Hop), followed by
1221 phosphorylation and activation of the STAT transcription factor (ZEIDLER AND BAUSEK 2013). The effect
1222 of altered JAK-STAT signaling was explored using a strong loss of function *stat* mutation and
1223 overexpression of Hop, as used in studies of adult FSC behavior (VIED *et al.* 2012; MELAMED AND
1224 KALDERON 2020). The spectrum of adult derivatives of *stat* mutant precursors induced at pupariation
1225 was very similar to that of *axn* mutant cells. There was a drastic loss of lineages with any marked
1226 terminal FCs (2% vs 22%), of FC-only lineages (4% vs 17%) and of lineages with FSCs (5% vs 15%),
1227 while EC-only lineages (90% vs 63%) increased greatly in frequency (Fig. 6A, B, G). However, in
1228 contrast to the behavior of *axn* mutant cells, the frequency of lineages containing only r1 ECs (46% vs
1229 49% control) or at least one r1 EC (64% vs 67% control) was not increased for *stat* mutant cells (Fig.
1230 6G). The frequency of labeled ovarioles was similar for *stat* mutant cells (43%) and the direct control
1231 (47%) in the same experiment, suggesting that marked cells had not been lost extensively. Thus, we
1232 deduce that all precursors posterior to EC-producing territory have preferentially moved anteriorly
1233 during pupal development in response to loss of JAK-STAT pathway activity, leading to a near-
1234 absence of posterior derivatives, FSCs and FCs.
1235 We also examined *stat* mutant lineages induced at 36h APF. As for *axn*, marked ovarioles with
1236 labeled terminal FCs (38%) were now as frequent as for controls (31%) (Fig. 6F; Supplementary
1237 spreadsheet "-3.5d stat November 2021 Numbers**"**), consistent with a conclusion that JAK-STAT
1238 signaling is critical in the first 48h of pupation for promoting posterior migration of precursors out of
1239 the germarium into the EGC and basal stalk. Marked ovarioles with labeled FSCs were very rare (3%
1240 vs control 13%) and the fraction of all labeled ECs and FSCs that were FSCs was much reduced (3% vs
1241 control 21%), as for lineages induced at pupariation. This is consistent with the possibility that JAK-
1242 STAT signaling is required for FSC formation during the second half of pupation, perhaps by
1243 promoting cell division.
1244 Expression of a *UAS-Hop* gene at 29C (or two copies at 25C) in adult FSCs leads to increased
1245 JAK-STAT activity and a variety of strong phenotypes, including increased FSC division and
1246 differentiation to FCs (VIED *et al.* 2012; MELAMED AND KALDERON 2020). In adults, the effects of increased
1247 JAK-STAT activity on cell location and differentiation could be studied in the absence of greatly
1248 altered cell division by co-expressing the CycE-Cdk2 inhibitor Dacapo (Dap) (LANE *et al.* 1996; MELAMED
1249 AND KALDERON 2020). Adult ovaries included very large numbers of labeled cells in *UAS-Hop* lineages
1250 induced at pupariation (Fig. 6D), indicating greatly increased cell division. The highly populated
1251 lineages included anterior, EC regions, which normally only include 2-4 marked cells. In adult ovaries,
1252 excess JAK-STAT can stimulate significant division in otherwise quiescent cells in the EC domain (VIED
1253 *et al.* 2012; MELAMED AND KALDERON 2020). The abundance of marked cells in pupal lineages precluded
1254 useful classification into clone types, other than noting that almost all lineages included ECs, FSCs and
1255 FCs.
1256 We therefore added *UAS-Dap*. MARCM clones induced at pupariation to initiate *UAS-Hop* (and
1257 *UAS-Dap*) expression might be expected to increase JAK-STAT activity only after a delay. However, we
1258 found that the fraction of lineages that included terminal FCs was increased significantly (50% vs 22%,
1259 Fig. 6G), suggesting that increased JAK-STAT promotes terminal FC production and that the transgene
1260 markedly alters JAK-STAT activity within the first 48h after clone induction. Precursors with increased
1261 JAK-STAT activity also produced an increased proportion of lineages containing FSCs (29% vs 15%)
1262 (Fig. 6C), while greatly reducing the frequency of EC-only lineages (40% vs 63%), r1 only lineages (33%

vs 49%) and lineages containing any r1 ECs (48% vs 68%) (Fig. 6G). The average number of cells in EC-only *UAS-Hop UAS-Dap* lineages was lower than for controls (1.1 vs 2.7). This is likely partly because many of the more posterior precursors that would normally produce only ECs shifted posteriorly to also produce FSCs (and FCs), so that EC-only lineages derived from only the most anterior precursors, which are the first to terminate division. The average number of ECs and FSCs in EC/FSC/FC lineages was similar to controls for *UAS-Hop UAS-Dap* lineages (8.0 vs 7.9 cells). Altogether, precursor division rates were likely similar to controls for this genotype, suggesting that the increase in FSC representation was due to direct effects on cell migration and not an increase in cell division rate, as observed for excess CycE expression.

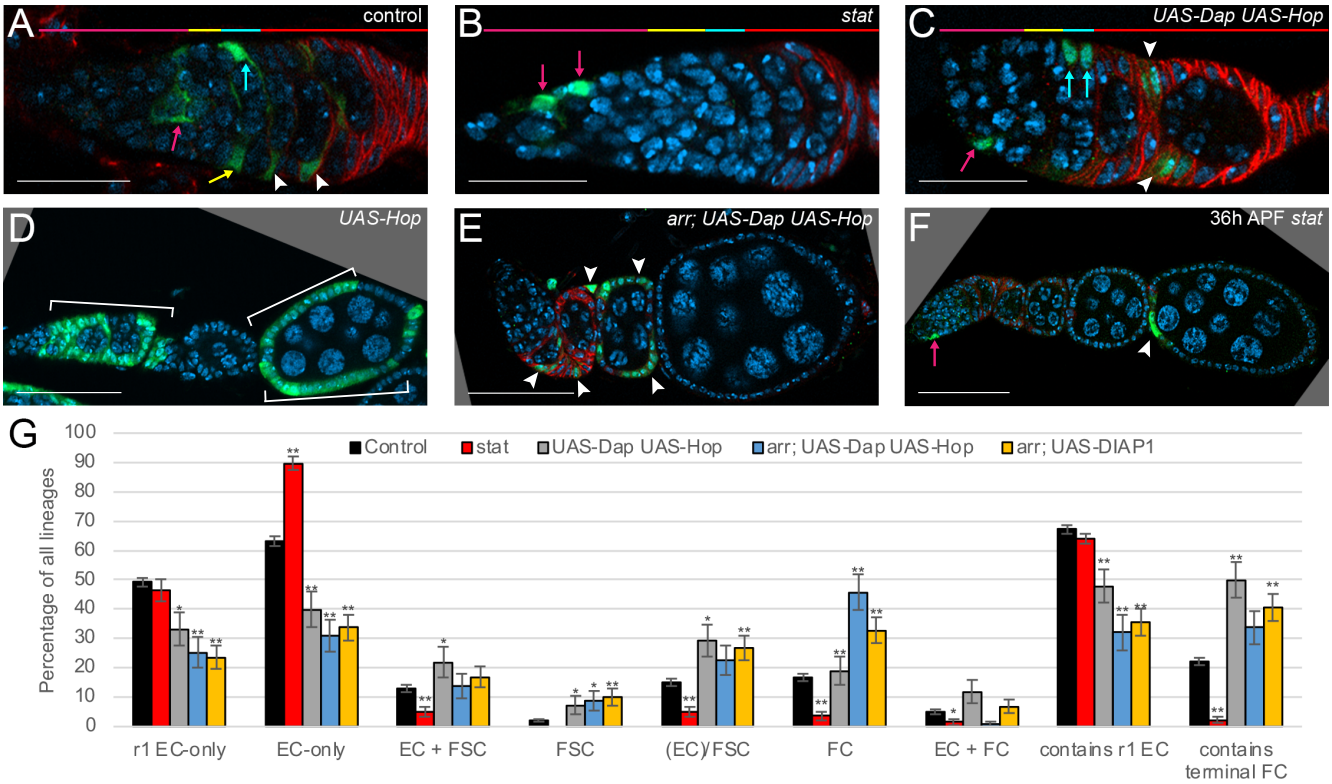

Figure 6: JAK-STAT pathway promotes posterior migration of precursors during pupation.
(A-F) Representative lineages induced at (**A-E**) 0h APF or (**F**) 36h APF for the indicated genotypes. White arrowheads indicate Follicle Cells; magenta arrows, r1 ECs; yellow arrows, r2a ECs; cyan arrows, FSCs. DAPI, blue; GFP, green; Fas3, red. (**A-C**) The r1 EC, r2a EC**,** FSC and FC domains are shown in corresponding colors in the horizontal bars above. **(A)** control EC/FSC lineage that includes r1 ECs, **(B)** *stat* EC-only lineage, **(C)** *UAS-Dap UAS-Hop* EC/FSC/FC lineage, **(D)** *UAS-Hop* lineage, illustrating an exceptionally high number of marked cells, likely due to increased cell division, and **(E)** *arr; UAS-Dap UAS-Hop* lineage, illustrating the common FC-only lineage outcome. **(F)** A *stat* lineage induced at 36h APF illustrating terminal FC marking, which is virtually absent for *stat* lineages induced at 0h APF. Scale Bar 20 µm for **(A-C)** and 50 µm for **(D-F)**. **(G)** Deduced frequency of the indicated types of single-cell lineage as a percentage of all lineages induced at 0h APF. Error bars show SEM. One asterisk (*) indicates p<0.05; two asterisks (**) indicates p<0.005 (Fisher's two-tailed exact test). Number of marked ovarioles = 739 (control), 142 (*stat*), 50 (*UAS-Dap UAS-Hop*), 57 (*arr; UAS-Dap UAS-Hop*), 95 (*arr; UAS-DIAP1*). For raw data and calculations please see supplementary spreadsheets titled 0h APF Graphs Fig4-10; Compilation of Numbers Figure 6 JAK-STAT.

Thus, increased JAK-STAT activity has the potential to promote posterior movement of all precursors, even from the most anterior r1 EC-producing locations. The restriction of the opposite phenotype for *stat* loss of function to cells posterior to the EC-producing domain (i.e., no increase in r1 EC-containing lineages) suggests that anterior regions of the developing ovariole may not normally experience significant levels of JAK-STAT signaling.

1293 We examined JAK-STAT pathway activity using reporters containing either ten tandem STAT
1294 binding sites upstream of GFP (BACH *et al.* 2007) or STAT-responsive promoter sequences from the
1295 Socs36E gene upstream of RFP (HE *et al.* 2019). Both reporters showed similar patterns in adult
1296 ovaries (MELAMED AND KALDERON 2020) and in pupal ovaries. There was very strong fluorescence
1297 surrounding each developing ovariole in both cases but this did not prevent signal detection in
1298 individual confocal sections of the developing ovarioles themselves (Fig. 7 and Supplementary Fig. 2).
1299 Activity was first detected clearly at about 30h APF, strongest around and anterior to the border
1300 between Fas3-positive and Fas3-negative somatic cells (Fig. 7A). Thereafter, reporter activity
1301 increased and spread posteriorly into Fas3-positive cells. The signal was lower in the anterior half of
1302 the developing germarium than in more posterior Fas3-negative somatic cells (Fig. 7B-D). These
1303 results are not sufficient to point to a specific cellular source of ligand. However, Fas3-positive cells
1304 are among the candidates. They may themselves initially be less responsive to ligand than Fas3-
1305 negative cells but reporter activity was as strong in Fas3-positive cells as in their anterior neighbors
1306 by 36h APF and thereafter (Fig. 7B-D; Supplementary Fig. 2). The higher pathway activity observed in
1307 somatic cells around, and posterior to, the three or four most mature germline cysts is consistent
1308 with the possibility that pathway activity in this region is necessary for a cell to maintain its position
1309 or to promote more posterior migration in order to seed FCs of the first budded egg chamber. We did
1310 not observe a clear gradient within this region (Fig. 7A-D).
1311 Shortly after the most posterior germline cyst had left the germarium to form the first egg
1312 chamber (around 60h APF), somatic cells anterior to that cyst had particularly strong reporter activity,
1313 similar to nascent stalk cells during adult oogenesis (Supplementary Fig. 2). By that time, both Castor
1314 staining and higher Fas3 staining than in surrounding cells indicate the presence of polar cells in the
1315 first egg chamber (REILEIN *et al.* 2021). Polar cells were similarly evident in the second egg chamber by
1316 about 84h APF, with strong STAT-GFP reporter activity in nearby somatic cells (Supplementary Fig. 2).
1317 The STAT-GFP signal extending into the germarium at 84h APF was significantly stronger than at
1318 earlier times and strongly resembled the adult pattern, with very little activity anterior to region 2a
1319 cysts (Supplementary Fig. 2). It is possible that the higher STAT-GFP signal is due to polar cells
1320 contributing JAK-STAT ligand. However, the overall spatial pattern of STAT-GFP was similar earlier and
1321 it is possible that the technical necessity of maintaining an intact ovary during dissection and staining
1322 of early pupal ovaries (rather than releasing individual ovarioles) limited GFP detection by antibody
1323 prior to 84h APF. Thus, there clearly is detectable JAK-STAT pathway activity prior to any polar cell
1324 formation in a pattern that largely excludes the anterior half of the developing germarium. It also
1325 appears that this pattern is significantly enhanced once polar cells have formed in the second budded
1326 egg chamber. The minimal levels of JAK-STAT pathway activity in anterior regions throughout the
1327 pupal period are consistent with the observation that marked r1 EC frequency is not altered by the
1328 absence of STAT activity, even though ectopic JAK-STAT can convert their precursors to adult cells in
1329 more posterior locations.
1330 In adults, altering JAK-STAT activity in either direction greatly affects the division rate of FSCs,
1331 while excess JAK-STAT can promote significant division of otherwise quiescent ECs (MELAMED AND
1332 KALDERON 2020; MELAMED *et al.* 2023). During pupation, loss of STAT activity barely altered the average
1333 number of cells in EC-only lineages (2.5 vs 2.7). This is likely partly because some of the precursors
1334 were originally in more posterior locations and set to divide faster. It is also consistent with the lack
1335 of net migration of r2a EC precursors to become r1 ECs and the observation of only low JAK-STAT
1336 activity in the normal EC precursor domain. There were insufficient *stat* mutant lineages in terminal
1337 egg chambers to measure average FC occupancy and insufficient FSC-containing lineages to measure
1338 the average number of marked ECs and FSCs. Thus, the strong anterior movement of *stat* mutant

derivatives precluded direct measurement of the normal role of JAK-STAT signaling in supporting the division of posterior precursors through pupation.

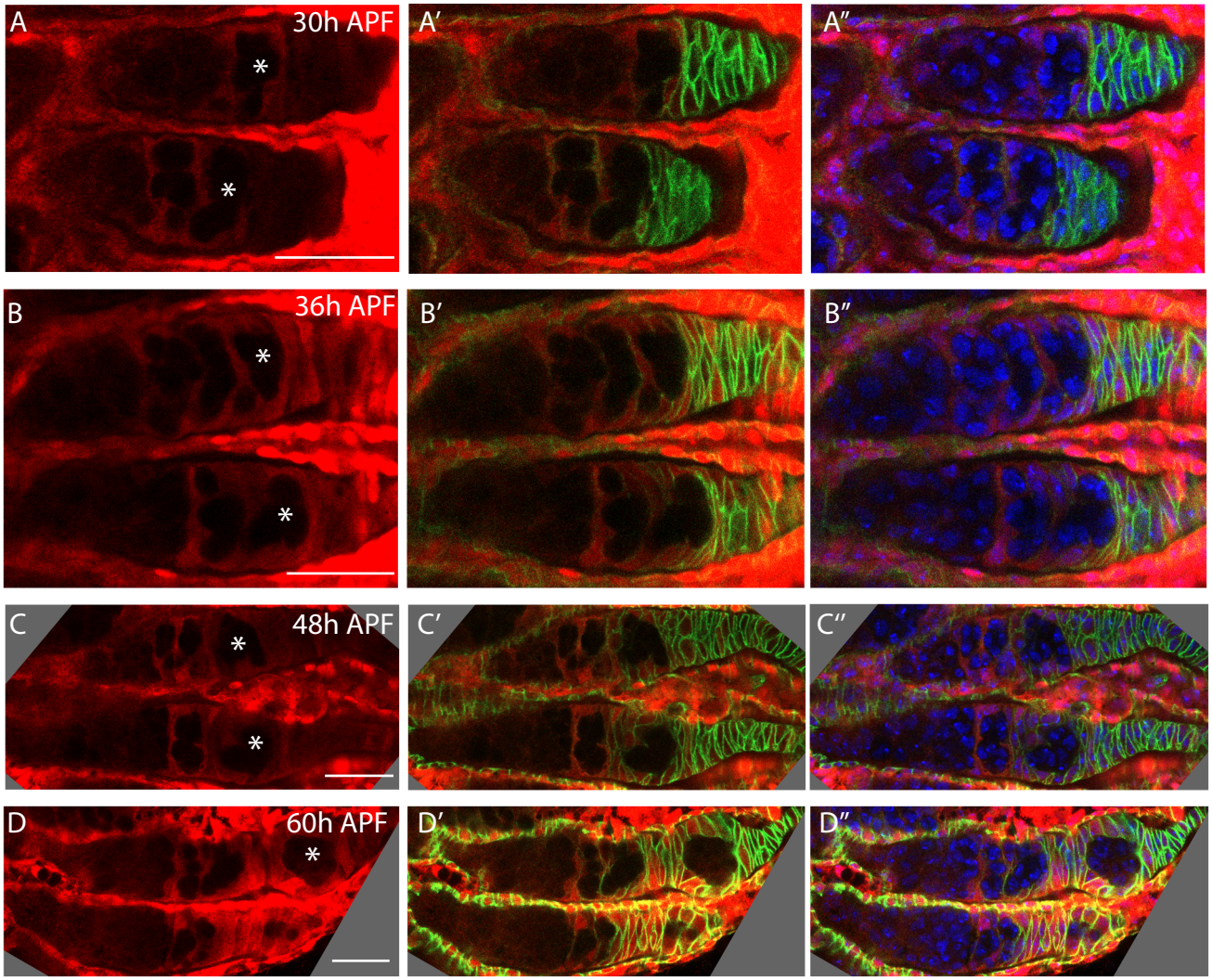

Figure 7: JAK/STAT signaling in pupal ovaries.
(A-D) Pupal ovaries expressing STAT-RFP were stained for RFP (red), Fasciclin 3 (green), and with DAPI (blue). STAT-RFP was strongly expressed in epithelial sheath cells surrounding each developing germarium and the entire ovary. STAT-RFP was first detectable in developing germaria at 30h APF, and increased in intensity over time. **(A)** At 30h APF, STAT-RFP was detected at low levels around the most mature cysts in the germarium and in the most anterior Fasciclin III-expressing cells posterior to the germarium (in the Extra-Germarial Crown (EGC)). **(B-D)** From 36h APF to 60h APF, STAT-RFP expression was seen around the most mature egg chambers and throughout the EGCs and basal stalks. **(D)** At 60h APF, STAT-RFP was also seen in follicle cells of the budding egg chamber. The most mature cyst in each germarium is marked with an asterisk. Scale Bars, 20 µm.

Since loss of Wnt and increased JAK-STAT signaling have similar outcomes of promoting posterior precursor movement, it might be expected that combining these changes would produce still stronger phenotypes, as seen for adult FSCs. Adding *UAS-Hop UAS-Dap* to loss of *arr* produced very little change in the various measured parameters, other than an increase in FC-only lineages (46% vs 33%, Fig. 6E, G). Comparison of the phenotype of *arr UAS-Hop UAS-Dap* with *UAS-Hop UAS-Dap* is less straightforward for technical reasons: the clone frequency for the latter genotype was

significantly higher, likely leading to incomplete resolution of double clones (suggested also by the comparatively high EC+FC frequency of 12% vs the exceptionally low value of 1% for the former genotype). Nevertheless, there are some clear changes imposed by loss of Wnt signaling. The frequency of r1 EC-only clones (25% vs 33%) and lineages containing any r1 ECs (32% vs 48%) was reduced, while the frequency of FC-only lineages was increased (46% vs 19%; or 47% vs 31% if EC+FC lineages are included), as was the fraction of lineages containing FCs but no FSC (46% vs 28%). These indicate greater posterior shifts for precursors in the normal EC and FSC producing domains. The effect on terminal FC production is less clear, likely because of the difference in clone frequencies and consequent limitations in deducing single lineages. Overall, the formation of terminal FCs, already increased by raising JAK-STAT activity, does not appear to be enhanced by additional elimination of Wnt pathway activity, contrasting with the effects on precursors in more anterior locations. Altogether, the loss of Wnt signaling was more influential in anterior regions, while excess JAK-STAT had a greater influence in more posterior regions. A similar conclusion was made regarding the much narrower spatial domain of FSCs in adults (MELAMED AND KALDERON 2020).

Yki activity primarily affects ovarian precursor survival and cell division

We were interested in examining the roles of Hedgehog (Hh) signaling and the Hippo/Yorkie pathway for two reasons. First, both have major inputs into adult FSC division rates (HARTMAN *et al.* 2013; HUANG AND KALDERON 2014; HSU *et al.* 2017) and we hoped to learn more about the regulation of somatic ovarian precursor proliferation. In adults, Hh stimulates FSC cell division through Yorkie (Yki) (HUANG AND KALDERON 2014). Second, Hh ligand is known to emanate from anterior locations in pupal ovaries (LAI *et al.* 2017), so that it might influence precursor cell migration, even though neither Hh nor Yki are known to have a significant effect on the migration or differentiation of adult FSCs.

Yki is a transcriptional co-activator frequently implicated in the regulation of cell and tissue growth. Yki activity is generally regulated, principally through inactivating phosphorylation, by upstream members of the Hippo (Hpo) pathway, including Hpo and Warts (Wts) protein kinases and a variable assortment of more upstream proteins (including Kibra) capable of sensing mechanical stimuli, including tension (MISRA AND IRVINE 2018). However, in adult ovaries, Yki is also transcriptionally regulated by the Hh signaling pathway (HUANG AND KALDERON 2014). In adult FSC lineages, loss of *yki* resulted in reduced division, increased apoptosis and rapid loss of FSCs. FSC maintenance was substantially improved by expression of excess CycE and excess DIAP1, both known transcriptional targets of Yki, to counter those deficiencies (HUANG AND KALDERON 2014).

When *yki* mutant lineages were induced at pupariation, the proportion of ovarioles with labeled cells was lower (19%) than for the direct side-by-side control (37%) but this deficit was largely restored by addition of *UAS-DIAP1* (32%) to inhibit apoptosis. Both the reduction relative to controls for *yki* (13% vs 59%) and restoration by *UAS-DIAP1* (to 60%) were observed in a second experiment. Although variation in the frequency of clone induction is potentially quite high because of the brief and moderate heat-shock protocol, these results suggest that some *yki* mutant lineages are lost to apoptosis during pupal development.

For each experiment, FSCs were rarely present in either *yki* (0% and 6%) or *yki; UAS-DIAP1* lineages (4% and 3%) relative to control averages (15%) (Fig. 8A, H). For *yki; UAS-DIAP1*, there was no significant difference in the fraction of lineages with either r1 ECs or terminal FCs relative to controls. This suggests that there is no strong overall A/P shift in precursor outcomes, contrasting with manipulations of Wnt or JAK-STAT pathways, and that FSC loss is therefore most likely to result from reduced division rates, as observed for *cycE* and *cutlet* mutations.

1406

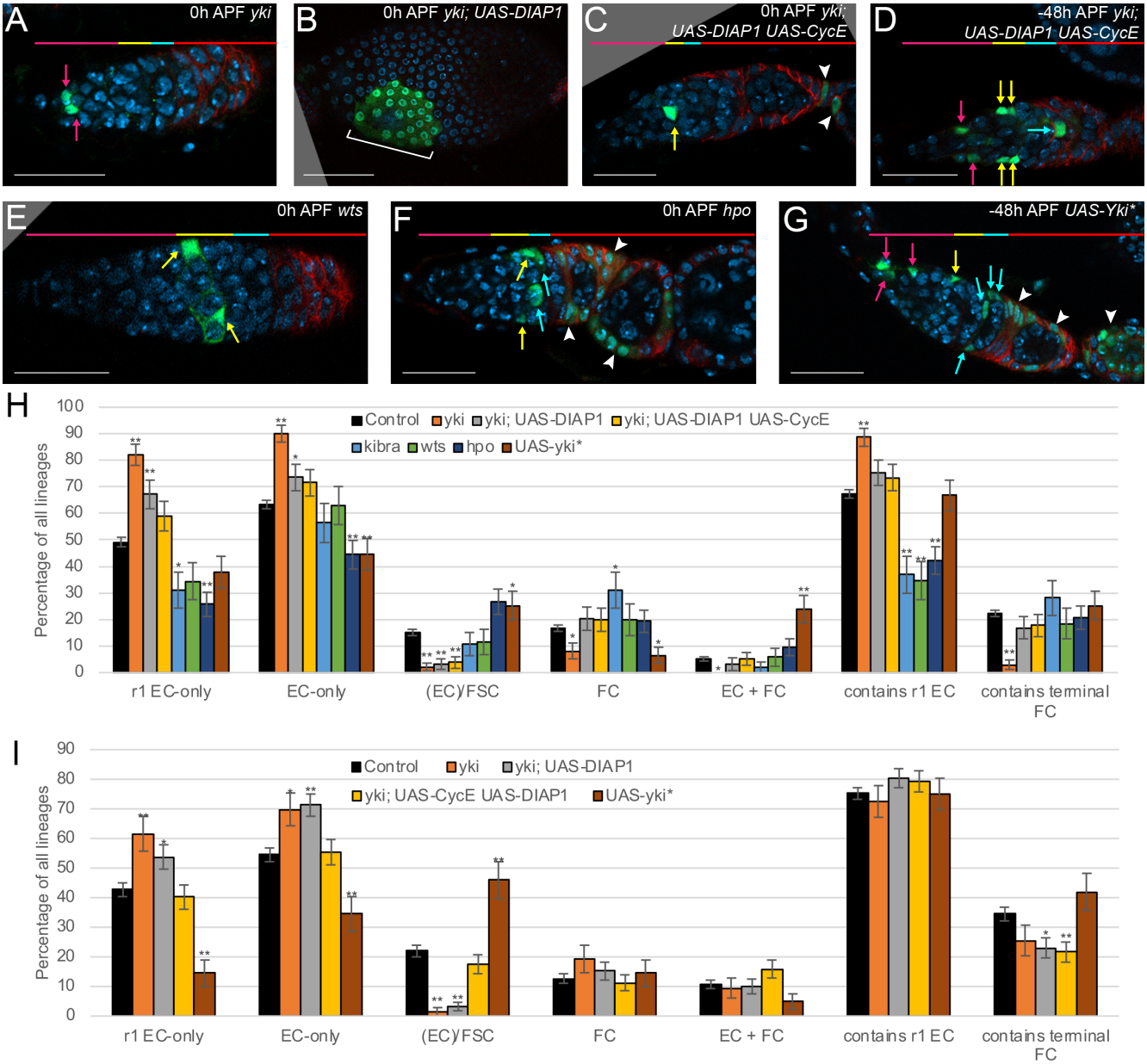

1407
1408 **Figure 8: Yki activity counters posterior derivative cell apoptosis, and promotes cell division rate to increase FSC**
1409 **representation.**
1410 **(A-G)** Representative lineages induced at (**A-C, E, F**) 0h APF or (**D, G**) 48h before pupariation for the indicated genotypes.
1411 White arrowheads indicate Follicle Cells; magenta arrows, r1 ECs; yellow arrows, r2a ECs; cyan arrows, FSCs. DAPI, blue;
1412 GFP, green; Fas3, red. The r1 EC, r2a EC**,** FSC and FC domains are shown in corresponding colors in the horizontal bars
1413 above images other than **(B)**. **(A)** *yki* commonly produced EC-only lineages, whereas **(B)** the addition of *UAS-DIAP1* greatly
1414 increased the representation of FCs, including terminal FCs, as shown here. **(C-D)** The further addition of *UAS-CycE*
1415 restored FSC-containing lineages for clones induced at **(D)** 48h before pupariation, as shown here, but not at **(C)** 0h APF;
1416 here showing an EC+FC lineage, characteristic of FSC loss. When *yki* mutant cells became FCs (generally requiring the
1417 presence of *UAS-DIAP1*)), they were frequently polar cells (arrowheads in **(C)**) but sometimes produced small patches of
1418 main-body FCs, as in **(B)**. **(E-G)** show lineages with increased Yki activity. **(E)** a *wts* lineage, illustrating the common r2a EC-
1419 only lineage, owing to a reduction in r1 EC fates, and **(F)** a *hpo* lineage, illustrating the increased frequency of EC/FSC/FC
1420 lineages, again in the absence of r1 ECs. **(G)** A UAS-Yki* (S168A) EC/FSC/FC lineage induced 48h before pupariation,
1421 illustrating the increase in such lineages and a large number of labeled cells, indicative of increased division rates. Scale
1422 Bar 20 µm for **(A, C-G)** and 50 µm for **(B)**. **(H, I)** Deduced frequency of the indicated types of single-cell lineage as a

1423 percentage of all lineages induced at **(H)** 0h APF and **(I)** -48h APF. Error bars show SEM. One asterisk (*) indicates p<0.05;
1424 two asterisks (**) indicates p<0.005 (Fisher's two-tailed exact test). (**H**) Number of marked ovarioles = 739 (control), 84
1425 (*yki*), 127 (*yki; UAS-DIAP1*), 67 (*yki; UAS-DIAP1 UAS-CycE*), 44 (*kibra*), 42 (*wts*), 82 (*hpo)*, 49 (*UAS-Yki**). (**I**) Number of
1426 marked ovarioles = 319 (control), 57 (*yki*), 101 (*yki; UAS-DIAP1*), 94 (*yki; UAS-CycE UAS-DIAP1*), 85 (*UAS-yki**). For raw data
1427 and calculations please see supplementary spreadsheets titled 0h APF Graphs Fig4-10; -2d APF Graphs**;** Compilation of
1428 Numbers Figure 8 yki hpo -5d; Compilation of Numbers Figure 8 yki hpo -5d.
1429
1430 Other changes in lineage outcomes suggest that loss of Yki does have some effect on final A/P
1431 cell locations, either by affecting precursor migration or spatially selective apoptosis. FC-only lineages
1432 were seen at lower frequency for *yki* (6% and 10%) relative to controls (average 17%), with no
1433 increase of EC/FC lineages (1% and 0% vs 5% for controls); correspondingly, there was a large
1434 increase in EC-only clones (95% and 86% vs 63% for controls). For *yki; UAS-DIAP1*, however, the
1435 average frequency of FC-only (20% vs 17%) and EC/FC lineages (3% vs 5%) was similar to controls.
1436 Addition of *UAS-CycE* together with *UAS-DIAP1* also resulted in frequencies of FC-only (20%) and
1437 EC/FC lineages (5%) similar to controls. Thus, the addition of *UAS-DIAP1* restored FC representation,
1438 including terminal FCs to control levels in two separate genetic tests, suggesting that posterior
1439 (would-be FCs) derivatives preferentially die in the absence of Yki. A caveat to this conclusion is that
1440 the restoration of FC lineages by *UAS-DIAP1* was seen only in one of two experiments for *yki; UAS-*
1441 *DIAP1* (5% and 35% for FC-only; 4% and 2% for EC/FC) (Fig. 8B, H). Moreover, the FC deficit seen for
1442 *yki* (with no *UAS-DIAP1*) in both experiments was not reproduced for lineages initiated 2d before
1443 pupariation (see below). A plausible explanation is that both a posterior bias of apoptosis induced by
1444 loss of Yki and elimination of that bias by addition of DIAP1 are variable (perhaps poised close to a
1445 threshold). In that case, the modest increase of EC-only lineage proportion and failure of lost FSC
1446 lineages to be converted to FC lineages for *yki; UAS-DIAP1*, as expected for reduced division, may be
1447 due to some residual preferentially posterior apoptosis, with no underlying direct effect of loss of Yki
1448 on A/P cell migration.
1449 To examine further whether loss of lineages with FSCs was due to lower division rates, we
1450 tested the effect of adding *UAS-CycE* to *yki; UAS-DIAP1* lineages. This did not substantially restore
1451 FSCs (present in only 4% of lineages, Fig. 8C) for lineages induced at pupariation. However, the
1452 MARCM system introduces a delay in the accumulation of *UAS-CycE* product because perduring
1453 GAL80 gene products must first be diluted or degraded. When lineages were induced 2d prior to
1454 pupariation the frequency of FSC-containing lineages was increased from 1% (*yki*) and 3% (*yki; UAS-*
1455 *DIAP1*) to 18% (Fig. 8D), closer to the control average of 22% (Fig. 8I), suggesting that reduced division
1456 is indeed the primary reason for the deficit of FSCs in *yki* mutant lineages.
1457 Other results from lineages induced 2d before pupariation showed some similarities and some
1458 differences to results from lineages induced at pupariation. The frequency of marked ovarioles for
1459 *yki; UAS-DIAP1* (74%) and *yki; UAS-CycE UAS-DIAP1* (73%) were once again higher than for *yki* (43%),
1460 suggesting some apoptotic loss of lineages for loss of Yki activity. The frequency of lineages with FCs
1461 but no FSCs (FC-only plus EC/FC) was similar to controls (23%) for the two types of *yki* lineage
1462 expressing DIAP1 (25% and 27%), as noted for clones induced at pupariation. However, *yki* lineages
1463 produced a similar result (28%) (Fig. 8I), rather than a reduction of these FC lineages, as observed for
1464 clones induced at pupariation (Fig. 8H). The fraction of lineages with labeled terminal FCs was also
1465 similar among all three *yki* genotypes (25%, 23% and 22%). Interestingly, these three values were all
1466 somewhat lower than the control average of 35%. This difference is particularly notable for the *yki;*
1467 *UAS-CycE UAS-DIAP1* genotype because all other lineage characteristics are similar to controls. Thus,
1468 loss of Yki results in reduced division, leading to a severe loss of FSCs, apoptosis with variable
1469 posterior cell (FC) selectivity, and a small decline in lineages with terminal FCs.

1470 In all cases, FCs that lacked *yki* function shared some characteristics. Labeled cells were
1471 preferentially found only in polar cells (most commonly), stalk cells or the basal stalk (Fig. 8C, data
1472 not shown). Labeled FCs in other locations were approximately equally split between two categories:
1473 either a pair of cells with strongly elevated Fas3, resembling ectopic polar cells, or a relatively normal
1474 FC patch (Fig. 8B). Adult-induced lineages were previously described as frequently including polar
1475 cells or ectopic polar cells (CHEN *et al.* 2011). Our results suggest that loss of *yki* greatly increase the
1476 chances that a FC derivative acquires the position or characteristics of a precursor of stalk and polar
1477 cells; cells that nevertheless become main-body FCs can develop further in a relatively normal fashion
1478 despite the absence of *yki* activity.
1479 The consequences of increasing Yki activity were examined using strong loss of function alleles
1480 for upstream regulators that can limit Yki activity. *kibra*, wts and *hpo* lineages, induced at pupariation,
1481 shared the phenotype of a reduced fraction of both r1 EC-only lineages (31% *kibra*, 34% *wts* and 26%
1482 *hpo* vs 49% control) and lineages containing any r1 ECs (37%, 35% and 42% vs 67%, respectively) (Fig.
1483 8H). These manipulations did not reproducibly change the proportion of lineages with marked
1484 terminal FCs (28%, 18% and 21% vs 22% control), while only specific mutations increased the
1485 proportion of lineages with FSCs (*hpo*; 27% vs 15%; others were 11%) (Fig. 8E, F, H). Neither the
1486 number of cells in EC-only lineages (*kibra* 1.8, *wts* 1.8 and *hpo* 2.2 vs control 2.7), nor the average
1487 sum of ECs and FSCs in EC/FSC/FC lineages were increased by these mutations (7.3, 9.8, 6.8 vs control
1488 8.6). Thus, it appears that cell division rates were not significantly increased.
1489 We also tested the effects of expressing a Yki derivative (Yki-S168A [*UAS-Yki**]) partially
1490 resistant to down-regulation by upstream pathway components (CHEN *et al.* 2011; HUANG AND
1491 KALDERON 2014). This resulted in an increase in lineages with FSCs (25% vs 15% control), as for *hpo*
1492 (but not the other Hpo pathway mutations), consistent with an expected consequence of an
1493 increased division rate. UAS-Yki* also produced a slightly reduced fraction of r1 EC-only lineages
1494 induced at pupariation (38% vs 49% control) but a normal fraction of lineages with any r1 ECs (67% vs
1495 67%) (Fig. 8H). The former decrease might simply be a consequence of increased division expanding
1496 some of the most anterior clones into region 2a.
1497 In *UAS-Yki** lineages initiated 2d before pupariation, the frequency of r1 EC-only (15% vs 43%)
1498 and EC-only lineages (35% vs 55%) was greatly reduced while lineages with marked FSCs were greatly
1499 increased (46% vs 22%) (Fig. 8G, I). Lineages with any marked r1 ECs (75% vs 75%) or terminal FCs
1500 (42% vs 35% control) were not greatly changed in frequency. The average size of EC-only clones (3.5
1501 vs 3.2) and the average number of ECs and FSCs in EC/FSC/FC clones (17.9 vs 14.5) were slightly
1502 increased. These results suggest that *UAS-Yki** is more effective when induced prior to pupariation,
1503 allowing an increase in cell division rate, that greatly increases FSC production; the increase was
1504 slightly greater than achieved by excess CycE expression overv the same time period. The depletion
1505 of r1 only and EC-only lineages without affecting the frequency of lineages containing an r1 EC or an
1506 EC may result from increased clone sizes, with some spreading into more posterior domains, rather
1507 than indicating an anterior to posterior shift of all derivatives. By contrast, there was a depletion of r1
1508 ECs amongst all clones for *kibra*, *wts* and *hpo* lineages induced at pupariation and the former two
1509 genotypes did not appear to affect cell division rate. Thus, Hippo pathway components primarily
1510 affected A/P movement of the most anterior precursors, whereas excess Yki primarily affected
1511 division rate and, hence, FSC representation.
1512
1513
1514

Hedgehog signaling promotes cell division, counters posterior derivative cell apoptosis and can influence A/P migration

The normal effect of Hh signaling on somatic ovarian precursors is most simply investigated by generating lineages homozygous for a strong *smoothened* (*smo*^{2}) loss of function mutation, preventing all responses to Hh (INGHAM 2022). When induced at pupariation, the proportion of ovarioles with labeled cells was consistently lower than for controls over three experiments (10% vs 28%, 12% vs 40%, 17% vs 34%). The yield of labeled ovarioles remained lower for clones of genotype *smo; UAS-DIAP1* (47% vs 73%, 19% and 17% vs 34%). Given the strong restoration of *yki* mutant clone frequency by *UAS-DIAP1* under analogous conditions, the results suggest that some *smo* mutant lineages are lost for reasons other than apoptosis or that the apoptotic signal is stronger than induced by *yki* and is not efficiently countered by *UAS-DIAP1*. The nature of recovered lineages was nevertheless influenced by the presence of *UAS-DIAP1*, as described below, suggesting some selective loss of cells by apoptosis. Expression of *UAS-DIAP1* alone did not alter any control phenotype significantly (Fig. 9D, E).

The phenotype shared by *smo* and *smo; UAS-DIAP1* (each cited as the average of three tests) was a reduction of lineages that include FSCs (3% each vs 15% control) (Fig. 9A, B, D). The average number of cells per EC-only clone (1.4 and 1.4 vs 2.7) and per EC/FSC clone (1.2 and 3.1 (both from fewer than five clones) vs 8.6) were reduced (Fig. 10H), as was the average size of a terminal FC patch (*smo* 15% vs 26% control, *smo; UAS-DIAP1* 15% vs 20% control; Fig. 10J). All of these data are consistent with a reduced division rate leading to loss of FSCs. That deficit alone might be expected to produce an increase in FC-only or EC/FC lineages. The frequency of FC-only plus EC/FC lineages was indeed significantly increased for *smo; UAS-DIAP1* lineages (37% + 7% = 44% vs 17% + 6% = 23% for control) but not for *smo* lineages (19% + 1% = 20%). There was also a reduction in lineages that included terminal FCs for *smo* (11% vs 22% control) but not for *smo; UAS-DIAP1* (24%) (Fig. 9A, B, D). These results suggest that some *smo* mutant FCs, including some of those contributing to the terminal egg chamber, are lost to apoptosis, reminiscent of the *yki* mutant genotype. For *smo; UAS-DIAP1* cells, there was a small reduction in the fraction of lineages including r1 ECs (56% vs 67%). The increase in FC-only lineages (37% vs 17%) noted above was also greater than expected to result only from loss of FSCs. Hence, loss of Hh signaling in the presence of *UAS-DIAP1* appears also to result in a posterior shift in precursor derivatives. This does not appear to extend to the most posterior precursors, since the proportion of lineages with labeled terminal FCs remained almost unchanged (24% vs 22%).

The phenotypes of *smo* and *smo; UAS-DIAP1* lineages were reproduced when induced 2d prior to pupariation. Clone frequency was reduced (17% and 21%, respectively versus 53% for the control, which expressed *UAS-DIAP1*) and lineages with FSCs were greatly reduced in both cases (1% and 1% vs 22% control average, Fig. 9E). The fraction of lineages with marked FCs in the absence of FSCs (FC-only plus EC/FC) was significantly increased only in the presence of DIAP1 (*smo* 26% and *smo; UAS-DIAP1* 44% vs 23% control), with a marked decrease in representation of terminal FCs amongst all lineages only in the absence of *UAS-DIAP1* (*smo* 20% and *smo; UAS-DIAP1* 31% vs 35% controls, Fig. 9E). Again, there was a decrease of lineages containing r1 ECs when DIAP1 was present (47% vs 75% control). These results are consistent with a posterior shift of all but the most posterior FC precursors in the absence of Hh signaling, together with some loss of FCs through apoptosis. This posterior shift would by itself increase FSC representation, based on the *arr* mutant phenotype, so the observed loss of FSCs is almost certainly due to reduced division rates. The addition of *UAS-CycE* to the *smo; UAS-DIAP1* genotype did not, however, increase FSC representation (Fig. 9E), contrasting with the

analogous rescue observed for *yki* mutant lineages. One possibility is that the reduction in cell division due to loss of *smo*, which may be more profound than from loss of *yki* (consistent with a greater FSC deficit), is not rescued effectively or in a timely fashion by *UAS-CycE*.

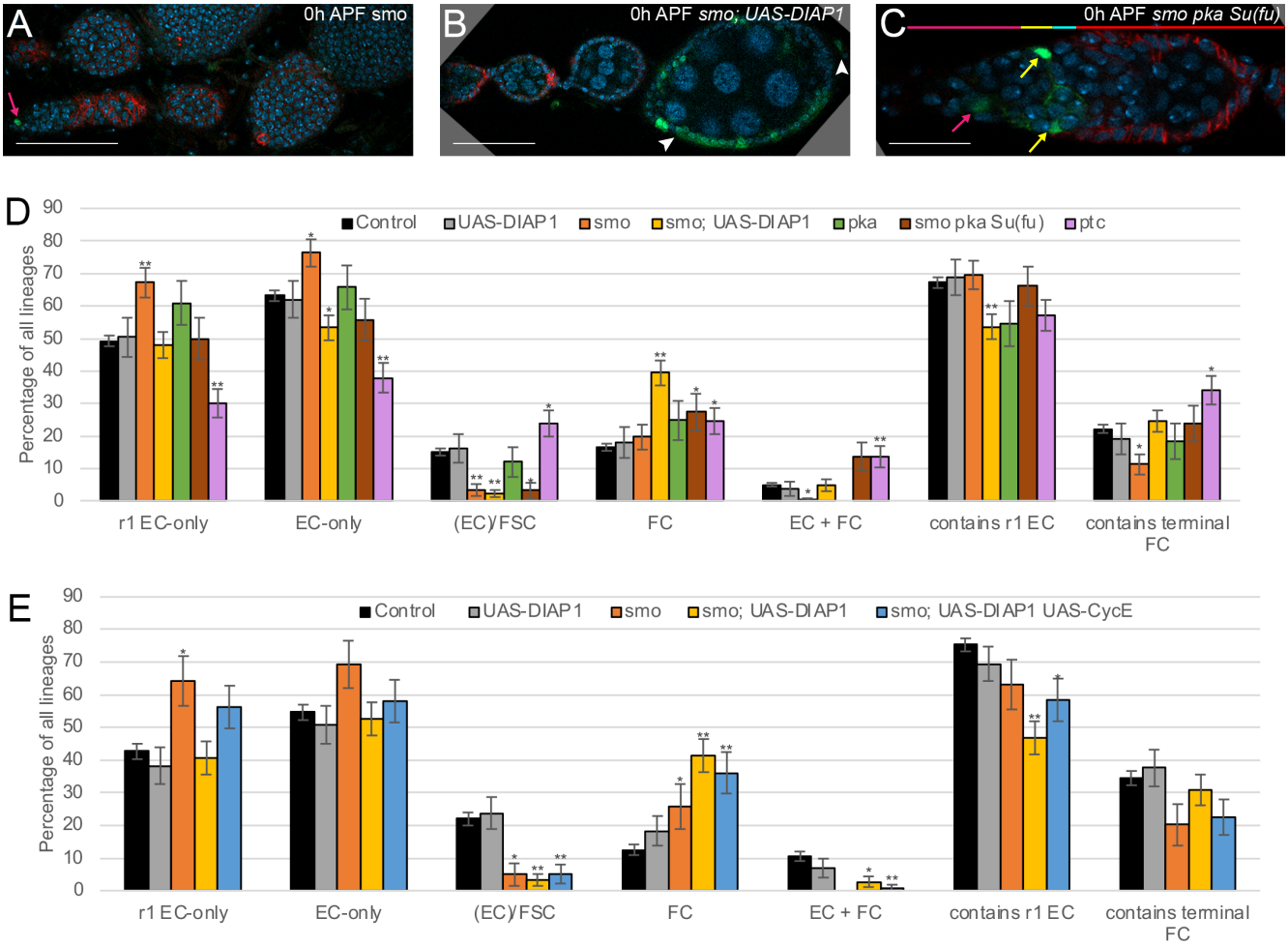

Figure 9. Hedgehog signaling promotes cell division and FSC representation, counters posterior derivative cell apoptosis and can influence A/P migration

(A-C) Representative lineages induced at 0h APF for the indicated genotypes. White arrowheads indicate Follicle Cells; magenta arrows, r1 ECs; yellow arrows, r2a ECs; cyan arrows, FSCs. DAPI, blue; GFP, green; Fas3, red. **(A)** A *smo* EC-only lineage and **(B)** a *smo; UAS-DIAP1* lineage with terminal FC marking, rarely seen in the absence of *UAS-DIAP1*. **(C)** A *smo pka Su(fu)* lineage, illustrating the common EC-only outcome. FSCs were rarely observed for all three illustrated genotypes. Scale Bar 20 µm for (**C**) and 50 µm for (**A, B**). **(D, E)** Deduced frequency of the indicated types of single-cell lineage as a percentage of all lineages induced at **(D)** 0h APF and **(E)** -48h APF. Error bars show SEM. One asterisk (*) indicates p<0.05; two asterisks (**) indicates p<0.005 (Fisher's two-tailed exact test). (**D**) Number of marked ovarioles = 739 (control), 59 (*UAS-DIAP1*), 98 (*smo*), 142 (*smo; UAS-DIAP1*), 38 (*pka*), 51 (*smo pka Su(fu)*), 85 (*ptc*). (**E**) Number of marked ovarioles = 319 (control), 58 (*UAS-DIAP1*), 37 (*smo*), 88 (*smo; UAS-DIAP1*), 55 (*smo; UAS-DIAP1 UAS-CycE*). For raw data and calculations please see supplementary spreadsheets titled 0h APF Graphs Fig4-10; -2d APF Graphs**;** Compilation of Numbers Figure 9 Hh -5d; Compilation of Numbers Figure 9 Hh -5d.

We also investigated the effects of partially compromising Hh signaling. In *Drosophila* wing discs, the loss of Protein Kinase A (PKA) compromises Smo activation by Hh but also blocks proteolytic processing of the full-length latent transcriptional activator Ci to a repressor form (Jia *et al.* 2003; Apionishev *et al.* 2005; Smelkinson *et al.* 2007; Little *et al.* 2020). It therefore produces an intermediate level of Hh pathway activity (high levels of full-length Ci but limited activation of Ci-155 by Smo-

1585 activated Fused kinase). Similarly, *smo pka: Su(fu)* mutant cells allow no activation of Fused but
1586 partially alleviate the requirement for Fu kinase activity because of the absence of Su(fu) (Suppressor
1587 of fused) restraint on full-length Ci activity (OHLMEYER AND KALDERON 1998). In wing discs, both *pka* and
1588 *smo pka; Su(fu)* genotypes produce relatively high levels of pathway activity but lower than maximal
1589 Hh signaling (manifest as strong transcriptional *patched* (*ptc*) induction but no induction of anterior
1590 Engrailed). In developing ovarioles, there was no significant reduction in clone frequency for these
1591 lineages induced at pupariation. Both genotypes led to a reduced fraction of lineages containing FSCs
1592 (12% and 3% vs 15% control, Fig. 9D). The effect was strongest for *smo pka Su(fu)* (Fig. 9C), suggesting
1593 that precursors in locations destined to produce FSCs normally receive high levels of Hh during some
1594 or all of pupal development. The FSC deficit was accompanied by an increase in lineages with FCs but
1595 no FSCs for *pka* and *smo pka; Su(fu)* (25% and 41% vs 22% for controls), without large changes in the
1596 fraction of lineages with terminal FCs (18% and 24% vs 22% control) or r1 ECs (54% and 66% vs 67%)
1597 (Fig. 9D). Thus, even intermediate reductions in Hh pathway activity reduce FSC production, likely
1598 through reduced cell division rates, while complete loss of pathway activity also results in a posterior
1599 shift of all but terminal FC precursors, accompanied by some loss of posterior precursor lineages
1600 through apoptosis.
1601 The maximal physiological level of Hh pathway activity is generally reproduced by loss of *ptc*
1602 function (INGHAM 2022). The phenotype of *ptc* mutant lineages induced at pupariation was consistent
1603 with an elevated division rate. The fraction of lineages that included an FSC was increased (24% vs
1604 15% control, Fig. 9D, Fig. 10A), as was the average size of an EC/FSC lineage (13.4 vs 8.6 control EC
1605 plus FSC cells; Fig. 10H). The fraction of all marked ECs and FSCs that were FSCs was also higher (28%
1606 vs 19% control average). The average size of a terminal FC patch was slightly higher (29% vs 24%; this
1607 measure excludes clones exclusively composed of polar cells, stalk cells or basal stalk cells; Fig. 10K).
1608 Since *ptc* marked FCs were generally very abundant (Fig. 10D) we wondered if these measures fully
1609 represented the division rate of *ptc* mutant cells. We therefore also measured indicators of the
1610 spread of clones as a further indicator of division rate. A precursor at pupariation that is destined to
1611 contribute to the terminal egg chamber also sometimes contributes to the penultimate egg chamber.
1612 As noted in the first section of Results, the lineage sometimes also contributes FCs occupying more
1613 anterior positions. A lineage that produces more cells is more likely to spread into each of these
1614 locations. Control lineages contributing to the terminal FC also populated the penultimate egg
1615 chamber with a frequency of 38% and more anterior egg chambers with a frequency of 25%. Those
1616 values were increased to 55% and 66%, respectively for *ptc* lineages (Fig. 10L). This measure does not
1617 correct for single-cell lineages and in other experiments the control values for penultimate egg
1618 chamber occupancy were higher (to give an average of 49%) (Fig. 10L). Thus, our cumulative evidence
1619 suggests that loss of *ptc* function may not increase the division rate of the most posterior precursors.
1620 The spread of FSC-containing lineages was estimated by counting the fraction of cysts with adjacent
1621 marked FCs. This value was much higher for *ptc* (80%) than for control FSC-containing lineages (Fig.
1622 10I), supporting the deduction from marked EC and FSC numbers in such lineages (Fig. 10H) that *ptc*
1623 increases division rate for precursors in the regions that can produce FSCs. The average size of an EC-
1624 only clone was not increased for *ptc* lineages (2.0 vs 2.7 control cells; Fig. 10H), suggesting that
1625 division is not increased in the most anterior regions, closest to the source of Hh.
1626 There also appears to be a posterior bias in the distribution of *ptc* mutant lineages, with fewer
1627 lineages including r1 ECs (57% vs 67% control) and more lineages including terminal FCs (34% vs
1628 22%), reflected also in an increased fraction of lineages containing FCs but no FSC (38% vs 22%) (Fig.
1629 9D). A posterior shift can also contribute to an increase of lineages with FSCs, as observed for *arr*
1630 lineages. Nevertheless, the *ptc* phenotype shows a lesser posterior shift than *arr*, a greater increase in

EC/FSC lineages and some direct evidence of increased division rates, affirming a significant contribution of division rate to FSC representation. The major effect of Hh signaling on cell division rate and FSC production was manifest by opposite *smo* and *ptc* phenotypes. Effects on cell location appear to be more complex: increased Hh signaling caused posterior displacement throughout the precursor domain, while loss of Hh signaling produced the same result (not the converse, as might be expected) for all but the most posterior precursors.

Relationship between Hh signaling and Yki activity

In adult FSC lineages, *ptc* increased *yki* RNA levels, *yki* was fully epistatic to *ptc* and substituting *yki* with a *tub-yki* transgene, preventing normal transcriptional regulation of *yki*, suppressed all *ptc* phenotypes (to produce roughly wild-type FSC properties) (HUANG AND KALDERON 2014). It was therefore concluded that *ptc* increased FSC representation (through enhanced division) via transcriptional induction of *yki*. Another report suggested a post-transcriptional regulation of Yki activity through the Hh pathway (LI *et al.* 2015), while the study of adult ECs deficient for *yki* or *smo* activity led to a conclusion of independent (albeit similar) Hh and Yki effects, each leading to EC dysfunction and consequently delayed or deficient germ cell differentiation (HUANG *et al.* 2017).

We explored the relationship between Hh signaling and Yki activity in ovarian precursors by manipulating both simultaneously. *ptc yki* lineages initiated at pupariation had phenotypes similar to *yki* phenotypes (Fig. 8A, Fig. 10B). Lineages with FSCs were less frequent than for controls (6% vs 15%; *yki* 2%), as were FC-only lineages (11% vs 17%; *yki* 8%) and the subset with only terminal FCs (5% vs 10%; *yki* 3%), while EC-only lineages were more frequent (71% vs 63%; *yki* 90%), as were r1 EC-only lineages (61% vs 49%; *yki* 82%) (Fig. 10G). Correspondingly, lineages that included labeled terminal FCs were less frequent (10% vs 22%; *yki* 3%) and those with r1 ECs were more abundant (82% vs 67%; *yki* 89%). All of these deviations from wild-type behavior are similar to those of *yki* lineages, though smaller in magnitude, and opposite to changes characteristic of *ptc* alone (Figs. 8 and 10). Thus, loss of *yki* is largely epistatic to loss of *ptc*, regarding the distribution of lineage types. All terminal FC samples for *ptc yki*, like *yki*, were mostly composed of polar cells or basal stalk cells, so a reliable measure of division rate for terminal epithelial FC precursors is not available. Similarly, there were too few FSC-containing lineages (just three) to provide a reliable estimate of division rate of EC/FSC precursors. Thus, the loss of FSC-containing *ptc yki* lineages is plausibly due to a reduced rate of precursor division, as deduced for *yki* lineages through rescue with *UAS-CycE*, but there is no direct supporting evidence.

The phenotype of marked *ptc yki* FCs commonly included the characteristic *yki* phenotype of occupying polar cell locations or producing ectopic polar-like cells with high Fas3, but also included multi-layering (Fig. 10E), with the marked cells in an outer layer, or the presence of multiple excess labeled cells between egg chambers. Those phenotypes were previously noted for *ptc* mutant FCs induced in adults (ZHANG AND KALDERON 2000) and were evident also in *ptc* mutant pupal lineages (Fig. 10D), where the FC patches were generally much larger than for *ptc yki* (supporting the hypothesis of a significantly lower division rate). We deduce that the multi-layering phenotype, indicative of a different affinity of *ptc* mutant FCs for germline cells and wild-type FCs, is not dependent on Yki activity.

Substitution of *yki* function with *tub-yki* resulted in lineages with phenotypes similar to controls (Fig. 10G). This result suggests that the levels of *yki* provided by the transgene are roughly normal (consistent with maintenance of healthy stocks with *tub-yki* replacing endogenous *yki* activity)

and that *yki* need not be regulated transcriptionally for roughly normal ovarian somatic cell precursor behavior.

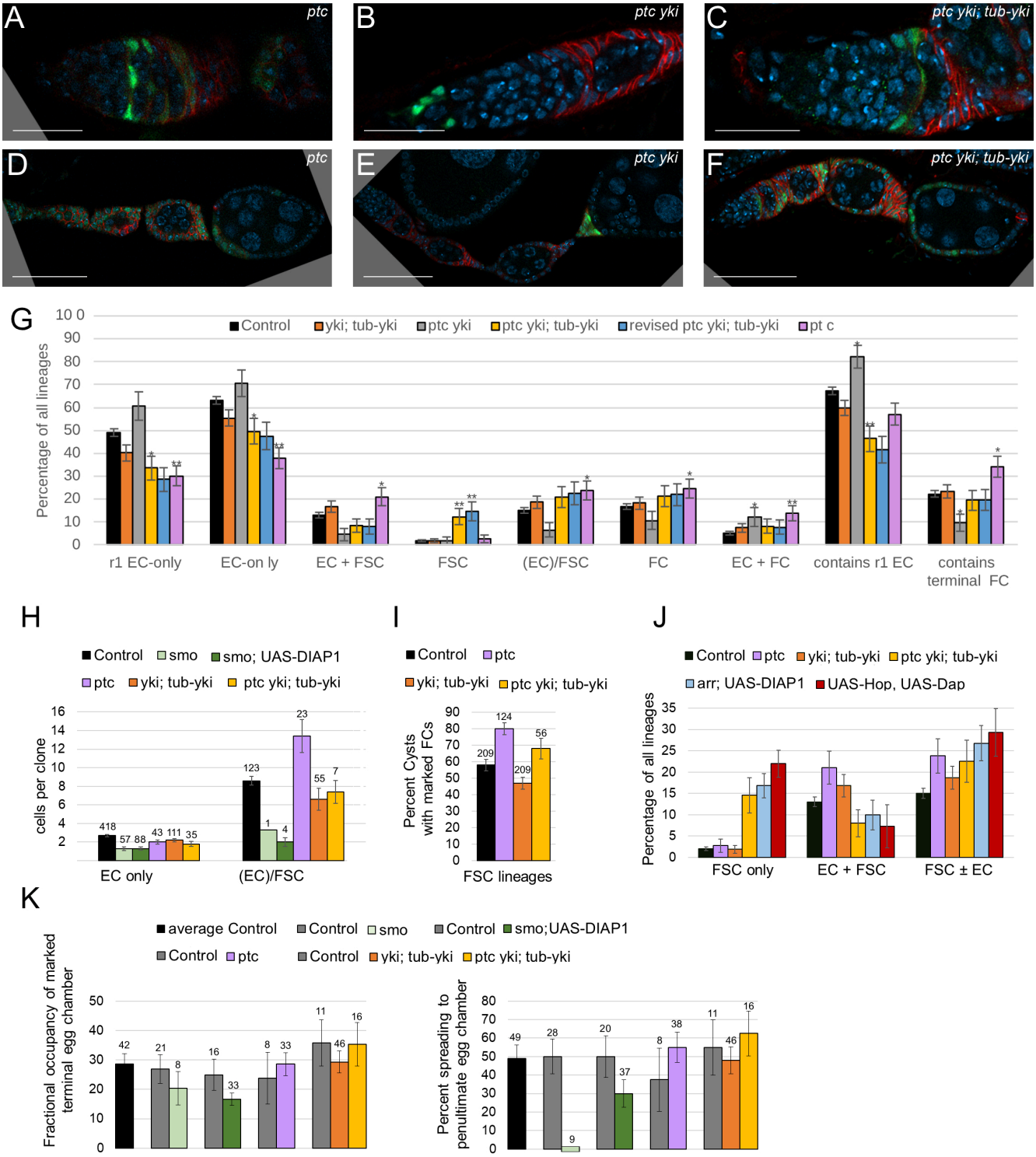

Figure 10: Dependence of *ptc* mutant phenotypes on transcriptional modulation of *yki*.
(A-F) Representative lineages induced at 0h APF for the indicated genotypes. White arrowheads indicate Follicle Cells; magenta arrows, r1 ECs; yellow arrows, r2a ECs; cyan arrows, FSCs. DAPI, blue; GFP, green; Fas3, red. The r1 EC, r2a EC, FSC and FC domains are shown in corresponding colors in the horizontal bars for **(A-C). (A)** A *ptc* EC/FSC/FC lineage showing a large number of marked cells, likely due to increased division. **(B)** A *ptc yki* EC-only lineage resembling a

common *yki* phenotype (Fig. 6A), and **(C)** a *ptc yki; tub-yki* EC/FSC/FC lineage with characteristically fewer cells than for *ptc*. **(D-F)** Ovarioles with *ptc* mutations induced at 0h APF produced ovarioles with multilayered FCs (paired white arrowheads) for **(D)** *ptc*, **(E)** *ptc yki* (which has relatively few marked FCs) and **(F)** *ptc yki; tub-yki*. Scale Bar 20 µm for **(A-C)** and 50 µm for **(D-F)**. **(G)** Deduced frequency of the indicated types of single-cell lineage as a percentage of all lineages induced at 0h APF. Error bars show SEM. One asterisk (*) indicates p<0.05; two asterisks (**) indicates p<0.005 (Fisher's two-tailed exact test). Animals occasionally lose the *tub-yki* transgene. Hence, data are reported for all scored ovaries for the *ptc yki; tub-yki* genotype and also as "revised" after removing samples from animals thought likely to have lost the *tub-yki* transgene based on phenotypes (low clone frequency, low frequency of FSCs and FCs) of all examined ovarioles. Number of marked ovarioles = 739 (control), 178 (*yki; tub-yki*), 59 (*ptc yki*), 76 (*ptc yki; tub-yki)*, 65 (revised *ptc yki; tub-yki*), 85 (*ptc*). **(H-K)** Measures of division rate and composition of FSC-containing lineages. **(H)** Average number of ECs in EC-only lineages, and the average sum of EC and FSC number in FSC-containing lineages. SEMs are based on raw data (prior to correction for single-cell lineages). n values (number of lineages scored) are above columns. **(I)** Percentage of cysts (includes region 2b, region 3 and all egg chambers) with adjacent marked FCs among FSC-containing lineages. n values (number of cysts scored) are above columns. **(J)** Percentage of all lineages with marked FSC but no EC, marked EC and FSC, marked FSC with or without EC. Number of marked ovarioles as in (G) for first four genotypes; 95 for *arr; UAS-DIAP1* and 50 for *UAS-Hop UAS-DIAP1*. **(K)** Left: average percentage of all FCs around the terminal egg chamber that are marked among lineages that include terminal FCs (but excluding those with only polar cells, stalk cells or basal stalk cells). Right: percentage of lineages with marked terminal FCs (no exclusions) with marked FCs on the penultimate egg chamber. n values (number of terminal egg chambers scored) are above columns. For raw data and calculations please see supplementary spreadsheets titled 0h APF Graphs Fig4-10; FC occupancy aggregate; Division Measures Hh/Yki**;** Compilation of Numbers Figure 10 Hh Hpo.

We noticed that the *tub-yki* transgene, marked by w^+, is sometimes spontaneously excised in stocks. This is, unfortunately not directly visible in stocks carrying the yki^{B3} allele, which itself has strong w^+ expression. We noted, however, that in our initial tests, many lineages expected to be of genotype *yki; tub-yki* showed characteristic *yki* mutant FC phenotypes (a high proportion of polar and stalk cells or elevated Fas3 expression). We therefore obtained the lineage results cited above by constructing a stock that is homozygous for *yki* together with one copy of *tub-yki*, so that the active transgene must be maintained for viability. The unstable *tub-yki* transgene also was lost over time from *ptc yki; tub-yki* stocks, as revealed by crosses to *yki* stocks to test viability, but here there was no solution to enforce *tub-yki* retention. We therefore measured *ptc yki; tub-yki* lineage phenotypes for two recently-derived stocks. In two flies derived from each stock, lineages resembled those seen for *ptc yki* (we score ovaries from individual flies separately). Results are therefore presented without any adjustment, likely representing a mix of *ptc yki; tub-yki* and *ptc yki* genotypes, and also after discarding the four sets of ovarioles very likely lacking *tub-yki*. Results were not greatly altered by the latter step, but we discuss here the second set of results ("revised *ptc yki; tub-yki*"), which likely represents the correct genotype.

The addition of *ptc* (to *yki; tub-yki*) increased the fraction of lineages with FSCs (Fig. 10C, F) from 18% to 23%, both higher than controls (15%) but not significantly (p>0.05) (Fig. 10D, J). The average number of cells per EC/FSC clone (7.4) was similar to the *yki; tub-yki* genotype (6.6) and to controls (8.6) but much lower than for *ptc* (13.4) (Fig. 10H). To probe division rate further in the neighborhood of precursors that can yield FSCs we also counted the frequency of marked FC patches in FSC-containing lineages. The very high proportion of germline cysts contacting marked FCs for *ptc* lineages (99/124; 80%), was not matched by *ptc yki; tub-yki* (38/56; 68%), yielding a value similar to the direct control for that experiment (35/51; 69%), slightly higher than the average of six such controls (121/209; 58%), and higher than for *yki;tub-yki* (98/209; 47%) (Fig. 10I). Thus, marked cells in FSC-containing lineages were less abundant in *ptc yki; tub-yki* ovarioles than for *pt*c when assessed both by EC/FSC numbers and a measure of FC production, suggesting that the faster division promoted by *ptc* is largely suppressed by *yki* substitution with *tub-yki*. That is consistent with the

1735 possibility that *ptc* increases division of precursors in intermediate FSC-producing locations largely
1736 through transcriptional induction of *yki*, as in adult FSC lineages. The average terminal FC clone size
1737 (35%) was very similar for *ptc yki; tub-yki* and the direct control (36%) but higher than for *yki; tub-yki*
1738 (29%) in the same experiment (Fig. 10K). The percentage of terminal FC clones that spread to the
1739 penultimate egg chamber was higher for *ptc yki; tub-yki* (63%) than both the control (55%) and *yki;*
1740 *tub-yki* (48%) (Fig. 10K). Thus, there may be a small loss of division of posterior precursors for *yki; tub-*
1741 *yki* and a small increase due to loss of *ptc* that does not rely on *yki* transcriptional induction. The
1742 phenotype of marked *ptc yki; tub-yki* FCs included multilayering and the accumulation of cells
1743 between egg chambers (Fig. 10F), confirming that these characteristics are caused by Hh signaling
1744 without using *yki* as an intermediate.
1745 The fractions of lineages including r1 ECs (47% vs 67%) and of EC-only lineages (48% vs 63%)
1746 were lower than controls, while the frequency of FC-only lineages was increased (22% vs 17%) for *ptc*
1747 *yki; tub-yki*, as observed for *ptc* alone (Fig. 10G). However, terminal FC labeling among all lineages
1748 was similar to controls (20% vs 22%), unlike *ptc* (34%). These results suggest that the posterior bias
1749 produced by excessive Hh signaling is not dependent on *yki* induction for precursors other than the
1750 most posterior, potential terminal FC precursors. It is interesting that loss of *yki* can lead to reduced
1751 terminal FC representation, while excess Yki increased representation (Fig. 8I). Those results are
1752 consistent with the possibility of *ptc* increasing terminal FC representation by inducing *yki*.
1753 Conversely, it is possible that reduced *yki* induction in *smo* mutant cells reduces terminal FC
1754 representation. This might balance a *yki*-independent consequence of *smo* that produces net
1755 posterior movement to result in the observed *smo* phenotype of posterior displacement of all but the
1756 most posterior clones. If correct, *smo* and *ptc* would have opposite *yki*-dependent changes in
1757 terminal FC formation, with Yki acting positively to promote terminal FC identity. For more anterior
1758 precursors, *smo* and *ptc* would both promote posterior movement in a Yki-independent manner.
1759 Increased posterior movement in the EC/FSC precursor domain, together with a roughly
1760 normal rate of cell division might account for the unusually high proportion of *ptc yki; tub-yki* lineages
1761 with labeled FSCs but no labeled ECs (15% vs 2% for controls, Fig. 10G, J). The other genotypes with a
1762 similar phenotype were *arr* (loss of Wnt signaling) and *UAS-DAP UAS-Hop* (increased JAK-STAT with
1763 an inhibitor of increased division), which causes posterior movement of all precursors with no
1764 apparent effect on cell division (Fig. 10J). The phenotype is not shared by *ptc*, presumably because
1765 increased division additionally replenishes EC precursors in EC/FSC lineages to balance posterior loss.
1766 Thus, although FSC-containing lineages are not much more abundant for *ptc* than for *ptc yki; tub-yki*,
1767 the contribution of increased division rate, which appears to rely on *yki* induction, is manifest by the
1768 markedly different frequencies of EC/FSC lineages (Fig. 10G and 10J).
1769
1770
1771

1772 **Discussion**
1773
1774 The replenishment of lost differentiated cells by adult stem cells is a vital physiological
1775 function for tissues with high cellular turnover, including human epidermal and intestinal cells. Adult
1776 stem cells must execute this function over a lifetime, overcoming natural variations and occasional
1777 extreme challenges, while their necessary continued replication and potential longevity make stem
1778 cells vulnerable to the accumulation of cancer-causing mutations. Adult stem cell studies are slowly
1779 revealing the cellular organizations and behaviors selected by these evolutionary pressures. In one
1780 large class of paradigms, which includes Drosophila FSCs and mammalian intestinal stem cells, stem
1781 cell division and differentiation are independent (Jones 2010; Reilein *et al.* 2017; Clevers and Watt
1782 2018; Reilein *et al.* 2018; Beumer and Clevers 2021; Greulich *et al.* 2021; Kalderon 2022). Hence,
1783 maintenance of a specific stem cell requires that division competes successfully with differentiation;
1784 this balance can be altered by genetic mutation, to produce a functional stem cell deficit or a hyper-
1785 competitive lineage with oncogenic potential. Moreover, differentiation in these paradigms is
1786 governed by the spatial distribution of extracellular signals and is initiated by changes in cell location
1787 (along the AP axis for FSCs and the crypt bottom/top axis for intestinal stem cells).
1788 Equally relevant, but less studied, are the developmental processes that create the requisite
1789 organization of stem cells and niche cells that produce key extracellular signals. Drosophila FSCs
1790 belong to a class of paradigm where stem cells are not set aside during development (Guiu *et al.*
1791 2019; Obernier and Alvarez-Buylla 2019; Bond *et al.* 2021; Reilein *et al.* 2021). Instead, a set of
1792 precursors simultaneously produces stem cells and the adult differentiated cells they will support. If
1793 differentiated cells are continuously irreversibly lost from the precursor pool through migration away
1794 from the future stem cell domain, as is true for FCs in the pupal Drosophila ovary and likely holds also
1795 for mammalian intestine, the survival of a specific precursor to produce a stem cell may depend on
1796 sufficient division activity during development to counter differentiation losses (Fig. 11 and Fig. 12).
1797 Also, if stem cell division and migration (leading to differentiation) must be balanced during
1798 development and in adults, the use of a similar set of extracellular factors might be expected. Our
1799 studies of the responses of single cells to specific genetic manipulations during Drosophila ovary
1800 development support both of these hypotheses (Fig. 11). These conclusions, based on experimental
1801 evidence for FSCs, are likely to apply generally to tissues supported by stem cells that develop
1802 alongside the mature tissue and act as a community with independent regulation of division and
1803 differentiation (Fig. 12).
1804
1805 **Origin of the first FCs**
1806
1807 It was previously shown that most FC-producing lineages induced at 36h APF contributed
1808 either no terminal FCs or only terminal FCs, suggesting segregation of terminal FC precursors by that
1809 stage (Reilein *et al.* 2021). This deduction was supported by live imaging, showing that only cells
1810 posterior to germline cells (in the Extra-Germarial Crown and Basal Stalk) from about 48h APF
1811 populated the terminal egg chamber (Reilein *et al.* 2021). Some of these cells accumulated anterior to
1812 the terminal egg chamber, destined to become FCs on the penultimate egg chamber, consistent with
1813 lineage studies. By contrast, FCs in more anterior egg chambers, together with ECs and FSCs, derived
1814 from germarial ICs. In this work, we found that lineages induced at pupariation often included
1815 marked FCs in the terminal egg chamber and also anterior to the penultimate egg chamber. The high
1816 frequency of those occurrences could not be explained by chance induction of two separate lineages;
1817 instead, most such occurrences report the behavior of single-cell lineages. Hence, we deduce that

1818 somatic cells intermingled with germline cells (ICs) in the developing germarium at pupariation can
1819 give rise to adult somatic ovary cells in every location, from the most anterior ECs to the most
1820 posterior FCs and the basal stalk protruding from the posterior of the terminal egg chamber (Fig.
1821 11A). Accordingly, the terminal FC precursors seen accumulating over the next 48h must largely
1822 derive from migration of ICs out of the germarium, distancing themselves from germline cells, even
1823 though such movements have not been directly observed by live imaging. Our lineage studies cannot
1824 exclude the possibility that some of the terminal FC population derive from a separate source but
1825 there is no specific evidence supporting that possibility. It seems most likely that all terminal FCs
1826 derive from ICs at pupariation.
1827 The alternative potential source of terminal FCs previously considered were "basal cells",
1828 already present posterior to developing germaria at pupariation but without the characteristic Fas3
1829 expression of cells in the subsequently enlarging Extra-Germarial Crown. Recent studies identified a
1830 population of cells, named Swarm cells, in larval ovaries, according to selective expression of Single-
1831 minded and Crossveinless-2 (Banisch *et al.* 2021). By using corresponding antibodies and GAL4 lines
1832 for lineage tracing, it was shown that these apical cells migrate basally from 72h to 120h after egg-
1833 laying to form the "basal cell" population at the larval/pupal transition. Swarm cell migration is
1834 initiated by an ecdysone pulse, while a second ecdysone pulse triggers the now-posterior Swarm cells
1835 to send a differentiation signal to posterior PGCs. Thereafter, Swarm cell lineages are lost during
1836 pupal development, leaving little residue in adults, consistent with an earlier surmise of basal cell
1837 death during pupation from electron micrographs (King *et al.* 1968). These deductions are consistent
1838 with our conclusion that ICs, and not basal cells, are the precursors of terminal FCs.
1839
1840 **Cell division rate strongly affects the likelihood of a precursor becoming a FSC**
1841
1842 Division rate is a key parameter for adult stem cells. For FSCs and all adult stem cells
1843 maintained by population asymmetry with division-independent differentiation, a genetic change
1844 that alters the division rate of a single stem cell necessarily has a strong effect on the likelihood that
1845 the stem cell lineage will amplify, survive or be extinguished (Reilein *et al.* 2018). A stem cell with
1846 increased division rate will likely be maintained, with an elevated chance of amplifying to occupy an
1847 entire niche, immortalizing the genetic change and possibly seeding a cancer. Conversely, a stem cell
1848 with reduced division that cannot contribute efficiently to the physiological function of the stem cell
1849 community tends to be eliminated quite rapidly. We found experimentally that there is an analogous
1850 effect of division rate on the likelihood of becoming an FSC during pupal development. Thus, very few
1851 precursors with reduced division due to *cycE* or *cutlet* mutations became FSCs (Fig. 11B), while a
1852 greater proportion than normal became FSCs as a consequence of faster division due to excess CycE
1853 or increased JAK-STAT or Hh signaling (Fig. 11C). The likely rationale for this outcome is similar to the
1854 situation for adult FSCs. Precursors in the A/P territory of a developing germarium that may become
1855 FSCs are continually depleted during pupation by irreversibly becoming FCs (Fig. 11A). This loss is
1856 potentially balanced by influx from more anterior positions and by precursor division. In the adult
1857 germarium there is no net flux of ECs to become FSCs (Kalderon 2022). It appears that the major
1858 means of FSC precursor survival during pupal development is also through replication, even though
1859 there is net posterior expansion of the germarium early in pupation and hence, the potential for
1860 substantial replenishment of the FSC precursor domain from the anterior. Thus, the competitive
1861 advantage of a faster-dividing potential FSC actually initiates even prior to FSC formation, likely
1862 beginning at pupariation. The genetic factors that regulate division rate may differ between pupal
1863 and adult stages but it appears from our studies that several are in common (*cycE*, *cutlet*, JAK-STAT

1864 and Hh signaling) (Fig. 11B, C). These findings can explain the stronger effect on FSC lineage
1865 prevalence of mutations that increase or reduce division rates when induced in larvae rather than
1866 adults, as noted long ago for alterations to Hh signaling (VIED *et al.* 2012). An analogous principle may
1867 hold for some human stem cells with division-dependent differentiation, allowing the amplification of
1868 potential cancer-initiating mutations even before adulthood or full tissue maturation.
1869
1870 **Regulation of cell division rate during pupation**
1871
1872 There is prominent spatial regulation of somatic ovary precursor cell division rate during pupal
1873 development, with EdU incorporation and FUCCI cell cycle reporters providing evidence of lower
1874 rates and early cessation of division anteriorly (REILEIN *et al.* 2021). Indeed, this spatial regulation of
1875 division is potentially instrumental in setting the appropriate number of adult ECs. Unfortunately, we
1876 can only measure division rate in selected regions and with some limitations during pupation,
1877 counting ECs in EC-only lineages, the ECs and FSCs of EC/FSC/FC lineages, and FCs in terminal FC
1878 lineages. These measures sufficed to provide reliable evidence of reduced or increased division in
1879 response to genetic manipulations but cannot provide precise details of changes in the spatial
1880 distribution of division rates. Thus, we have evidence of decreased division for loss of function
1881 alterations to *cycE*, *cutlet*, *smo* and *yki*, together with increased division for excess CycE, activated Yki,
1882 *ptc* and increased JAK-STAT signaling, measured over the whole duration of pupation. Very little
1883 information was revealed for alterations, like loss of *stat* and excess Wnt pathway activity, which
1884 resulted in the production of almost exclusively ECs.
1885 Since Hh pathway activity had a positive effect on precursor division and Hh pathway activity
1886 is known to decline from anterior to posterior in pupal ovaries (LAI *et al.* 2017), this pathway cannot
1887 contribute to the greater division rate of posterior cells. Excess JAK-STAT activity produced lineages
1888 with very large numbers of marked cells, partly obscuring the likely A/P position of the original
1889 precursor. Nevertheless, there were very few examples of the highly prevalent (>50%) typical wild-
1890 type EC-only clone with just 2-3 labeled cells. It seems clear, therefore, that excess JAK-STAT signaling
1891 increased division of even the most anterior precursors. Thus, it is surely important to limit JAK-STAT
1892 pathway activity in anterior precursors. Once an egg chamber has budded to produce polar cells,
1893 which are a key source of JAK-STAT pathway ligand, we observed strong pathway reporter signal in all
1894 egg chambers and the posterior half of the germarium, as in adults (VIED *et al.* 2012; MELAMED AND
1895 KALDERON 2020). It therefore seems inevitable that, as in the adult, JAK-STAT pathway activity
1896 promotes division of posterior FSC/FC precursors but not anterior EC precursor germarial cells during
1897 the second half of pupation.
1898 A key question is whether JAK-STAT is an important stimulator of FSC or FC precursor division
1899 over the first 48h. There were few or no FSC- or FC-containing *stat* mutant lineages to measure cell
1900 numbers directly. Moreover, the severe loss of *stat* FSC lineages, which might be caused by reduced
1901 division rates, by anterior precursor movement or both, could have occurred during the second half
1902 of pupation. We did not see a strong JAK-STAT pathway reporter signal prior to 30h APF. Thereafter,
1903 however, reporter signal was stronger in posterior germarial cells and extra-germarial cells than in
1904 the anterior half of the germarium (Fig. 7), so it is plausible that graded JAK-STAT pathway activity
1905 may also contribute to faster division of more posterior cells over the first half of pupation (Fig. 12).
1906 Inferred division rates of germarial pupal precursors are roughly inversely correlated to Wnt
1907 pathway activity reported by Fz3-RFP. Thus, EC precursors have low or undetectable pathway activity
1908 only early in pupation while anterior precursors are still dividing; more posterior precursors
1909 consistently have only low Wnt pathway activity and do not arrest. Loss of Wnt pathway activity (*arr*)

did not, however, increase the average size of EC-only lineages or EC/FSC lineages. Almost all *axn* mutant precursors become ECs, so it is not known whether abnormally high (and potentially supra-physiological) Wnt pathway activity would impede posterior precursor cell division, as found for adult FSCs (MELAMED AND KALDERON 2020). Thus, despite the spatial correlation between higher Wnt signaling levels and lower division rates, we have no direct evidence of Wnt signaling reducing precursor division rates during pupation.

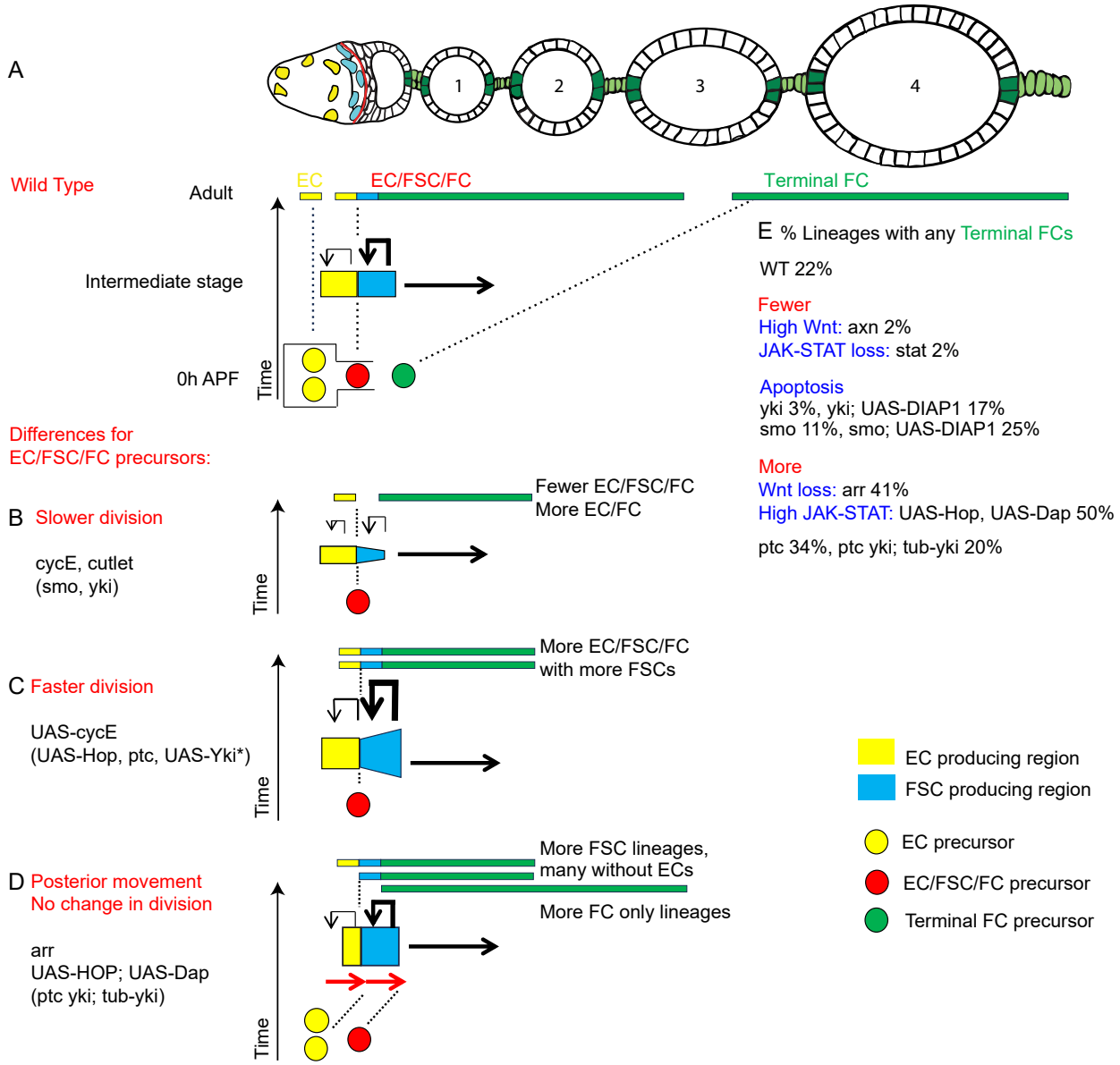

Figure 11: Summary of key influences on FSC formation and formation of the first FCs
(A) Ovariole diagram with ECs in yellow, FSCs in cyan, specialized stalk and polar cell FCs in green and other FCs in white. Representative precursors of EC-only (yellow), EC/FSC/FC (red) and terminal FC lineage (green) precursors are shown for oh APF. EC-only precursors are the most abundant, so two yellow cells are shown. An intermediate developmental time (such as 48h APF) is shown for EC/FSC/FC precursors to highlight the increased A/P range of derivates destined to become ECs (yellow) and FSCs (cyan), as well as the constant loss of EC/FSC precursors to become FCs to the posterior (horizontal arrow). The more posterior EC/FSC precursors divide faster than anterior EC/FSC precursors, especially later in pupation (larger renewal arrow). Our studies show that this renewal is important for FSC precursors to persist, compensating for

losses from continued FC formation. **(B-D)** Differences from wild-type behavior that affect precursors becoming FSCs. Experimental results are summarized and the underlying rationalization is illustrated (showing only relevant precursors). (**B**) Cell-autonomous reduction of division rate of an EC/FSC/FC (red) precursor among other wild-type precursors leads to progressive loss of FSC precursors throughout pupation because FSC precursor division no longer matches losses from differentiation to FCs. Consequently, many potential EC/FSC/FC lineages become EC/FC lineages. This behavior was seen most clearly for reduced activity of *cycE* and *cutlet*, but also for *smo* and *yki* when apoptosis was inhibited. **(C)** Conversely, a genetic cell-autonomous increase in division rate relative to other precursors leads to a progressive increase of FSC precursors during pupation, ensuring survival of FSC precursors and giving rise to EC/FSC/FC lineages with more FSCs than usual. Experimentally, this condition increased the frequency of EC/FSC/FC lineages, implying that some potential FSC lineages are normally lost in wild-type ovarioles because of insufficient division. This behavior was seen most clearly for increased activity of *cycE.* Similar results were seen for excess activated Yki (but not for regulators of Hippo pathway activity expected to increase Yki activity) and lesser, similar changes were observed for *ptc*. Excess JAK-STAT (*UAS-Hop*) produced many FSC-containing lineages but there were too many marked cells altogether to quantify lineage results. (**D**) A genetic change deduced to cause cell-autonomous posterior movement of all precursors (as seen for *arr*) resulted in fewer EC-only lineages, more FSC-containing lineages and more FC-only lineages. The increase in FSC-producing is because there are initially more potential EC-only (yellow) precursors than EC/FSC/FC precursors. Hence, a posterior shift relative causes more precursors originally in EC-only locations to move into FSC-producing territory than the number of precursors moving out of EC/FSC/FC territory to become FCs. Many of the resulting FSC-containing lineages lacked ECs. That is presumably because precursors entering the EC/FSC/FC-producing domain can continue to move posteriorly through that domain (red arrows) and are sustained, in part, through normal rates of cell division. Division continues in the FSC-producing (cyan) region but not in the EC-producing (yellow) region in the second half of pupation, so that many lineages maintain FSCs but not ECs. A high proportion of FSC lineages without ECs was seen also for *UAS-Hop; UAS-Dap* and *ptc yki; tub-yki* genotypes, supporting the deduction that they cause posterior movement around the FSC precursor region without affecting cell division rate. **(E)** The most posterior ICs at pupariation (green in (**A**)) were deduced from lineage studies here to migrate out of the germarium over the first 48h of pupation and then become the first FCs, occupying the terminal egg chamber (and sometimes also the penultimate egg chamber). The frequency of this outcome (producing Terminal FCs) was greatly decreased by loss of JAK-STAT or increased Wnt signaling; it was increased by reciprocal changes in those pathways. Reduced terminal FC contributions in the absence of *yki* and *smo* activity appeared to be due to spatially selective apoptosis. Increased Hh signaling (*ptc*) increased terminal FC lineage frequency, apparently dependent on normal *yki* gene regulation.

Wnt signaling promotes anterior migration

We found strong and consistent alterations in precursor outcomes for genetic alterations of Wnt pathway activity. Loss of activity caused an extensive posterior shift in outcomes, with a large increase in lineages containing terminal FCs and only FCs, together with a large reduction in lineages containing only ECs or containing any r1 ECs. The frequency of lineages containing FSCs was substantially increased and an unusually high fraction of FSC lineages did not include any ECs. This is an interesting outcome: loss of Wnt signaling causes increased FSC loss in adults (because of greater conversion to FCs and apparently no replenishment from the anterior) but increased FSC production during pupal development. This can be rationalized on the basis that there are normally many more EC-only than FC-only precursors (63% vs 17%), so more cells have the potential to enter FSC-producing regions from the anterior than from the posterior (Fig. 11D). Moreover, continued posterior movement appears to convert many potential EC/FSC/FC lineages to FSC/FC lineages. The resulting high frequency of FSC/FC lineages plausibly constitutes a distinguishing characteristic of genotypes that promote posterior migration without altering division rates for a given location (Fig. 10J and 11D).

Increased Wnt pathway activity produced strong phenotypes, which were broadly the converse of those observed for loss of Wnt pathway activity (more EC-only lineages; fewer FC-only and terminal FC-containing lineages). Amongst EC outcomes, there was only a small shift in favor of r1 ECs (contrasting with the large converse effect of loss of pathway activity), suggesting that

precursor migration in the most anterior regions of the developing germarium, where Wnt signaling appears to be roughly uniform, may not normally be driven by differential Wnt pathway activity. There was also a reduction in *axn* FSC-containing lineages, all of which included ECs, from 15% to 6%. If anterior displacement caused all prospective FSC precursors to become ECs and all FC-precursors to form FSC-containing lineages, there would be a net gain in FSC lineages because the initial FC-only precursor pool is larger than the FSC precursor pool. Since FSC lineages are depleted we might infer that FC-only precursors migrated beyond the FSC domain to form EC-only lineages. An additional contribution to FSC loss could be a reduction in cell division rate. There were too few FC- and FSC-containing *axn* lineages to assess division rate in these posterior regions. However, adult FSC division is severely reduced by loss of *axn* (Reilein *et al.* 2017; Melamed and Kalderon 2020) and the properties of FSC precursors during the last 2 days of pupation are likely highly similar to adult FSCs because they appear to exist in a very similar environment. Hence, some contribution of reduced division rate to the observed paucity of FSC-containing lineages is likely.

We attempted to measure the temporal effects of Wnt pathway activity by initiating genetic alterations at different times during pupation. These results cannot easily be interpreted quantitatively but indicated directly that Wnt signaling influenced outcomes in the latter stages and indirectly (inferred from greater severity when initiated early) that Wnt signaling levels were also influential early in pupation. Also, since terminal FC fates were greatly reduced for *axn* lineages induced at pupariation but not when induced 36h later, we infer that the primary deficit is likely migration of precursors posteriorly out of the germarium into the EGC and basal stalk during the first 48h of pupation. Thus, terminal FC formation relies on limiting Wnt pathway activity (Fig. 11E), as found for FC production from adult FSCs (Reilein *et al.* 2017; Melamed and Kalderon 2020). Throughout pupal development, Wnt pathway activity, reported by Fz3-RFP, declined to undetectable levels roughly coincident with the anterior extent of strong Fas3 expression, which appears to mark FC precursors. Thus, very low or absent Wnt pathway activity appears to be a significant factor in allowing FC formation throughout pupation, as in adults.

JAK-STAT signaling promotes posterior cell migration

The situation for JAK-STAT pathway signaling is roughly the mirror-image of that described for Wnt signaling, with a couple of significant differences (Fig. 11). First, increased JAK-STAT activity greatly stimulated precursor division. Second, although increased JAK-STAT activity (together with *UAS-Dap* to block changes in cell division rate) reduced the incidence of lineages with r1 ECs, loss of *stat* activity did not have the converse effect. Thus, even the most anterior precursors can be shifted more posterior in response to JAK-STAT but slightly more posterior EC precursors do not rely on JAK-STAT pathway activity to prevent anterior movement (unlike FC precursors and FSC precursors). The most likely explanation is that JAK-STAT activity is low, as observed directly, and functionally insignificant in the anterior half of the germarium throughout pupation. Interestingly, as for *arr* mutations, there was an increase in FSC-containing lineages lacking marked ECs for the *UAS-Hop UAS-Dap* genotype, consistent with the phenotype originating from posterior migration from EC-producing regions, rather than an increase in division rate (there was no indication of increased division for this genotype).

The large deficit of *stat* mutant lineages with marked terminal FCs (Fig. 11E) was a particularly important finding. The deficit was not observed for lineages induced 36h after pupariation and therefore appears to originate from a failure of precursors to migrate posteriorly out of the germarium over the first 48h of pupation. This is consistent with JAK-STAT pathway activity

universally favoring FC formation in adults and pupae. The *stat* mutant phenotype suggests that low Wnt pathway activity, as seen in the most posterior pupal precursors, is not sufficient for normal terminal FC production, although the condition of eliminating both Wnt and JAK-STAT pathway simultaneously has not been directly tested.

In adults there is always a nascent or just-formed egg chamber budding from the germarium with anterior polar cells producing a JAK-STAT ligand that produces a posteriorly-biased gradient in the vicinity of FSCs to promote FC formation (VIED *et al.* 2012). Prior to formation of the first egg chamber there are no polar cells as a source of ligand. The genetic results show that STAT must have significant activity during this period because very few precursors lacking *stat* activity become terminal FCs. The small number of mutant terminal FCs formed were found in different locations in different ovarioles. Had all marked FCs been found, for example, in the basal stalk, that might have suggested that the most posterior precursors do not need to respond to a JAK-STAT signal to maintain their position and might therefore be the source of JAK-STAT pathway ligand.

We were able to detect pathway activity from 30h APF onwards. Activity was strongest in regions surrounding and posterior to the most posterior germline cyst, consistent with the possibility that this heightened activity promotes posterior migration of precursors out of the germarium prior to production of the first egg chamber. It will be important to determine which cells might be a source of ligand for the JAK-STAT pathway in the period prior to polar cell production. The pattern of pathway activity at 48h APF is consistent with the possibility of production of ligand by Fas3-positive cells (and/or efficient passage through Fas3-positive cells) and is similar, albeit weaker, to the pattern in adult germaria. That observation raises the question of whether the graded JAK-STAT pathway activity in adult germaria results entirely from ligand produced in polar cells or might also be contributed by early Fas3-positive FCs. Selective inhibition of Upd ligand production in adult polar cells using *neur-GAL4* strongly reduced STAT-GFP with partial penetrance (around 70%), while inhibition with *109-30-GAL4*, which is expressed in all early FCs and slightly higher in polar cells, was also effective (VIED *et al.* 2012). Those results argue strongly for a primary role of polar cells but also allow the possibility that early FCs may provide an additional source of JAK-STAT pathway ligand in adult germaria.

Hedgehog signaling and Yki as an intermediate; division rate and some location effects

The contributions of Hh signaling and Yki activity to the behavior of adult germarial cells are relatively clear. Both Hh signaling and Yki promote FSC division and are required to limit apoptosis, while both are necessary in ECs to limit BMP production and hence allow normal germ cell maturation. In FSCs, Hh pathway activity can increase Yki activity through transcriptional regulation of *yki* (HUANG AND KALDERON 2014), while in ECs different reports suggested independent actions of Hh and Yki (HUANG *et al.* 2017) or post-transcriptional regulation of Yki activity by Hh (LI *et al.* 2015).

Manipulation of Hh signaling and Yki activity during pupal development also produced some related phenotypes, reminiscent of effects on adult FSCs. Both increased Hh signaling (*ptc* mutation) and increased activated Yki (*UAS-YkiS168A*) expression increased measures of precursor division and increased FSC representation, as would be predicted as a consequence (Fig. 11C). However, Hpo pathway inactivation (via *hpo*, *wts* and *kibra*), which is expected to activate Yki post-transcriptionally, did not appear to increase division or FSC representation consistently. The increase in semi-quantitative measures of precursor division and of FSC representation observed for *ptc* were mostly reduced when *tub-yki* substituted for *yki*, suggesting that the increased division rate may, as in adult FSCs, depend on transcriptional induction of *yki*. However, there were exceptions, limiting the

2070 evidence that responses to *ptc* require normal transcriptional regulation of *yki*. Moreover, the
2071 inferred division rates and overall distribution of cell types for the *yki; tub-yki* genotype were quite
2072 similar to controls, suggesting that transcriptional regulation of *yki* activity can be substituted quite
2073 well by a constitutive promoter, as in adult FSCs.
2074 There was a clear loss of *yki* mutant lineages that was suppressed by expressing DIAP1 to
2075 inhibit apoptosis but this appeared only to affect posterior precursors giving rise to FC lineages. The
2076 paucity of *yki; UAS-DIAP1* FSC-containing lineages was likely due primarily to reduced precursor
2077 division because it was suppressed by adding excess CycE together with DIAP1 (in lineages initiated
2078 2d before pupariation to allow timely initiation of expression of the *UAS*-driven transgenes in MARCM
2079 lineages), strongly suggesting that Yki normally contributes to requisite precursor division rates.
2080 A variety of other observations suggest some additional contributions of Hh signaling and Yki
2081 activity but these deductions are tempered by the limited magnitude or significant variability in some
2082 of the noted effects. First, there did appear to be some consequences for A/P movement of
2083 precursors. Loss of *yki* in the presence of *UAS-DIAP1* did not result in any notable changes of
2084 representation of r1 ECs but did reduce the representation of terminal FCs in lineages initiated 2d
2085 before pupariation. Increased Yki activity consistently (*kibra*, *wts*, *hpo*, *UAS-YkiS168A*) reduced r1 EC
2086 representation but only *UAS-YkiS168A* modestly (and not significantly) increased terminal FC
2087 production. Increased Hh signaling modestly decreased r1 EC representation, while increasing
2088 terminal FC representation. The effect on r1 ECs was retained when *yki* was substituted by *tub-yki*,
2089 while the effect on terminal FC representation was lost. This suggests that increased Hh signaling
2090 reduces r1 EC production independent of Yki, even though increased Yki activity has the same effect,
2091 while terminal FC representation, which is modestly increased by *UAS-YkiS168A* and decreased by
2092 loss of *yki*, is only increased by excess Hh signaling when transcriptional regulation of *yki* is allowed.
2093 These deductions align with earlier conclusions about adult ovaries: Hh signaling acts through Yki to
2094 influence more posterior cells (FSCs), while Hh and Yki act independently, albeit with similar
2095 consequences, for anterior cells (ECs) (HUANG AND KALDERON 2014; HUANG *et al.* 2017).
2096 The interpretation of *smo* phenotypes, representing loss of Hh pathway activity, has an
2097 additional caveat. Clone frequency was lower than for controls and was not restored by *UAS-DIAP1*,
2098 even though lineage phenotypes were altered by DIAP1. Thus, there is significant precursor loss or
2099 death (either non-apoptotic or apoptosis is not efficiently rescued by *UAS-DIAP1*) with unknown
2100 spatial selectivity. In *smo; UAS-DIAP1* lineages there was a loss of FSCs, plausibly due to limited cell
2101 division (Fig. 11B). This would be expected to increase the frequency of FC-only or EC/FC lineages. FC-
2102 only lineage frequency was increased but beyond that expected from FSC loss alone, and r1 EC
2103 representation was modestly reduced, with no change in terminal FC representation. Thus, loss of Hh
2104 signaling, at least among surviving cells, appears to cause a modest posterior shift over most of the
2105 precursor domain, excluding the most posterior regions. This deduction stands alongside a deduction
2106 of (stronger) posterior shifts also for increased Hh signaling. The latter deduction relates to potential
2107 consequences of Hh signaling, whereas the former reports the normal influence of Hh signaling. Thus,
2108 with significant caveats, it appears that Hh signaling might normally promote retention of anterior
2109 positions for most of the precursor domain. This is easily reconciled with the anterior bias of Hh
2110 pathway activity and the likelihood that posterior precursors soon fall out of the range of Hh
2111 signaling.
2112 Another study examined the consequences of manipulating Hh pathway activity in all somatic
2113 cell ovary precursors (rather than clonally) and concentrated mainly on genetic changes initiating
2114 prior to pupariation, to conclude that Hh signaling promotes retention of ICs in the developing gonad
2115 (LAI *et al.* 2017). It is conceivable that the shortfall of *smo* lineages we observed is due to migration of

some precursors away from the developing ovary. However, such losses might plausibly affect the most posterior precursors most strongly, and we found no selective shortage of terminal FC representation in *smo; UAS-DIAP1* lineages. Hence, we favor limited cell death as a more likely explanation. The effects of Hpo pathway inhibition (to increase Yki activity) have also been reported for early ovary development using manipulation of gene activity in all precursors, leading to a conclusion that the IC pool was increased in response, plausibly due to increased division (SARIKAYA AND EXTAVOUR 2015). This result is commensurate with our deductions from clonal analyses with UAS-YkiS168A and loss of *hpo*, though neither *kibra* nor *wts* mutations elicited a discernible indicator of increased division.

Summary conclusions and open questions

In the adult ovary, FSCs are maintained within a narrow A/P domain. At the posterior edge of that domain, some FSCs move posteriorly into territory with lower Wnt signaling and higher JAK-STAT signaling to become FCs (Fig. 12). Genetic reduction of Wnt or increase of JAK-STAT signaling greatly increase the chance, cell autonomously, of an individual FSC becoming an FC, suggesting that the magnitudes of these pathways are major drivers of FSC movement (VIED *et al.* 2012; REILEIN *et al.* 2017; MELAMED AND KALDERON 2020). The converse genetic argument holds for FSC conversion to ECs but the frequency of EC production is much lower than for FCs, perhaps because FSCs less frequently stray into more anterior territory, which is stably occupied by quiescent ECs, while space to the posterior of FSCs is constantly vacated by the process of egg chamber formation and budding. We previously found that the nature or behavior of somatic ovarian precursor cells, like FSCs, appears to be guided solely by location (REILEIN *et al.* 2021). Thus, the precursors that become FSCs are simply those that end up in the location of FSCs at the end of pupation.

Here, we found that the external signals guiding the location of precursors during pupal development overlap extensively with those used in adults (Fig. 12). This is relatively easily rationalized for Wnt signaling because Cap cells, located at the anterior of the germarium, are already differentiated at pupariation and appear to be a source of Wnt signals throughout pupation and adulthood. It is likely that an additional source of Wnt arises progressively during pupation as EC precursors stop dividing and adopt mature cell characteristics of producing Wnt ligands (SAHAI-HERNANDEZ AND NYSTUL 2013; WANG AND PAGE-MCCAW 2018) while the distance from Cap cells to FSC and FC precursors increases (Fig. 12). The net consequence is that from early pupation onwards there is graded Wnt signaling that declines to undetectable levels at the point of FC specification, which coincides with the onset of strong Fas3 expression (Fig. 5).

The involvement of JAK-STAT signaling was not predictable because a major source of ligand in adults are the anterior polar cells associated with an egg chamber budding from the germarium (Fig. 12). The first egg chamber produced during pupation has no antecedent and there is therefore no polar cell source of JAK-STAT ligand as a subset of somatic cells move posteriorly out of the developing germarium during the first 48h to acquire strong Fas3 expression and become the first FCs. We nevertheless detected JAK-STAT pathway activity around this precursor to FC transition zone and found that formation of the first FCs is strongly dependent on JAK-STAT activity, just as it depends on low Wnt activity. We do not know the source of the JAK-STAT ligand or whether pathway activity is graded over this transition zone, though it is clearly lower in more anterior regions. Hh pathway activity declines from anterior to posterior in both pupal and adult ovaries (FORBES *et al.* 1996; VIED *et al.* 2012; LAI *et al.* 2017). Although there were some effects of manipulating Hh signaling on A/P precursor outcomes (contrasting with adult studies, where only cell division rate appears to

be affected), these were much weaker than observed for Wnt or JAK-STAT pathways, suggesting that the latter two pathways are the major determinants of developmental formation of ECs, FSCs and FCs, just as they have the greatest influence on FSCs becoming ECs or FCs or remaining as FSCs in adults.

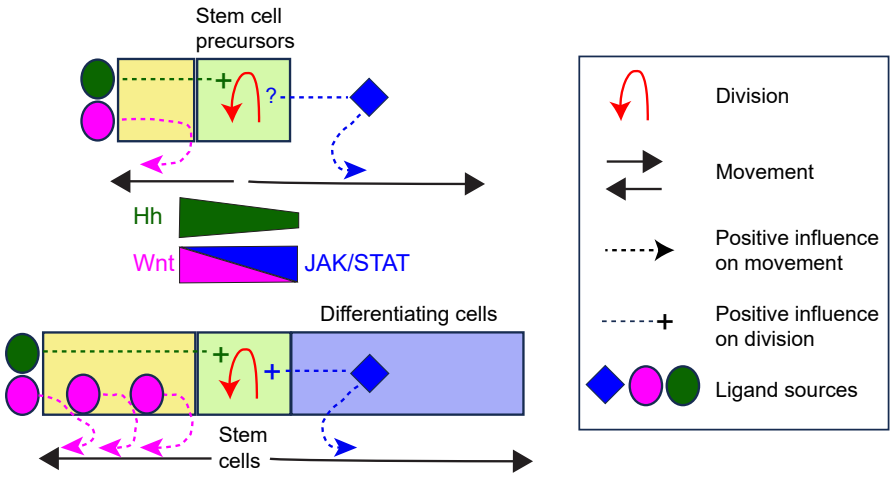

Figure 12. General principles illustrated by FSC development.
The cartoon depicts a pool of precursors on top and the adult tissue they form at the bottom. If a set of precursors (in the pale green space) produce both stem cells and differentiated tissue extending away from the source during development, then the probability that a given precursor will remain in the stem cell zone and become an adult stem cell depends on its division rate competing successfully against movement out of the stem cell zone. In paradigms with independent division and differentiation of adult stem cells, the same competition applies to maintaining a given stem cell. Both division rate and cell movements are likely to be regulated by external signals. It would generally be economical to use largely similar signals to regulate those processes during both development and adulthood, as we have found for Drosophila ovarian FSCs. Most simply, this is achieved by signals from niche cells established early in development. In the Drosophila ovary, two such signals come from Cap cells, which form prior to pupation: Hh promotes division and Wnt promotes anterior movement. There are two other features of ovary development, which might also be used in other paradigms. First, the primitive Cap cell niche is elaborated or expanded during pupal development by the production of additional niche cells (Escort Cells; pale yellow region) that supplement signaling from the anterior by producing additional Wnt ligands. Second, there is an important signal in adults (activating the JAK-STAT pathway) that originates from differentiated cells posterior to the stem cells. This signal promotes both stem cell division and posterior exit from the stem cell zone. During development, the same pathway promotes exit from the stem cell zone and has the potential to stimulate division; our data do not show whether division is stimulated at the earliest times during pupation or what is the exact cellular source of JAK-STAT pathway ligand prior to production of the first differentiated cells. Some stem cell paradigms, like mouse gut crypts, may not have the feature of FSCs that differentiated cells are produced in two directions (the yellow territory may be absent altogether or not replenished by the stem cells). The general principles still remain that (i) division rate is important for both development and maintenance of stem cells because it competes with cells moving out of the stem cell zone, and (ii) niche cells may produce a set of signals that act in a graded fashion over distance to regulate division rate and movement of both stem cell precursors and their adult stem cell derivatives.

The factors regulating proliferation of pupal precursors also were found to be very similar to those regulating adult FSC division rate, although the developmental data are much more limited and semi-quantitative at best. JAK-STAT and Hh signaling, via *yki* induction, are major stimulators of cell division, while Wnt signal normally has no significant influence (Fig. 12). The role of cell division rate in producing FSCs during pupal development was also found to be analogous to its role in maintaining FSCs. In both situations, it appears that the major loss of cells in a location with potential to act as an FSC is from posterior movement to become FCs. Although some cells may move from an EC-centered

precursor domain to final FSC positions during pupal development, the maintenance of precursors that become FSCs and of adult FSCs themselves, despite posterior loss, both depend principally on a sufficient cell division rate. Hence, both the formation and the maintenance or expansion of FSC lineages is favored by genetic cell-autonomous changes that increase division rate (Fig. 11).

We suggest that two major findings of our study are likely to apply to other stem cell paradigms that share major characteristics with FSCs (Fig. 12). First, if stem cells of a specific tissue are specified during the entire period that the rest of the tissue is specified, rather than being set aside early during development, it is likely that the same signals contribute to stem cell development and stem cell maintenance in adults. Second, in such scenarios where, additionally, the division and differentiation of adult stem cells are separate processes, the probability of an appropriately located precursor becoming a stem cell and of an adult stem cell being maintained both depend on the division rate of that cell relative to competitors vying to become stem cells or remain as adult stem cells.

Data Availability

Drosophila stocks used in this study are available upon request. The authors affirm that all data necessary for confirming the conclusions of the article are present within the article, figures, and supplementary spreadsheets deposited with the article.

Acknowledgments

We thank the Bloomington Drosophila stock center, the Developmental Studies Hybridoma Bank (DSHB), and Laura Johnston (Columbia University) for reagents, FlyBase as an information resource, and the confocal microscope resource provided by the Department of Biological Sciences, Columbia University. We thank Aron Choi, Brian Heubel, Pegah Khosravi-Kamrani and Karen Sophia Park for experimental assistance, David Melamed, Hoyon Kim, Laura Johnston and Iva Greenwald for discussions.

Study funding

This study was funded by NIH grant RO1 GM079351 to DK.

2246 **References**
2247

2248 Apionishev, S., N. M. Katanayeva, S. A. Marks, D. Kalderon and A. Tomlinson, 2005 Drosophila
2249 Smoothened phosphorylation sites essential for Hedgehog signal transduction. Nature Cell
2250 Biology 7**:** 86-92.
2251 Asaoka, M., and H. Lin, 2004 Germline stem cells in the Drosophila ovary descend from pole cells in
2252 the anterior region of the embryonic gonad. Development 131**:** 5079-5089.
2253 Assa-Kunik, E., I. L. Torres, E. D. Schejter, D. S. Johnston and B. Z. Shilo, 2007 Drosophila follicle cells
2254 are patterned by multiple levels of Notch signaling and antagonism between the Notch and
2255 JAK/STAT pathways. Development 134**:** 1161-1169.
2256 Bach, E. A., L. A. Ekas, A. Ayala-Camargo, M. S. Flaherty, H. Lee *et al.*, 2007 GFP reporters detect the
2257 activation of the Drosophila JAK/STAT pathway in vivo. Gene Expr Patterns 7**:** 323-331.
2258 Banisch, T. U., M. Slaidina, S. Gupta, M. Ho, L. Gilboa *et al.*, 2021 A transitory signaling center controls
2259 timing of primordial germ cell differentiation. Dev Cell 56**:** 1742-1755 e1744.
2260 Beumer, J., and H. Clevers, 2021 Cell fate specification and differentiation in the adult mammalian
2261 intestine. Nat Rev Mol Cell Biol 22**:** 39-53.
2262 Beumer, J., and H. Clevers, 2024 Hallmarks of stemness in mammalian tissues. Cell Stem Cell 31**:** 7-24.
2263 Biteau, B., C. E. Hochmuth and H. Jasper, 2011 Maintaining tissue homeostasis: dynamic control of
2264 somatic stem cell activity. Cell Stem Cell 9**:** 402-411.
2265 Bond, A. M., G. L. Ming and H. Song, 2021 Ontogeny of adult neural stem cells in the mammalian
2266 brain. Curr Top Dev Biol 142**:** 67-98.
2267 Boyle, M., and S. DiNardo, 1995 Specification, migration and assembly of the somatic cells of the
2268 Drosophila gonad. Development 121**:** 1815-1825.
2269 Chen, H. J., C. M. Wang, T. W. Wang, G. J. Liaw, T. H. Hsu *et al.*, 2011 The Hippo pathway controls
2270 polar cell fate through Notch signaling during Drosophila oogenesis. Dev Biol 357**:** 370-379.
2271 Clevers, H., and F. M. Watt, 2018 Defining Adult Stem Cells by Function, not by Phenotype. Annu Rev
2272 Biochem 87**:** 1015-1027.
2273 Dai, W., A. Peterson, T. Kenney, H. Burrous and D. J. Montell, 2017 Quantitative microscopy of the
2274 Drosophila ovary shows multiple niche signals specify progenitor cell fate. Nat Commun 8**:**
2275 1244.
2276 Duhart, J. C., T. T. Parsons and L. A. Raftery, 2017 The repertoire of epithelial morphogenesis on
2277 display: Progressive elaboration of Drosophila egg structure. Mech Dev 148**:** 18-39.
2278 Eliazer, S., and M. Buszczak, 2011 Finding a niche: studies from the Drosophila ovary. Stem Cell Res
2279 Ther 2**:** 45.
2280 Forbes, A. J., A. C. Spradling, P. W. Ingham and H. Lin, 1996 The role of segment polarity genes during
2281 early oogenesis in Drosophila. Development 122**:** 3283-3294.
2282 Gancz, D., and L. Gilboa, 2013 Insulin and Target of rapamycin signaling orchestrate the development
2283 of ovarian niche-stem cell units in Drosophila. Development 140**:** 4145-4154.
2284 Gancz, D., T. Lengil and L. Gilboa, 2011 Coordinated regulation of niche and stem cell precursors by
2285 hormonal signaling. PLoS Biol 9**:** e1001202.
2286 Gao, S., Y. Zhang and F. Liu, 2023 Revisiting the lineage contribution of hematopoietic stem and
2287 progenitor cells. Development 150.
2288 Giedt, M. S., and T. L. Tootle, 2023 The Vast Utility of Drosophila Oogenesis. Methods Mol Biol 2626**:**
2289 1-36.
2290 Gilboa, L., 2015 Organizing stem cell units in the Drosophila ovary. Curr Opin Genet Dev 32**:** 31-36.

2291 Godt, D., and F. A. Laski, 1995 Mechanisms of cell rearrangement and cell recruitment in Drosophila
2292 ovary morphogenesis and the requirement of bric a brac. Development 121: 173-187.
2293 Grammont, M., and K. D. Irvine, 2001 fringe and Notch specify polar cell fate during Drosophila
2294 oogenesis. Development 128: 2243-2253.
2295 Greulich, P., B. D. MacArthur, C. Parigini and R. J. Sanchez-Garcia, 2021 Universal principles of lineage
2296 architecture and stem cell identity in renewing tissues. Development 148.
2297 Guiu, J., E. Hannezo, S. Yui, S. Demharter, S. Ulyanchenko *et al.*, 2019 Tracing the origin of adult
2298 intestinal stem cells. Nature 570: 107-111.
2299 Hartman, T. R., T. I. Strochlic, Y. Ji, D. Zinshteyn and A. M. O'Reilly, 2013 Diet controls Drosophila
2300 follicle stem cell proliferation via Hedgehog sequestration and release. J Cell Biol 201: 741-
2301 757.
2302 Hayashi, Y., Y. Yoshinari, S. Kobayashi and R. Niwa, 2020 The regulation of Drosophila ovarian stem
2303 cell niches by signaling crosstalk. Curr Opin Insect Sci 37: 23-29.
2304 He, L., R. Binari, J. Huang, J. Falo-Sanjuan and N. Perrimon, 2019 In vivo study of gene expression with
2305 an enhanced dual-color fluorescent transcriptional timer. Elife 8.
2306 Hsu, T. H., C. Y. Yang, T. H. Yeh, Y. C. Huang, T. W. Wang *et al.*, 2017 The Hippo pathway acts
2307 downstream of the Hedgehog signaling to regulate follicle stem cell maintenance in the
2308 Drosophila ovary. Sci Rep 7: 4480.
2309 Huang, J., and D. Kalderon, 2014 Coupling of Hedgehog and Hippo pathways promotes stem cell
2310 maintenance by stimulating proliferation. J Cell Biol 205: 325-338.
2311 Huang, J., A. Reilein and D. Kalderon, 2017 Yorkie and Hedgehog independently restrict BMP
2312 production in escort cells to permit germline differentiation in the Drosophila ovary.
2313 Development 144: 2584-2594.
2314 Ingham, P. W., 2022 Hedgehog signaling. Curr Top Dev Biol 149: 1-58.
2315 Jemc, J. C., 2011 Somatic gonadal cells: the supporting cast for the germline. Genesis 49: 753-775.
2316 Jia, J., C. Tong and J. Jiang, 2003 Smoothened transduces Hedgehog signal by physically interacting
2317 with Costal2/Fused complex through its C-terminal tail. Genes & Development 17: 2709-2720.
2318 Jones, P. H., 2010 Stem cell fate in proliferating tissues: equal odds in a game of chance. Dev Cell 19:
2319 489-490.
2320 Kahney, E. W., J. C. Snedeker and X. Chen, 2019 Regulation of Drosophila germline stem cells. Curr
2321 Opin Cell Biol 60: 27-35.
2322 Kalderon, D., 2022 Investigating Adult Stem Cells Through Lineage analyses. Stem Cell Rev Rep 18: 2-
2323 22.
2324 Kalderon, D., D. Melamed and A. Reilein, 2021 The number of Follicle Stem Cells in a Drosophila
2325 ovariole. bioRxiv: 2021.2010.2025.465475
2326 King, R. C., S. K. Aggarwal and U. Aggarwal, 1968 The development of the female Drosophila
2327 reproductive system. J Morphol 124: 143-166.
2328 Kirilly, D., S. Wang and T. Xie, 2011 Self-maintained escort cells form a germline stem cell
2329 differentiation niche. Development 138: 5087-5097.
2330 Lai, C. M., K. Y. Lin, S. H. Kao, Y. N. Chen, F. Huang *et al.*, 2017 Hedgehog signaling establishes
2331 precursors for germline stem cell niches by regulating cell adhesion. J Cell Biol 216: 1439-
2332 1453.
2333 Lane, M. E., K. Sauer, K. Wallace, Y. N. Jan, C. F. Lehner *et al.*, 1996 Dacapo, a cyclin-dependent kinase
2334 inhibitor, stops cell proliferation during Drosophila development. Cell 87: 1225-1235.

2335 Lee, T., and L. Luo, 2001 Mosaic analysis with a repressible cell marker (MARCM) for Drosophila
2336 neural development.[erratum appears in Trends Neurosci 2001 Jul;24(7):385]. Trends in
2337 Neurosciences 24: 251-254.
2338 Li, C., L. Kan, Y. Chen, X. Zheng, W. Li *et al.*, 2015 Ci antagonizes Hippo signaling in the somatic cells of
2339 the ovary to drive germline stem cell differentiation. Cell Res 25: 1152-1170.
2340 Li, M. A., J. D. Alls, R. M. Avancini, K. Koo and D. Godt, 2003 The large Maf factor Traffic Jam controls
2341 gonad morphogenesis in Drosophila. Nat Cell Biol 5: 994-1000.
2342 Little, J. C., E. Garcia-Garcia, A. Sul and D. Kalderon, 2020 Drosophila hedgehog can act as a
2343 morphogen in the absence of regulated Ci processing. Elife 9.
2344 Losick, V. P., L. X. Morris, D. T. Fox and A. Spradling, 2011 Drosophila stem cell niches: a decade of
2345 discovery suggests a unified view of stem cell regulation. Dev Cell 21: 159-171.
2346 Margolis, J., and A. Spradling, 1995 Identification and behavior of epithelial stem cells in the
2347 Drosophila ovary. Development 121: 3797-3807.
2348 McGregor, J. R., R. Xi and D. A. Harrison, 2002 JAK signaling is somatically required for follicle cell
2349 differentiation in Drosophila. Development 129: 705-717.
2350 Melamed, D., A. Choi, A. Reilein, S. Tavare and D. Kalderon, 2023 Spatial regulation of Drosophila
2351 ovarian Follicle Stem Cell division rates and cell cycle transitions. PLoS Genet 19: e1010965.
2352 Melamed, D., and D. Kalderon, 2020 Opposing JAK-STAT and Wnt signaling gradients define a stem
2353 cell domain by regulating differentiation at two borders. Elife 9.
2354 Merkle, J. A., J. Wittes and T. Schupbach, 2020 Signaling between somatic follicle cells and the
2355 germline patterns the egg and embryo of Drosophila. Curr Top Dev Biol 140: 55-86.
2356 Misra, J. R., and K. D. Irvine, 2018 The Hippo Signaling Network and Its Biological Functions. Annu Rev
2357 Genet 52: 65-87.
2358 Murray, S. M., S. Y. Yang and M. Van Doren, 2010 Germ cell sex determination: a collaboration
2359 between soma and germline. Curr Opin Cell Biol 22: 722-729.
2360 Obernier, K., and A. Alvarez-Buylla, 2019 Neural stem cells: origin, heterogeneity and regulation in the
2361 adult mammalian brain. Development 146.
2362 Ohlmeyer, J. T., and D. Kalderon, 1998 Hedgehog stimulates maturation of Cubitus interruptus into a
2363 labile transcriptional activator. Nature 396: 749-753.
2364 Panchal, T., X. Chen, E. Alchits, Y. Oh, J. Poon *et al.*, 2017 Specification and spatial arrangement of
2365 cells in the germline stem cell niche of the Drosophila ovary depend on the Maf transcription
2366 factor Traffic jam. PLoS Genet 13: e1006790.
2367 Pignoni, F., and S. L. Zipursky, 1997 Induction of Drosophila eye development by decapentaplegic.
2368 Development 124: 271-278.
2369 Post, Y., and H. Clevers, 2019 Defining Adult Stem Cell Function at Its Simplest: The Ability to Replace
2370 Lost Cells through Mitosis. Cell Stem Cell 25: 174-183.
2371 Reilein, A., H. V. Kogan, R. Misner, K. S. Park and D. Kalderon, 2021 Adult stem cells and niche cells
2372 segregate gradually from common precursors that build the adult Drosophila ovary during
2373 pupal development. Elife 10.
2374 Reilein, A., D. Melamed, K. S. Park, A. Berg, E. Cimetta *et al.*, 2017 Alternative direct stem cell
2375 derivatives defined by stem cell location and graded Wnt signalling. Nat Cell Biol 19: 433-444.
2376 Reilein, A., D. Melamed, S. Tavare and D. Kalderon, 2018 Division-independent differentiation
2377 mandates proliferative competition among stem cells. Proc Natl Acad Sci U S A 115: E3182-
2378 E3191.
2379 Sahai-Hernandez, P., and T. G. Nystul, 2013 A dynamic population of stromal cells contributes to the
2380 follicle stem cell niche in the Drosophila ovary. Development 140: 4490-4498.

2381 Sarikaya, D. P., and C. G. Extavour, 2015 The Hippo pathway regulates homeostatic growth of stem
2382 cell niche precursors in the Drosophila ovary. PLoS Genet 11: e1004962.
2383 Slaidina, M., T. U. Banisch, S. Gupta and R. Lehmann, 2020 A single-cell atlas of the developing
2384 Drosophila ovary identifies follicle stem cell progenitors. Genes Dev 34: 239-249.
2385 Smelkinson, M. G., Q. Zhou and D. Kalderon, 2007 Regulation of Ci-SCFSlimb binding, Ci proteolysis,
2386 and hedgehog pathway activity by Ci phosphorylation. Dev Cell 13: 481-495.
2387 Song, X., G. B. Call, D. Kirilly and T. Xie, 2007 Notch signaling controls germline stem cell niche
2388 formation in the Drosophila ovary. Development 134: 1071-1080.
2389 Song, X., and T. Xie, 2003 Wingless signaling regulates the maintenance of ovarian somatic stem cells
2390 in Drosophila. Development 130: 3259-3268.
2391 Spradling, A. C., M. de Cuevas, D. Drummond-Barbosa, L. Keyes, M. Lilly *et al.*, 1997 The Drosophila
2392 germarium: stem cells, germ line cysts, and oocytes. Cold Spring Harbor Symposia on
2393 Quantitative Biology 62: 25-34.
2394 St Johnston, D., 2023 Polarity and axis formation in the Drosophila female germ line. Curr Top Dev
2395 Biol 154: 73-97.
2396 Vermeulen, L., and H. J. Snippert, 2014 Stem cell dynamics in homeostasis and cancer of the intestine.
2397 Nat Rev Cancer 14: 468-480.
2398 Vied, C., and D. Kalderon, 2009 Hedgehog-stimulated stem cells depend on non-canonical activity of
2399 the Notch co-activator Mastermind. Development 136: 2177-2186.
2400 Vied, C., A. Reilein, N. S. Field and D. Kalderon, 2012 Regulation of stem cells by intersecting gradients
2401 of long-range niche signals. Dev Cell 23: 836-848.
2402 Vlachos, S., S. Jangam, R. Conder, M. Chou, T. Nystul *et al.*, 2015 A Pak-regulated cell intercalation
2403 event leading to a novel radial cell polarity is involved in positioning of the follicle stem cell
2404 niche in the Drosophila ovary. Development 142: 82-91.
2405 Voog, J., and D. L. Jones, 2010 Stem cells and the niche: a dynamic duo. Cell Stem Cell 6: 103-115.
2406 Wang, S., Y. Gao, X. Song, X. Ma, X. Zhu *et al.*, 2015 Wnt signaling-mediated redox regulation
2407 maintains the germ line stem cell differentiation niche. Elife 4: e08174.
2408 Wang, X., and A. Page-McCaw, 2014 A matrix metalloproteinase mediates long-distance attenuation
2409 of stem cell proliferation. J Cell Biol 206: 923-936.
2410 Wang, X., and A. Page-McCaw, 2018 Wnt6 maintains anterior escort cells as an integral component of
2411 the germline stem cell niche. Development 145.
2412 Wang, Z. A., J. Huang and D. Kalderon, 2012 Drosophila follicle stem cells are regulated by
2413 proliferation and niche adhesion as well as mitochondria and ROS. Nat Commun 3: 769.
2414 Wang, Z. A., and D. Kalderon, 2009 Cyclin E-dependent protein kinase activity regulates niche
2415 retention of Drosophila ovarian follicle stem cells. Proc Natl Acad Sci U S A 106: 21701-21706.
2416 Ward, E. J., H. R. Shcherbata, S. H. Reynolds, K. A. Fischer, S. D. Hatfield *et al.*, 2006 Stem cells signal
2417 to the niche through the Notch pathway in the Drosophila ovary. Curr Biol 16: 2352-2358.
2418 Wiese, K. E., R. Nusse and R. van Amerongen, 2018 Wnt signalling: conquering complexity.
2419 Development 145.
2420 Xi, R., J. R. McGregor and D. A. Harrison, 2003 A gradient of JAK pathway activity patterns the
2421 anterior-posterior axis of the follicular epithelium. Developmental Cell 4: 167-177.
2422 Zamfirescu, A. M., A. S. Yatsenko and H. R. Shcherbata, 2022 Notch signaling sculpts the stem cell
2423 niche. Front Cell Dev Biol 10: 1027222.
2424 Zeidler, M. P., and N. Bausek, 2013 The Drosophila JAK-STAT pathway. JAKSTAT 2: e25353.
2425 Zhang, H., and Y. Cai, 2020 Signal transduction pathways regulating Drosophila ovarian germline stem
2426 cells. Curr Opin Insect Sci 37: 1-7.

2427 Zhang, Y., and D. Kalderon, 2000 Regulation of cell proliferation and patterning in Drosophila
2428 oogenesis by Hedgehog signaling. Development 127: 2165-2176.
2429 Zhang, Y., and D. Kalderon, 2001 Hedgehog acts as a somatic stem cell factor in the Drosophila ovary.
2430 Nature 410: 599-604.
2431 Zhu, C. H., and T. Xie, 2003 Clonal expansion of ovarian germline stem cells during niche formation in
2432 Drosophila. Development 130: 2579-2588.
2433
2434
2435
2436
2437
2438
2439
2440
2441
2442
2443
2444
2445
2446
2447
2448
2449
2450
2451

2452 **Supplementary Materials**
2453
2454 **Supplementary Figure 1: Wnt signaling influences over different periods of pupation.**
2455
2456 **Supplementary Figure 2: JAK/STAT signaling in pupal germaria after stalk and polar cell formation.**
2457
2458 **Supplementary spreadsheets with raw data and calculations underlying all presented data**
2459
2460 **Single-cell 0hAPF calculations**
2461 All summary clone data for lineages induced at 0h APF together with the calculations converting data
2462 to estimations of single-cell lineage data and averaging of all control values and other genotypes
2463 tested in more than one experiment.
2464
2465 **Single-cell -2dAPF calculations**
2466 All summary clone data for lineages induced at -2d APF together with the calculations converting data
2467 to estimations of single-cell lineage data and averaging of all control values and other genotypes
2468 tested in more than one experiment.
2469
2470 **0h APF Significance Fisher** and **-2d APF Significance Fisher**
2471 Copies of the two previous spreadsheets (numbers only, no formulae exposing the calculation
2472 methods) with additional columns to show p values of significant differences to controls if $p<0.05$
2473 using Fisher's exact two-tailed test.
2474
2475 **0h APF Controls Variation**
2476 Calculation of SD and SEM for single-cell lineage parameters among control experiments and
2477 comparison to expectations from probabilistic labeling of precursors in different A/P locations.
2478
2479 **0h APF Graphs Fig1,3**
2480 First sheet is 0h APF master sheet (from the single-cell calculation sheet). Others show data for Figs.
2481 1B-D and Fig. 3I.
2482
2483 **0h APF Graphs Fig4-10**
2484 First sheet is 0h APF master sheet (from the single-cell calculation sheet). Others show data for Figs.
2485 4, 6, 8H, 9D, 10G
2486
2487 **-2d APF Graphs**
2488 First sheet is -2d APF master sheet (from the single-cell calculation sheet). Others show data for Figs.
2489 3J, 8I, 9E.
2490
2491 **-3.5d axn August 2023 Numbers**
2492 Control and *axn* lineages initiated 3.5d before eclosion (36h APF); raw data and deduced frequencies
2493 of clone types.
2494
2495 **-4d arr DIAP Numbers**
2496 Control and *arr; UAS-DIAP1* lineages initiated 4d before eclosion (24h APF); raw data and deduced
2497 frequencies of clone types.

Fig. S1 Graph Data
Data for Supplementary Fig. 1.

Fig5 Fz3RFP Graph
Data for Fig. 5 graph of Fz3-RFP Wnt reporter intensities over the germarium at different times.

-3.5d stat November 2021 Numbers
stat lineages initiated 3.5d before eclosion (36h APF); raw data and deduced frequencies of clone types.

FC occupancy aggregate
Raw data and aggregation for fraction of terminal egg chamber occupied by marked FCs and frequency of additional FC labeling in penultimate or more anterior egg chambers for cycE and cutlet genotype lineages (initiated at 0h APF and -2d APF, leading to graph in Fig. 3F), and for selected Hedgehog and Yorkie genotypes (0h APF Hh Yki TermFC). Raw cell number data for EC-only and EC/FSC lineages of select Hh Yki genotypes to estimate SEM (Cell#). Summary data for fraction of available cysts with marked FCs in FSC-containing lineages (%cystsMarkedFCs 0h APF).

Division Measures Hh/Yki
Summary data for graphs in Fig. 10H-K.

Raw data lineage spreadsheets: "**Compilation of Numbers**" named by Figure and time of lineage initiation ("-5d" = 0h APF, "-7d" = -2d APF).
First sheet in a pair is the raw tabulation of marked cells for each sample of a given genotype. The second sheet compiles the raw data to give a variety of measures, including those transferred to the master spreadsheets used to estimate single-cell lineage parameters ("calculations" spreadsheets).